

Mechanisms of control in *Mycobacterium tuberculosis* infection

by

Mariëtta M. Ravesloot-Chávez

A dissertation submitted in partial satisfaction of the

requirements for the degree of

Doctor of Philosophy

in

Microbiology

in the

Graduate Division

of the

University of California, Berkeley

Committee in Charge:

Professor Sarah A. Stanley, Chair

Professor Laurent Coscoy

Professor David H. Raulet

Spring 2022



## ABSTRACT

Mechanisms of control in *Mycobacterium tuberculosis* infection

by

Mariëtta M. Ravestloot-Chávez

Doctor of Philosophy in Microbiology

University of California, Berkeley

Professor Sarah A. Stanley, Chair

*Mycobacterium tuberculosis* is an obligate pathogen that has evolved to survive exclusively in the human population and remains a leading cause of mortality due to bacterial infections. The immune responses against *M. tuberculosis* are diverse, with some people controlling the infection for their lifetime without showing symptoms, whereas others develop progressive disease leading to the spread of the bacterium among people. The underlying causes for the obvious differences in susceptibility to infection are not well understood. Some genes have been associated with severe disease, including genes involved in the interferon- $\gamma$  (IFN- $\gamma$ ) and interleukin-12 (IL-12) signaling pathways. However, many questions remain about the genetic factors that contribute to susceptibility and resistance to infection.

In chapter 1 we highlight our current knowledge about the innate immune responses that are crucial for the recognition of infection and activation of adaptive immune responses. A successful pro-inflammatory response to infection is well-balanced, accomplishing control of infection while limiting excessive pro-inflammatory responses that damage the host. Cytokines such as TNF- $\alpha$  and IL-1 are important for protection, yet excessive or insufficient cytokine production results in progressive disease. Macrophages phagocytose *M. tuberculosis* and are capable of cell-intrinsic antimicrobial control. Furthermore, they are important for initiating and maintaining inflammation. Neutrophils are highly abundant during infection and are normally associated with control of bacterial infections. However, they can be drivers of hyperinflammatory responses that benefit *M. tuberculosis* growth and result in host mortality. The role of other innate cells, including natural killer cells and innate T cells, remains enigmatic.

Chapter 2 describes the use of a genetically diverse mouse cohort to identify underlying mechanisms of susceptibility to infection. The diverse mouse lines showed a range of susceptibility to infection with several lines harboring 100-fold more bacterial in the lungs compared to the classical C57BL/6 mice. In addition, the abundance of neutrophils in the lung seems to correlate with outcome of infection, showing that high neutrophilic influx associates with high bacterial burden in the lung. Furthermore, we identified a mouse line that controls *M. tuberculosis* infection in the absence of high numbers of CD4<sup>+</sup>IFN $\gamma$ <sup>+</sup> T cells, which have been shown to drive control of infection in the classic B6 model.

Restriction of *M. tuberculosis* growth by macrophages occurs at the onset of the adaptive immune responses with CD4<sup>+</sup> T cells producing IFN- $\gamma$  that activates macrophages to exert their antimicrobial programs. A master regulator of IFN- $\gamma$  is the transcription factor HIF-1 $\alpha$ , which induces the upregulation of several pathways involved in maintenance of the macrophage's glycolytic metabolism and bactericidal responses against *M. tuberculosis*. Many questions remain on how HIF-1 $\alpha$  mediates these effects and how HIF-1 $\alpha$  is regulated by IFN- $\gamma$  signaling. In chapter 3 we investigate the factors involved in the constitutive degradation of HIF-1 $\alpha$  in resting macrophages. HIF-1 $\alpha$  seems to be degraded through a non-canonical pathway that requires the activity of ubiquitin ligase VHL. Although VHL is known for targeting proteins to proteasome-dependent degradation, HIF-1 $\alpha$  is degraded by the lysosome, suggesting the involvement of additional proteins that contribute to the activation of the correct degradation pathway. Inhibition of HIF-1 $\alpha$  degradation, including the deletion of the gene encoding VHL, results in enhanced cell-intrinsic control in macrophages. This effect is mediated through production of nitric oxide (NO). Surprisingly, very little is known about the pathways downstream of NO and HIF-1 $\alpha$  signaling that result in microbicidal responses. Our data shows that expression of a family of solute carrier (SLC) transporter proteins is highly dependent of IFN- $\gamma$  and HIF-1 $\alpha$  expression. The requirement for SLC metabolite transporters in macrophage glycolytic metabolism makes this protein family essential for maintaining the antimicrobial function of macrophages. In Chapter 3 we describe the development of a targeted forward genetics CRISPR approach to identify which SLC transporters are required for cell-intrinsic control of *M. tuberculosis* infection in macrophages. Taken together, this project aims to elucidate the antimicrobial mechanisms in the host that contribute to cell-intrinsic and -extrinsic control of infection.

*Equipped with his five senses, man explores the universe around him  
and calls the adventure Science.*

-Edwin Powell Hubble

## **Dedication**

To Freddy, who's support and true enjoyment of science has been an inspiration at every step along the way.

## Table of contents

<b>Chapter 1. Background on the innate immune response to <i>Mycobacterium tuberculosis</i> infection.....</b>	<b>1</b>
1.1 Abstract. ....	2
1.2 Recognition of <i>M. tuberculosis</i> by pattern recognition receptors of the innate immune system.....	3
1.3 Innate cytokines.....	3
1.3.1 TNF- $\alpha$ . ....	3
1.3.2 GM-CSF. ....	4
1.3.3 IL-1. ....	5
1.3.4 Type I interferons. ....	7
1.3.5 IL-10. ....	7
1.3.6 TGF- $\beta$ . ....	8
1.4 Macrophage-based mechanisms of innate control. ....	8
1.4.1 Autophagy. ....	8
1.4.2 Vitamin D and cathelicidin.....	9
1.4.3 Reactive oxygen species.....	9
1.4.4 iNOS. ....	10
1.4.5 Interferon-inducible GTPases.....	10
1.4.6 Aerobic glycolysis and metabolic regulation of infection.....	11
1.5 Cell death and eicosanoids.....	11
1.6 Other innate cells.....	12
1.6.1 Neutrophils in host defense. ....	12
1.6.2 Destructive inflammation mediated by neutrophils.....	12
1.6.3 Alveolar macrophages and innate cells during early infection.....	12
1.6.4 Dendritic cells.....	13
1.6.5 Natural killer cells. ....	13
1.7 Harnessing the innate immune response. ....	14
1.7.1 Innate immunity and adjuvant development for protein subunit vaccines. ....	14
1.7.2 Trained immunity. ....	15
1.8 Conclusions and perspectives. ....	16
<b>Chapter 2. Variation in immune responses and tuberculosis susceptibility in a novel cohort of genetically diverse mice.....</b>	<b>17</b>

2.1 Summary of results.....	18
2.3 Results. ....	20
2.3.1 Mouse lines collected from different latitudes display variability in immune responses and susceptibility to <i>M. tuberculosis</i> infection.....	20
2.3.2 Macrophages from Manaus lines respond to IFN- $\gamma$ stimulation during <i>M. tuberculosis</i> infection. ....	23
3.3.3 High bacterial burden correlates with high neutrophil influx in MANC lines.....	25
3.3.4 SARA mice show low numbers of CD4 <sup>+</sup> IFN- $\gamma$ <sup>+</sup> T cells in the lung.....	27
2.4 Discussion. ....	27
2.5 Materials and Methods.....	30
2.6 Supplemental figures.....	32
<b>Chapter 3. Intrinsic effects of interferon-<math>\gamma</math> signaling.</b> .....	36
3.1 Summary of results.....	37
3.2 Introduction .....	38
3.2.1 IFN- $\gamma$ signaling is essential for induction of antimicrobial pathways in macrophages. ..	38
3.2.2 HIF-1 $\alpha$ activity is regulated through a constitutively active degradation pathway. ....	38
3.2.3 IFN- $\gamma$ regulates the expression of metabolite transporters.....	39
3.3 Results .....	40
3.3.1 HIF-1 $\alpha$ protein levels are stabilized by inhibition of lysosomal acidification. ....	40
3.3.2 Ubiquitin ligase VHL is involved in an uncanonical HIF-1 $\alpha$ degradation pathway. ...	41
3.3.3 Enhanced HIF-1 $\alpha$ -dependent NO production results in increased bacterial restriction. ....	42
3.3.4 HIF-1 $\alpha$ regulates expression of metabolite transporters.....	43
3.3.5 GBP activity does not benefit the host during <i>M. tuberculosis</i> infection.....	44
3.3.6 Identifying the role of SLC transporters in IFN- $\gamma$ dependent cell-intrinsic control. A	45
3.4 Discussion. ....	48
3.5 Materials and Methods.....	50
3.6 Supplemental Figures.....	53
<b>Chapter 4. Conclusions and future directions.</b> .....	57
4.1 Summary of results.....	58
4.2 Remaining questions and future directions. ....	59
4.2.1 Chapter 2 and the abundance of neutrophils in the Manaus lines. ....	59
4.2.2 Chapter 3 and HIF-1 $\alpha$ regulation.....	59



4.2.3 Chapter 3 and the function of SLC.....	60
Final thoughts and speculation into the future. ....	60
<b>References</b> .....	62

## List of Figures

### Chapter 1:

Figure 1.1 PRRs implicated in detecting <i>M. tuberculosis</i> infection and initiating the production of important innate cytokines.....	4
Figure 1.2 A combination of antimicrobial function and regulation of inflammation is required for successful control of <i>M. tuberculosis</i> infection.....	6

### Chapter 2:

Figure 2.1 Mouse lines from different latitudes show variable susceptibility to <i>M. tuberculosis</i> infection. ....	21
Figure 2.2 Variation in bacterial burden and immune cells present in the lung between locales. 22	
Figure 2.3 The MANC line does not show obvious defects in intrinsic control of infection. ....	24
Figure 2.4. In vivo signaling of IL-1 is not correlated to high neutrophil influx in the Manaus lines. ....	25
Figure 2.5 scRNAseq analysis of infected mouse lungs reveals a lower expression of inflammatory cytokines in neutrophils from MANC mice. ....	26
Figure 2.6 SARA mice show increased bacterial restriction in the absence of high numbers of CD4 <sup>+</sup> IFN $\gamma$ <sup>+</sup> cells. ....	28
Supplemental Figure 2.1 Mouse lines from within and among different locations show variability in <i>M. tuberculosis</i> susceptibility. ....	32
Supplemental Figure 2.2 Correlation between CFU and the proportion CD4 <sup>+</sup> IFN $\gamma$ <sup>+</sup> cells in the lung of B6 and Saratoga mice. ....	33
Supplemental Figure 2.3 Expression of genes involved in intrinsic control of infection are differentially expressed in MANC mice. ....	34
Supplemental Figure 2.4 Differences in abundance of T cell subsets do not explain the underlying mechanism for bacterial restriction in SARA mice. ....	35

### Chapter 3:

Figure 3.1. Interferon- $\gamma$ signaling restricts <i>M. tuberculosis</i> growth in macrophages. ....	41
Figure 3.2. HIF-1 $\alpha$ degradation in macrophages is inhibited by lysosomal inhibitors.....	42
Figure 3.3. VHL is required for HIF-1 $\alpha$ degradation and control of infection.....	43
Figure 3.4. HIF-1 $\alpha$ regulates expression of metabolite transporters downstream of IFN- $\gamma$ signaling.....	44
Figure 3.5. Lack of individual GBPs does not impair intrinsic control of <i>M. tuberculosis</i> infection in macrophages. ....	45
Figure 3.6. <i>Slc</i> gene expression do not contribute to IFN- $\gamma$ dependent control of infection. ....	46
Figure 3.7. Model of forward genetics screen to identify <i>Slc</i> genes that are required for IFN- $\gamma$ dependent control of infection. ....	47
Supplemental Figure 3.1. Model of HIF-1 $\alpha$ expression and protein degradation. ....	53
Supplemental Figure 2. Absence of HIF-1 $\alpha$ specific K48 and K63 ubiquitin staining.....	54
Supplemental Figure 3. Loss of various individual genes in BMDM does not result in enhanced bacterial growth in the presence of IFN- $\gamma$ .....	55
Supplemental Figure 4. Transduction efficiency various among cell types. ....	56

## Acknowledgments

I especially want to thank my mentor, Sarah A. Stanley. Thank you for your unwavering support and guidance throughout my PhD. Your passion for science and drive to tackle big questions is incredibly inspiring. You are always sharp, yet compassionate and you always seek out opportunities to collaborate and learn from other scientists. I hope to emulate these values in my future career in science. You often remind me to think about the bigger picture, in science and also in life, and this is a lesson I will always keep close to my heart. It is truly a privilege working with you.

To all those I overlapped with during my time in the Stanley lab, Daniel Fines, Kayla Dinshaw, Erik Van Dis, Ira Jain, Sagar Rawal, Xammy Nguyenla, Ronald Rodriguez, Nick Campbell-Kruger, Alex Zalinkas, Sam Berry, Andrea Anaya Sanchez, Robyn Jong, Katie Lien, Kimberley Sogi, Matthew Knight, Douglas Fox and Jonathan Braverman, I enjoyed my time in lab because of all of you. Together you create such a friendly, stimulating and inclusive environment. I could not have wished for better colleagues to be on this journey with.

To Laurent and David, thank you sincerely for your support. Your input, critical perspectives, and general enthusiasm for my project during my thesis meeting have been vital in motivating me to keep moving forward.

To Rocío, thank you for making me feel welcome and for always being there to chat, give advice and simply listen.

I am thankful to the PMB department, and the faculty, staff and students that comprise it, for providing me the opportunity to be a part of such a great program. In addition to being an open community that shares the wide scope of high quality science done by everyone, the numerous seminars, symposia and retreats create such an interactive and warm community that I am very happy I was a part of this.

## Chapter 1

### Background on the innate immune response to *Mycobacterium tuberculosis* infection

Sections of this chapter were published in Annual Review of Immunology:  
Raveslout-Chávez MM\*, Van Dis E\*, Stanley SA. The innate immune response to  
*Mycobacterium tuberculosis* infection. Annual Review of Immunology 2021. 39:611-37  
<https://doi.org/10.1146/annurev-immunol-093019-010426>. PMID: 33637017

\*These authors contributed equally

## 1.1 Abstract.

It is estimated that 2 billion people are infected with *Mycobacterium tuberculosis*. The majority of these individuals mount an immune response that is sufficient to maintain infection in a latent state and will never experience clinical signs of disease. However, the vast reservoir of infection means that even though only ~10% of infected individuals experience active disease, in 2017 there were an estimated 10 million incident cases of active TB, resulting in 1.6 million deaths<sup>1</sup>. Recent studies have renewed hope that it will be possible to develop an effective vaccine for tuberculosis. However, in order to use rational strategies to improve upon this progress, a better understanding of the immune response to infection is required. This chapter discusses the immune cells that are required for the innate immune response to *M. tuberculosis* infection. Cells of the innate immune system are the first to encounter *M. tuberculosis*, and their response shapes the entire course of infection, forming the battleground through which the host-pathogen interaction is enacted. Antigen presenting cells (APC) migrate to draining lymph nodes to activate the CD4 T cell response, which is crucial for control of infection, however manipulating the timing of the migration and the phenotype of the APC itself is a major mechanism used by *M. tuberculosis* to subvert adaptive immunity and establish chronic infection. Similarly, although macrophages are key to controlling bacterial replication and establishing resistance to infection, they also serve as a bacterial niche for growth, and can contribute to a hyper-inflammatory response that harms the host and promotes transmission of infection. Most immune responses to *M. tuberculosis* encompass a similar duality. Achieving the proper balance of innate cytokines is key to protecting the host as excessive or insufficient production of either pro or anti-inflammatory cytokines results in progressive disease. In this context, the tight regulation of neutrophils is essential for host protection, as neutrophilic infiltration is also associated with hyper-inflammatory responses that drive host mortality. Finally, there is increasing appreciation for the fact that innate lymphocytes, such as NK cells, and innate like T cells, such as MAIT and  $\gamma\delta$  T cells, display interesting correlations with disease progression and treatment responses in humans, and may in fact play a role in protective immunity. Understanding innate immunity is central to understanding how hosts successfully control infection with *M. tuberculosis*. Furthermore, understanding how to provoke an innate immune response that can confer the protective, and not the detrimental aspects of the host immune response, will be key to developing a successful vaccine.

**1.2 Recognition of *M. tuberculosis* by pattern recognition receptors of the innate immune system.** The first step in initiating an immune response to *Mycobacterium tuberculosis* is detection by pattern recognition receptors (PRRs). Several classes of PRRs, including Toll-like receptors (TLRs), nucleotide-binding domain and leucine-rich repeat-containing receptors (NLRs), C-type lectin receptors (CLRs), and cyclic GMP-AMP synthase (cGAS)/stimulator of interferon genes (STING), have been proposed to contribute to recognition of *M. tuberculosis* (Figure 1.1). Studies of mouse models have identified TLR2, which recognizes lipoproteins and lipoglycans from *M. tuberculosis*, and TLR9, which recognizes unmethylated CpG DNA, as the most important TLRs for control of *M. tuberculosis* infection<sup>2-5</sup>. Mice lacking both TLR2 and TLR9 are more susceptible than TLR2<sup>-/-</sup> or TLR9<sup>-/-</sup> single knockout mutants, suggesting that each TLR makes a nonredundant contribution to the immune response<sup>5</sup>. The importance of TLR sensing stems from production of inflammatory cytokines, in particular IL-12, which is necessary for priming IFN- $\gamma$ -producing T cells that mediate control of *M. tuberculosis* infection<sup>5-7</sup>. In addition to TLRs, several CLRs have been proposed to play a role in immune recognition of *M. tuberculosis*. The cell wall glycolipid mannose-capped lipoarabinomannan can be recognized by DC-SIGN, mannose receptor, or Dectin-2<sup>8-11</sup>, and trehalose dimycolate can be recognized by Mincle or Marco<sup>11,12</sup>. However, experiments using mutant mice have suggested a limited role for individual CLRs<sup>11,13-15</sup>, which may be partially explained by redundancy in function. Finally, the NLR NOD2, which senses small muramyl peptides derived from bacterial cell wall peptidoglycan, contributes to cytokine responses to *M. tuberculosis* in myeloid cells cultured in vitro<sup>16-22</sup>. However, mice lacking NOD2 are largely resistant to infection, exhibiting modest susceptibility only six months after infection<sup>20,23</sup>. The NLR NLRP3, a component of the inflammasome, is reviewed in the Section titled IL-1.

cGAS is a cytosolic DNA sensor that produces cyclic GMP-AMP (cGAMP) upon DNA binding<sup>24,25</sup>. STING signaling is initiated by binding of cGAMP or other cyclic dinucleotides exported by pathogenic bacteria<sup>26-28</sup>. STING induces expression of type I interferons, a family of cytokines that are detrimental to host control of *M. tuberculosis* infection<sup>29-32</sup>. Activation of STING by *M. tuberculosis* and production of type I interferon require perforation of the vacuolar membrane by the ESX-1 type VII secretion system<sup>33</sup>. Three independent reports demonstrated that cGAS is required for type I interferon induction, suggesting that DNA is the pathogen-associated molecular pattern (PAMP) that leads to STING activation<sup>34-36</sup>. However, it was also reported that *M. tuberculosis* induces type I interferon by direct STING recognition of cyclic-di-AMP produced by the bacterium<sup>37</sup>. Whereas TLRs, CLRs, and NLRs have been proposed to benefit the immune response to *M. tuberculosis* by promoting the production of proinflammatory cytokines and chemokines, the cGAS-STING pathway may be an example in which a bacterial pathogen engages an antiviral pathway to promote pathogenesis.

### **1.3 Innate cytokines.**

**1.3.1 TNF- $\alpha$ .** TNF- $\alpha$  was one of the first cytokines associated with tuberculosis and is crucial for control of infection. Macrophages and DCs are the primary producers of TNF- $\alpha$  during infection; however, TNF- $\alpha$  is also produced abundantly by CD4 T cells<sup>38</sup>. Mice lacking TNF- $\alpha$  or the TNF receptor are highly susceptible to infection and exhibit poor activation of myeloid cells, a defect in chemokine production, and diffuse inflammation that lacks organized structure<sup>39-42</sup>. Evidence for the importance of TNF- $\alpha$  in human tuberculosis infection comes primarily from patients treated with anti-TNF agents for inflammatory disorders, who have a high propensity for reactivation of tuberculosis disease<sup>43-45</sup>. Nonhuman primate and mouse models support the idea

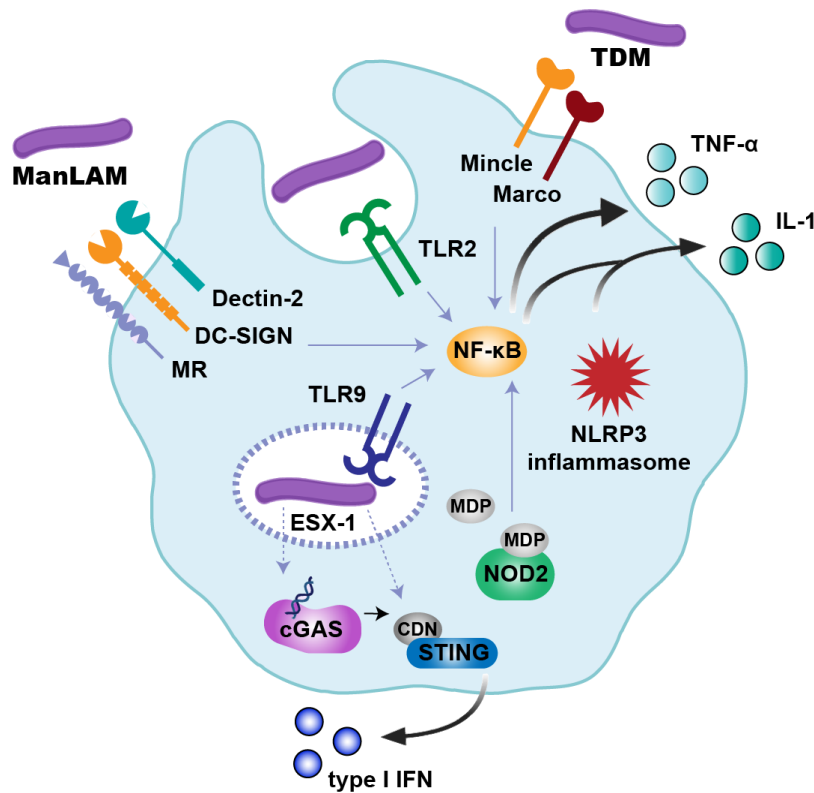


**Figure 1.1 PRRs implicated in detecting *M. tuberculosis* infection and initiating the production of important innate cytokines.**

*M. tuberculosis* is detected by multiple classes of PRRs. The CLR MR, DC-SIGN, and Dectin-2 have been proposed to recognize the glycolipid ManLAM, whereas Mincle and Marco recognize TDM on the surface of bacteria. TLR2 recognizes lipoproteins and/or lipoglycans on the surface, whereas TLR9 recognizes DNA released in the phagolysosome. The NLR NOD2 recognizes MDP released from bacterial peptidoglycan. NLRP3 triggers inflammasome activation upon *M. tuberculosis* infection. The ESX-1 secretion system promotes detection by cytosolic sensors by perforating the phagosomal membrane and allowing bacterial pathogen-associated molecular patterns to enter the cytosol, resulting in activation of cGAS/STING. CLRs, TLRs, and NOD2 signal through NF- $\kappa$ B to activate transcription of inflammatory cytokines including IL-1 and TNF- $\alpha$ . Processing and activation of IL-1 $\beta$  are promoted by the NLRP3 inflammasome. The cGAS-STING pathway leads to the expression of type I interferon, which is detrimental to the host. Abbreviations: CDN, cyclic dinucleotide; cGAS, cyclic GMP-AMP synthase; CLR, C-type lectin receptor; ManLAM, mannose-capped lipoarabinomannan; MDP, muramyl dipeptide; MR, mannose receptor; NLR, nucleotide-binding domain and leucine-rich repeat-containing receptor; PRR, pattern recognition receptor; STING, stimulator of interferon genes; TDM, trehalose dimycolate; TLR, Toll-like receptor.

that TNF- $\alpha$  is important for granuloma formation, structure, and integrity<sup>46–48</sup>. However, studies using the zebrafish model of infection with *Mycobacterium marinum*, which is particularly well-suited to studying granuloma formation<sup>49</sup>, have suggested that TNF- $\alpha$  maintains granuloma structure indirectly by restricting mycobacterial growth<sup>50,51</sup>; this has also been suggested by mouse studies<sup>52</sup>. Furthermore, the zebrafish model has demonstrated that excess TNF- $\alpha$  can lead to increased macrophage cell death, which promotes hyperinflammation and death of the host. This finding illustrates the concept that in innate immunity to tuberculosis, excessive production of protective factors can be detrimental<sup>53,54</sup> (Figure 1.2).

**1.3.2 GM-CSF.** The cytokine granulocyte-macrophage colony-stimulating factor (GM-CSF) was originally implicated in myeloid cell and granulocyte differentiation. However, mice lacking the

GM-CSF gene, *Csf2*, have normal steady-state myelopoiesis but lack alveolar macrophages (AMs) <sup>55</sup>. Lungs of *Csf2*<sup>-/-</sup> mice exhibit a buildup of pulmonary surfactant due to impaired catabolism by AMs, as well as pulmonary lymphoid hyperplasia at baseline <sup>56</sup>. GM-CSF levels rise in the lungs of wild-type mice for at least 60 days after *M. tuberculosis* infection, and *Csf2*<sup>-/-</sup> mice are highly susceptible to *M. tuberculosis*, succumbing rapidly after infection <sup>57</sup>. While nonhematopoietic cells are the primary producers of GM-CSF, *Csf2*<sup>-/-</sup> mice are partially rescued by adoptive transfer of wild-type but not *Csf2*<sup>-/-</sup> CD4 T cells, implying a minor role for T cell-derived GM-CSF <sup>58</sup>. *Csf2*<sup>-/-</sup> mice have a defect in their production of inflammatory cytokines and chemokines in response to infection, resulting in impaired recruitment of both myeloid cells and T cells to the lungs <sup>57</sup>. *Csf2*<sup>-/-</sup> infected mice also exhibit a significant increase in bacterial burden in the lungs compared with wild-type mice, suggesting a potential antibacterial role for GM-CSF <sup>57</sup>. Indeed, addition of exogenous GM-CSF to *M. tuberculosis*-infected peritoneal macrophages and human monocytes results in enhanced control of infection <sup>58,59</sup>. However, whereas treatment of wild-type mice with anti-GM-CSF neutralizing antibodies results in significant weight loss and larger granulomas in the lungs, it induces no change in lung colony-forming units, suggesting a role for GM-CSF in immune regulation rather than control of *M. tuberculosis* growth <sup>60</sup>. A clear role for GM-CSF in activating the microbicidal capabilities of macrophages in vivo has yet to be demonstrated. Furthermore, the fact that *Csf2*<sup>-/-</sup> mice have baseline alterations in lung function complicates the interpretation of results from these mice <sup>59,61,62</sup>.

**1.3.3 IL-1.** The first interleukin to be described was IL-1, discovered as a potent modulator of innate immunity. The IL-1 family members IL-1 $\alpha$  and IL-1 $\beta$ , are produced during infection with *M. tuberculosis* by inflammatory monocyte-macrophages, inflammatory DCs, and neutrophils <sup>31,63</sup>. They play critical and nonredundant protective roles early during infection, despite signaling through the same receptor. Neutralization of both IL-1 $\alpha$  and IL-1 $\beta$  has a more significant impact on morbidity after infection than neutralization of either protein individually <sup>64</sup>. Similarly, mice doubly deficient for IL-1 $\alpha$  and IL-1 $\beta$  (*Il1a*<sup>-/-</sup>/*Il1b*<sup>-/-</sup>) are more susceptible to *M. tuberculosis* infection and show higher bacterial burdens in the lung compared to mice lacking the individual cytokines <sup>31,52,65</sup>. The protective function of IL-1 is further confirmed by blocking receptor signaling with anti-IL-1R antibodies or in an *Il1r*<sup>-/-</sup> mouse model; the mice become highly susceptible to *M. tuberculosis* infection and show increased bacterial burden in the lungs <sup>31,32,63,64,66</sup>. Interestingly, loss of IL-1 signaling does not result in diminished TNF- $\alpha$ , IL1-2p40, inducible nitric oxide synthase (iNOS), or IFN- $\gamma$  responses <sup>31</sup>. In other bacterial infections, the protective function of IL-1 is often ascribed to recruitment of neutrophils; however, neutrophils are not known to be protective in the context of tuberculosis, and it remains unclear why IL-1 signaling is critical for resistance. IL-1R signaling in *trans* by infected bystander cells is sufficient to induce restriction of intracellular bacterial growth in infected myeloid cells that lack IL-1R <sup>67</sup>, suggesting that IL-1 promotes production of a soluble protective factor. Finally, a protective role of IL-1 during human tuberculosis infection has been suggested based on case studies in which rheumatoid arthritis patients treated with IL-1R antagonist anakinra occasionally showed reactivation of tuberculosis <sup>68,69</sup>.

IL-1 $\beta$  is produced as a precursor protein and is cleaved into a mature form by inflammasome and caspase-1 activation and then released to act systemically. Unlike the case of IL-1 $\beta$ , IL-1 $\alpha$



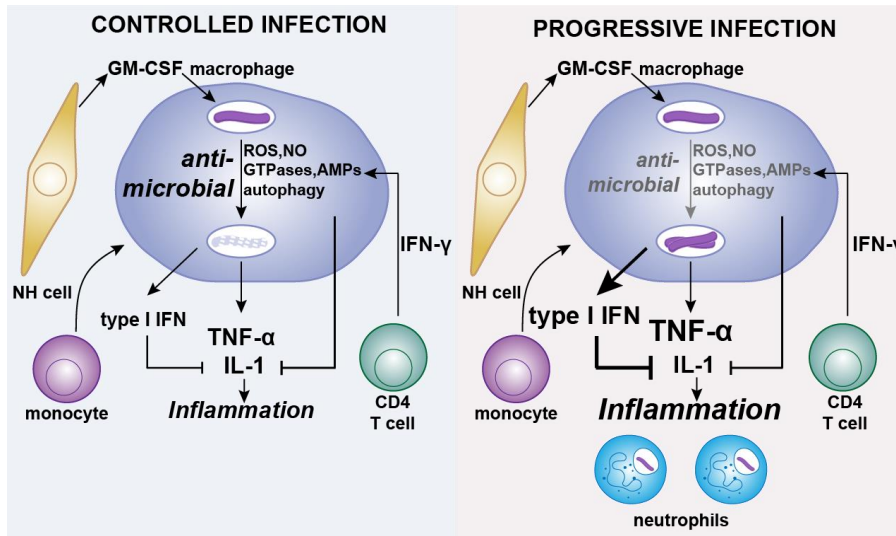


**Figure 1.2 A combination of antimicrobial function and regulation of inflammation is required for successful control of *M. tuberculosis* infection.**

Successful control of *M. tuberculosis* infection is associated with robust macrophage-based control of bacterial replication by antimicrobial mechanisms. Mechanisms that have been proposed to contribute to cell-intrinsic control of infection include autophagy, interferon-inducible GTPases, ROS, NO, and antimicrobial peptides. Cytokines such as GM-CSF produced by nonhematopoietic cells and IFN- $\gamma$  produced by CD4 T cells promote the microbicidal functions of macrophages. In controlled infection, there is appropriate production of inflammatory cytokines including TNF- $\alpha$  and IL-1; type I interferon, which blocks IL-1 function, is produced at low levels. Indeed, some of the susceptibility of mice lacking factors formerly assumed to be directly antimicrobial may be attributed to inflammatory imbalances. In contrast, uncontrolled infection may result from either a failure of antimicrobial control or imbalanced cytokine production. If antimicrobial mechanisms fail, the increased bacterial burden can drive the excessive production of inflammatory cytokines, leading to the recruitment of neutrophils that contribute to excessive inflammation. Alternatively, increased type I interferon production can functionally block IL-1 signaling, leading to immune failure. In most cases in mice, susceptible strains can be rescued by depletion of neutrophils, suggesting that in the mouse model diverse failures of immunity converge on a single neutrophil-driven mechanism of mortality. Abbreviations: AMP, antimicrobial peptide; GM-CSF, granulocyte-macrophage colony-stimulating factor; NH, nonhematopoietic; NO, nitric oxide; ROS, reactive oxygen species.

activity does not require proteolytic processing by caspase-1. The main inflammasome that becomes activated upon *in vitro* infection with *M. tuberculosis* appears to be NLRP3. This requires the ESX-1 secretion system<sup>70-74</sup>, although the exact mechanism remains controversial. Despite detection of *M. tuberculosis* by the inflammasome, *Nlrp3*<sup>-/-</sup>, *Asc*<sup>-/-</sup>, and *Casp1*<sup>-/-</sup> mice are not nearly as susceptible to infection as mice deficient in IL-1 $\alpha$  and/or IL-1 $\beta$  or IL-1R<sup>66,73,75-78</sup>. Furthermore, IL-1 $\beta$  production is still present in *Nlrp3*<sup>-/-</sup> or *Casp1*<sup>-/-</sup> mice<sup>66,73</sup>, indicating that pro-IL-1 $\beta$  can be processed and released through an inflammasome-independent mechanism<sup>79-82</sup>. An excess of IL-1 has been linked to an increased influx of neutrophils and lung inflammation, which result in high bacterial burden and mortality<sup>83</sup> (Figure 1.2). However, IL-1 $\alpha$  and IL-1 $\beta$  regulation is complex, and postsecretion, their activity is controlled further by the presence of IL-1R antagonist (IL-1Ra), complicating the interpretation of IL-1 protein levels. For example, *Sst1*<sup>S</sup> mice, which are highly susceptible to *M. tuberculosis* infection, have elevated levels of IL-1 protein in the lungs during infection. However, they also have high levels of IL-1Ra, which limit IL-1 activity, causing a functional deficiency in IL-1 signaling and increased *M. tuberculosis* susceptibility<sup>32</sup>.

**1.3.4 Type I interferons.** Type I interferons comprise a family of cytokines that signal through the interferon receptor to induce interferon-stimulated genes. Most cell types produce type I interferon upon stimulation of cytosolic DNA or RNA sensors that normally sense cytosolic viruses or through signaling via specific TLRs. In the case of *M. tuberculosis* infection, type I interferon is induced when the ESX-1 secretion system perforates the vacuolar membrane, leading to activation of the cGAS/STING pathway<sup>29,33,84</sup>. Although type I interferon is critical for resistance to viral infections, the effect of type I interferon during *M. tuberculosis* infection is primarily detrimental. Tuberculosis patients with active disease show a distinct upregulation of type I interferon-inducible transcripts in blood neutrophils and monocytes. This gene expression profile correlates with disease severity and may predict the transition from active to latent disease<sup>85-90</sup>. In mice, type I interferon is detrimental to *M. tuberculosis* infection; however, the severity of the phenotype appears to be background dependent. In C57BL/6 wild type mice, loss of the type I IFN receptor or other signaling components results in only modest enhancement of control of infection<sup>29,32,91-94</sup>. However, if these mice are stimulated to produce higher levels of type I interferon than are naturally produced during *M. tuberculosis* infection by administration of intranasal TLR3 ligand poly-ICLC, increased lung pathology and mortality during *M. tuberculosis* infection is observed, demonstrating that increasing type I interferon levels in the C57BL/6 background results in highly impaired immunity<sup>95</sup>. Furthermore, the susceptibility of B6.*Sst1*<sup>S</sup> congenic mice that carry the tuberculosis susceptibility allele of the *Sst1* locus derived from the highly susceptible C3H/HeBFeJ strain was recently shown to be primarily driven by type I interferon, as crossing these mice with *Ifnar*<sup>-/-</sup> mice alleviated the exacerbated disease<sup>32</sup>. Type I interferons inhibit IL-1 signaling indirectly through strong upregulation of IL-1Ra expression during *M. tuberculosis* infection<sup>32</sup>. Blocking IL-1Ra in B6.*Sst1*<sup>S</sup> mice restores IL-1 protective signaling and rescues the type I interferon-induced susceptibility to infection, suggesting that the type I interferon-based susceptibility observed in these mice is almost entirely explained by inhibition of IL-1 signaling<sup>32</sup>. Although several mechanisms by which type I interferons inhibit host defenses have been proposed, including modulating eicosanoids, iNOS production, and IL-10<sup>31,32,96-98</sup>, it is likely that the primary impact of type I interferon on *M. tuberculosis* immunity is to impair the production of IL-1, which is critical for protection against infection. Despite deleterious effects of high levels of type I interferon on the host immune response, it is possible that type I interferon is protective in some contexts, particularly in the absence of IFN- $\gamma$ . The balance of deleterious and protective responses of type I interferon is further reviewed by Moreira-Teixeira et al.<sup>99</sup>.

**1.3.5 IL-10.** IL-10 is an anti-inflammatory cytokine that downregulates both innate and adaptive immune responses. Pulmonary tuberculosis patients have elevated levels of plasma IL-10, and their T cells exhibit both enhanced *Il10* expression and evidence of IL-10 stimulation<sup>100,101</sup>. Studies of the role of IL-10 in mice have yielded mixed results, likely reflecting the complex role of IL-10 and other immunosuppressive cytokines in infection. One study showed that *Il10*<sup>-/-</sup> C57BL/6 mice experience a significant increase in bacterial numbers in the lungs and increased mortality starting late in infection<sup>102</sup>, while another study found that *Il10*<sup>-/-</sup> mice on the C57BL/6 and BALB/C backgrounds have reduced bacterial burdens in the lungs during the late stage of infection<sup>103</sup>. CBA/J mice, which are highly susceptible to *M. tuberculosis*, are clearly impacted by IL-10 deficiency, as *Il10*<sup>-/-</sup> mice on this background exhibit lower bacterial numbers in the lungs and spleen throughout the course of infection when compared with wild-type<sup>104</sup>. Furthermore, treatment of CBA/J mice with an anti-IL-10R blocking antibody during the chronic

stage of *M. tuberculosis* infection lowers bacterial numbers in the lungs and improves survival compared to untreated CBA/J mice<sup>105</sup>. The seemingly contradictory results in the mouse model likely reflect the fact that IL-10 has a context-dependent role in infection; while it can contribute to restraining detrimental inflammation in the context of a potential hyperinflammatory response (such as CBA/J mice), it can also harm the host by suppressing effective responses.

**1.3.6 TGF- $\beta$ .** Transforming growth factor  $\beta$  (TGF- $\beta$ ) is an immunosuppressive cytokine that plays a crucial role in immune homeostasis and peripheral tolerance. TGF- $\beta$  is known to have a suppressive effect on cells that play a key role in regulating *M. tuberculosis* infection, including macrophages, dendritic cells, neutrophils, and T cells (reviewed in<sup>106</sup>. High levels of TGF- $\beta$  are found in the lungs of patients with active pulmonary tuberculosis<sup>107,108</sup> and serum levels of TGF- $\beta$  correlate with disease severity<sup>109</sup>. Similarly, high TGF- $\beta$  levels are associated with active diseases in murine and in non-human primate models, where successful antibiotic therapy is results in diminished TGF- $\beta$  levels<sup>110,111</sup>. Although production of TGF- $\beta$  is crucial to prevent hyper-inflammation and autoimmunity<sup>106</sup>, several lines of evidence suggest that TGF- $\beta$  may suppress effective immune responses to *M. tuberculosis* to the detriment of the host. In mice, blocking TGF- $\beta$  signaling using neutralizing antibody, recombinant TGF- $\beta$  receptor, or small molecule inhibitors results in increased control of disease as measured by bacterial burden in the lungs<sup>112,113</sup>. A recent study suggests that the specific mechanism by which TGF- $\beta$  suppresses host immunity is by preventing CD4 T cells from producing IFN- $\gamma$  in granuloma cores, thereby limiting effective macrophage activation<sup>114</sup>. Thus, pharmacological inhibition of TGF- $\beta$  may be an attractive strategy for managing patients with active TB disease.

#### **1.4 Macrophage-based mechanisms of innate control.**

Macrophages are programmed to detect invading pathogens, activate microbicidal mechanisms, and coordinate the subsequent immune response. However, in the absence of adaptive immunity, macrophages are not capable of controlling *M. tuberculosis* infection. Although for many years it was speculated that *M. tuberculosis* resisters (individuals whose purified protein derivative (PPD) and IFN- $\gamma$  release assay (IGRA) results never convert despite considerable exposure to *M. tuberculosis*) were able to clear infection via innate immunity, deeper immunological analysis of these individuals revealed the existence of class-switched antibodies, solid evidence of an adaptive response to infection<sup>115</sup>. Indeed, in both mouse and nonhuman primate models, growth of *M. tuberculosis* is unrestricted in macrophages until the arrival of CD4 T cells in the lungs<sup>116,117</sup>. The primary role of CD4 T cells in macrophage activation is understood to be the production of IFN- $\gamma$ , which can directly activate macrophages to control infection<sup>7</sup>. In addition, there appear to be IFN- $\gamma$ -independent mechanisms that have yet to be identified<sup>118</sup>. Although several decades of research have focused on understanding the cell-intrinsic mechanisms of bacterial killing downstream of macrophage activation, recent revisions in our understanding of the functions of antimicrobial responses have left holes in our knowledge of effectors that have direct antimicrobial activity (Figure 1.2).

**1.4.1 Autophagy.** Autophagy (self-eating) is a conserved cellular process with important roles in homeostasis, development, and metabolism. In addition, it is well-established that a form of selective autophagy known as xenophagy is a major contributor to innate immune defense against microbial infections (reviewed in<sup>119</sup>. The first evidence for an antimycobacterial effect of autophagy was the observation that starvation or rapamycin treatment leads to restriction of *M.*

*tuberculosis* growth in RAW macrophages<sup>120</sup>. Subsequently it was found that autophagic targeting of *M. tuberculosis* occurs as a response to perforation of the phagosome by the bacterial ESX-1 secretion system and stimulation of cGAS-STING<sup>34,35,37,84</sup>. TBK1 activation downstream of STING leads to ubiquitin-mediated autophagic targeting of the *M. tuberculosis*-containing phagosome. The E3 ubiquitin ligases Parkin and Smurf promote autophagic targeting of *M. tuberculosis*, and mice deficient in these factors are susceptible to *M. tuberculosis*<sup>121,122</sup>. In addition, *Atg5<sup>fl/fl</sup>Lyz2Cre* mice, which lack the core autophagy effector ATG5 in myeloid cells, are hypersusceptible to *M. tuberculosis*<sup>84,123</sup>. However, subsequent detailed analyses of autophagy-deficient mice have shown the role of autophagy to be complex. While *Atg5<sup>fl/fl</sup>Lyz2Cre* mice succumb rapidly to *M. tuberculosis*, mice deficient in other core autophagy effectors have no significant weight loss or inability to restrict bacterial replication through several months of infection<sup>124</sup>. The susceptibility of *Atg5<sup>fl/fl</sup>Lyz2Cre* mice is rescued by depletion of neutrophils, and much of the susceptibility is recapitulated in *Atg5<sup>fl/fl</sup>Mrp8Cre* mice, which lack ATG5 specifically in neutrophils<sup>124</sup>. This suggests there is a unique role for ATG5 in the regulation of inflammation and neutrophil recruitment, discrete from its role in autophagic targeting of bacteria. Taken together, these findings provide significant evidence that autophagy plays a role in *M. tuberculosis* infection but not all effects are intrinsic to the macrophage.

**1.4.2 Vitamin D and cathelicidin.** Vitamin D has been used to treat tuberculosis since the mid-1800s. Multiple cohort studies show an association between low serum vitamin D levels and tuberculosis disease risk<sup>125,126</sup>. However, clinical trials have not clearly demonstrated that vitamin D treatment of tuberculosis patients already receiving antibiotics improves outcomes<sup>127,128</sup>. In vitro treatment of *M. tuberculosis*-infected cells with vitamin D restricts growth of the bacteria, indicating that vitamin D leads to cell-intrinsic control of *M. tuberculosis*<sup>129,130</sup>. A major effect of vitamin D treatment in *M. tuberculosis*-infected human monocytes is expression of the cathelicidin antimicrobial peptide LL-37<sup>129,131</sup>. LL-37 has antibacterial activity against *M. tuberculosis* in liquid culture<sup>132</sup>, and administration of LL-37 to *M. tuberculosis*-infected mice starting 60 days postinfection significantly reduced the bacterial load in the lungs<sup>132</sup>. *Cramp<sup>-/-</sup>* mice, which lack the gene for murine cathelicidin, have enhanced mortality and a defect in controlling bacterial growth after *M. tuberculosis* infection compared to wild-type mice<sup>133</sup>. Importantly, in other studies researchers have observed no effect of exogenous vitamin D on *M. tuberculosis* growth in human monocytes<sup>134,135</sup>. Thus, although low vitamin D levels may correlate with tuberculosis disease, whether the main function of vitamin D is to activate microbicidal mechanisms remains unclear.

**1.4.3 Reactive oxygen species.** The production of reactive oxygen species (ROS) is a crucial defense against phagocytosed pathogens. The production of ROS is initiated by the NADPH oxidase complex, which catalyzes the production of superoxide. Through a series of reactions, multiple other ROSs are then produced, including hydrogen peroxide, hypochlorous acid, and hydroxyl radicals. Data suggest that NADPH oxidase is required for control of tuberculosis in humans. Patients with chronic granulomatous disease (CGD), who have inherited defects in NADPH oxidase, have presented with active tuberculosis or disseminated bacillus Calmete-Guérin (BCG) disease upon vaccination<sup>136</sup>. Macrophages isolated from a CGD patient were unable to control growth of *M. tuberculosis*, suggesting that ROSs are important for cell-intrinsic control of *M. tuberculosis* infection in humans<sup>137</sup>. However, studies on the role of ROSs in control of *M. tuberculosis* in the mouse model are inconclusive. Mice lacking components of

NADPH oxidase display no increase in bacterial burden in the lungs or, at most, a mild and transient increase<sup>138,139</sup>. A recent study in the mouse model revealed a potential immunoregulatory role for ROSs, independent of bactericidal potential. While *Cybb*<sup>-/-</sup> mice, which lack the NADPH oxidase component gp91, are able to control *M. tuberculosis* growth similar to wild-type mice, they experience greater weight loss and have a significant increase in mortality associated with excessive neutrophil recruitment<sup>139</sup>. Blocking IL-1 signaling in *Cybb*<sup>-/-</sup> mice reduces neutrophil infiltration and rescues susceptibility, demonstrating that ROSs may limit harmful inflammation<sup>139</sup>.

**1.4.4 iNOS.** The importance of IFN- $\gamma$  during *M. tuberculosis* infection has been attributed to its ability to activate microbicidal mechanisms of macrophages, most importantly expression of the enzyme iNOS, encoded by the gene *Nos2*<sup>140</sup>. iNOS catalyzes the production of the bactericidal/static radical nitric oxide (NO). Human tuberculosis patients exhibit iNOS expression in the lungs and are known to exhale NO, confirming that this molecule is produced during human *M. tuberculosis* infection<sup>141-143</sup>. The importance of NO for control of *M. tuberculosis* infection is clear, as *Nos2*<sup>-/-</sup> mice are extremely susceptible to infection<sup>144</sup>. However, studies of mixed bone marrow chimeras that examined different genotypes in the same inflammatory environment have demonstrated no difference in *M. tuberculosis* burden in wild-type and *Nos2*<sup>-/-</sup> cells, raising the possibility that NO does not function in a cell intrinsic manner for control of bacterial numbers. Indeed, it has been proposed that NO limits IL-1 $\beta$  production by two mechanisms. First, by nitrosylation and inhibition of the NLRP3 inflammasome, NO may limit neutrophil recruitment and subsequent destruction of host tissue<sup>83,145</sup>. Depleting neutrophils in *Nos2*<sup>-/-</sup> mice rescues the increase in bacterial burden in the lungs at 24 days after infection<sup>83</sup>. Second, NO may also limit IL-1 $\beta$  transcription by inhibiting NF- $\kappa$ B signaling<sup>146</sup>. However, the facts that the ability to resist NO is an important virulence trait for *M. tuberculosis*<sup>147</sup> and that iNOS-deficient macrophages suffer from increased bacterial burdens in vitro make it clear that NO can impact cell-intrinsic antimicrobial activity of macrophages, independent of the inflammatory context. Thus, a role for NO in cell-intrinsic control of infection in vivo cannot be ruled out, and there is likely more to learn about the contribution of NO to control of infection in vivo.

**1.4.5 Interferon-inducible GTPases.** Interferon-inducible GTPases are a family of proteins that encompass myxovirus resistance proteins (Mxs), guanylate-binding proteins (GBPs), immunity-related guanosine triphosphatases (IRGs), and very large inducible GTPase proteins (VLIGs). Both GBPs and IRGs are IFN- $\gamma$ -inducible proteins that have been implicated in mycobacterial infections. Almost a decade ago, it was demonstrated that Gbp1 is required for control of *Mycobacterium bovis* BCG infection in vivo<sup>148</sup>. However, mice with a chromosomal deletion that removes six GBPs, including GBP1, are only mildly susceptible to *M. tuberculosis*, with a modest increase in bacterial burden emerging at 100 days after infection<sup>149</sup>. A gene expression signature associated with the transition from latent to active disease contains *GBP1*, providing some relevance to human disease<sup>90,150</sup>. Although the IRG family member *Irgm1* was shown to mediate host resistance to *M. tuberculosis* in mice<sup>151</sup>, the significance of this finding is difficult to interpret in light of the emerging understanding that these knockout mice exhibit baseline alterations in immunity<sup>152</sup>. Nonetheless, results from human studies suggest a role for IRGM1 in resistance to *M. tuberculosis* (reviewed in<sup>153</sup>). Therefore, more research is needed into a potential role for these proteins in antituberculosis immunity.

**1.4.6 Aerobic glycolysis and metabolic regulation of infection.** The metabolic program of aerobic glycolysis is associated with differentiation of macrophages into the M1 phenotype. It is now understood that changes in levels of metabolites during aerobic glycolysis impact specific programs of gene expression and cellular differentiation. *M. tuberculosis*-infected macrophages transition to aerobic glycolysis, and this transition is required for effective control of bacterial growth<sup>154,155</sup>. During *M. tuberculosis* infection, aerobic glycolysis impacts gene expression by promoting the activity of the transcription factor hypoxia-inducible factor 1 $\alpha$  (HIF-1 $\alpha$ )<sup>156</sup>. HIF-1 $\alpha$  is a crucial mediator of IFN- $\gamma$ -dependent immunity required for host defense against *M. tuberculosis* and is essential for expression of inflammatory cytokines, production of host-protective eicosanoids, and cell-intrinsic control of bacterial replication<sup>155</sup>. How HIF-1 $\alpha$  and/or aerobic glycolysis promote cell-intrinsic control of infection is yet unknown.

**1.5 Cell death and eicosanoids.** There are multiple mechanisms by which the host cell can undergo cell death during *M. tuberculosis* infection, and the field has coalesced around a paradigm in which apoptotic death benefits the host whereas necrotic death benefits the bacterium. However, this paradigm is based largely on in vitro experiments and is difficult to establish conclusively, as there is no experimental means to selectively eliminate either form of death in vivo without also affecting other parameters of the immune response. In general, several attenuated strains and mutants of *M. tuberculosis* have been found to induce apoptotic cell death in macrophages<sup>157–159</sup>. Apoptotic cells can be phagocytosed by DCs and subsequently stimulate T cell priming and activation<sup>160–164</sup>. Efferocytosis of apoptotic cells by uninfected macrophages is thought to result in killing of bacteria through fusion of the efferocytic phagosome with lysosomes, and macrophage apoptosis is therefore considered beneficial for host survival<sup>164,165</sup>. In contrast, macrophages infected with virulent *M. tuberculosis* undergo necrosis<sup>159,166</sup>. Recent findings with a zebrafish model of *Mycobacterium marinum* infection showed that excess TNF- $\alpha$  can induce necrosis through interaction of multiple signaling pathways, including activation of RIP kinases, production of mitochondrial ROSs, and subsequent activation of cyclophilin D<sup>53</sup>. TNF- $\alpha$  was also implicated in apoptosis induced by eicosanoid synthesis<sup>167</sup>. Production of the eicosanoid PGE<sub>2</sub> promotes apoptosis in macrophages infected with avirulent *M. tuberculosis*<sup>168</sup>. In contrast, PGE<sub>2</sub> production is inhibited by LXA<sub>4</sub>, which is induced during infection with virulent strains and leads to necrosis. Mice lacking prostaglandin E synthase (*Ptges*<sup>-/-</sup>) show a higher bacterial burden in the lungs, whereas *Alox5*<sup>-/-</sup> mice, which are unable to synthesize certain eicosanoids (including LXA<sub>4</sub> and LTB<sub>4</sub>), are more resistant to *M. tuberculosis* infection<sup>166</sup>. This suggests that PGE<sub>2</sub> has a protective effect against virulent *M. tuberculosis*. However, whether this effect is mediated through regulation of cell death or regulation of inflammation is unclear. PGE<sub>2</sub> has both pro- and anti-inflammatory functions, including the regulation of cytokine expression in DCs and T cell differentiation<sup>169</sup>. In addition, lipoxins have been described as negative regulators of acute inflammatory processes and together with PGE<sub>2</sub> regulate neutrophil recruitment<sup>145,170</sup>. Interestingly, polymorphisms in the promoter region of leukotriene A4 hydrolase (*lta4h*), which catalyzes the production of eicosanoid LTB<sub>4</sub>, have been associated with mortality and response to anti-inflammatory treatment in patients with tuberculosis meningitis, further supporting the notion that eicosanoids are important for regulating inflammatory processes<sup>171,172</sup>.

## 1.6 Other innate cells

**1.6.1 Neutrophils in host defense.** Polymorphonuclear neutrophils are short-lived cells of the innate immune response that are highly abundant during bacterial infections. Neutrophils possess a potent antimicrobial arsenal effective against many bacterial and fungal pathogens<sup>173</sup>. In the case of *M. tuberculosis*, while there is some evidence that neutrophils participate in protective immunity, a clear role in host defense has yet to be defined. In some settings, they may promote *M. tuberculosis* infection. Recruitment of neutrophils to the lung after *M. tuberculosis* infection is rapid and is mediated through multiple chemokines, including IL-17, CXCL5, and KC, and by eicosanoids produced by 12/15-lipoxygenase<sup>145,174,175</sup>. Neutrophils take up bacteria in vivo<sup>145,164,176</sup>. However, studies examining whether neutrophils are able to effectively kill phagocytosed *M. tuberculosis* are inconclusive and contradictory<sup>177</sup>, in part because of the difficulty of working with primary neutrophils ex vivo and the paucity of appropriate cell lines for neutrophil research. Studies of neutrophil function in vivo are also inconclusive. Neutrophils harboring bacteria may die by apoptosis, which is followed by efferocytosis by resident macrophages, possibly facilitating control of infection<sup>165</sup>. Alternatively, it has also been proposed that neutrophils are a permissive niche for growth and persistence in vivo<sup>178,179</sup>. Separate from their ability to kill bacteria, neutrophils may have an influence on priming of adaptive immunity. Depletion of neutrophils at early stages of infection in resistant mouse strains has yielded differing results, with some studies finding no impact and other studies finding that depletion of neutrophils compromises host defense<sup>176,180</sup>.

**1.6.2 Destructive inflammation mediated by neutrophils.** In human tuberculosis, neutrophils are generally associated with active disease, caseous necrosis, and exacerbated pathogenesis<sup>181</sup>, and neutrophils may be drivers of the pathology associated with active disease. Indeed, animal models established that excessive accumulation of neutrophils in the lungs drives destructive inflammation and susceptibility to infection. Furthermore, the phenotypes of many mice known to be susceptible to *M. tuberculosis* infection, including *Nos2*<sup>-/-</sup>, *Atg5*<sup>-/-</sup>, *Irg1*<sup>-/-</sup>, and *Card9*<sup>-/-</sup> mice, can be at least partially rescued by depletion of neutrophils<sup>124,145,182,183</sup>. These data suggest that defects in immunity resulting from disparate perturbations lead to a common pathway of neutrophil-driven susceptibility (Figure 2). However, many questions remain. First, it is unclear whether neutrophils are a common driver of susceptibility in humans. Second, the mechanisms by which neutrophils are recruited to excess under specific conditions, and how they drive destructive inflammation, are unclear. Finally, it is possible that neutrophils are in fact more heterogeneous in tuberculosis disease than is currently appreciated and that specific subsets of neutrophils participate in host defense, whereas others contribute to pathology.

**1.6.3 Alveolar macrophages and innate cells during early infection.** AMs are a subset of tissue-resident macrophages that reside within the lung airspace and play crucial roles in lung homeostasis, surfactant metabolism, and tissue repair<sup>184</sup>. AMs are the first cell type to encounter *M. tuberculosis*. Studies of human AM infections are difficult, as the AM phenotype is programmed and maintained in the tissue niche and is rapidly lost in cell culture<sup>185</sup>. In mice, a productive *M. tuberculosis* infection starts with infection of AMs that reside in the lung alveoli<sup>186,187</sup>. Depletion of AMs with liposome-encapsulated dichloromethylene diphosphonate prior to infection reduces the bacterial burden in the lungs and increases survival, suggesting that AMs form a replicative niche early after infection<sup>188,189</sup>. Indeed, infected AMs initially exhibit an anti-inflammatory NRF2-dependent antioxidant response<sup>187,189,190</sup>. Approximately 10 days after

infection is initiated, AMs exhibit a more proinflammatory transcriptional state that precedes their transition from the airway into the pulmonary interstitium at approximately 14 days postinfection<sup>186,187</sup>. AMs in the interstitium localize in infectious foci, a process that is mediated by IL-1R signaling in nonhematopoietic cells<sup>186</sup>. At two weeks, AMs appear to be the predominant infected cell type in the lung<sup>191,192</sup>. Shortly thereafter, however, *M. tuberculosis* disseminates to monocyte-derived cells and neutrophils<sup>189,193</sup>. Interstitial macrophages show a glycolytic transcriptional profile, express iNOS and IL-1, and restrict intracellular growth of *M. tuberculosis* more efficiently than AMs<sup>189</sup>. In addition, mycobacterial growth in the lungs appears to be sustained by a constant influx of new monocytes into the lungs<sup>194</sup>. Thus, although airway AMs are a more permissive niche for growth early after infection, *M. tuberculosis* replication in the lungs can be sustained through dynamic infection of new monocytes that provide *M. tuberculosis* with new cellular niches that become rapidly infected.

**1.6.4 Dendritic cells.** DCs bridge innate and adaptive immunity, traveling from sites of infection and inflammation to secondary lymphoid tissues for activation of T cells. Both classical/resident and monocyte-derived DCs are present in the lungs during *M. tuberculosis* infection<sup>195</sup>. Antibody-based depletion of CD11c<sup>+</sup> cells, which transiently eliminates both classical and monocyte-derived DCs, results in defective CD4 T cell priming and increased susceptibility to *M. tuberculosis* infection, demonstrating the importance of DCs for host defense<sup>196</sup>. Several studies using CCR2<sup>-/-</sup> mice have suggested that inflammatory monocytes, and not DCs, may be responsible for trafficking *M. tuberculosis* to the draining lymph nodes for activation of T cell responses<sup>197,198</sup>. However, a more recent study using diphtheria toxin to selectively ablate CCR2 at different stages of infection found that while interstitial macrophages traffic bacteria to the draining lymph nodes, classical DCs are largely responsible for priming CD4 T cell responses<sup>199</sup>. Human data have suggested that the onset of adaptive immunity to *M. tuberculosis* is significantly delayed<sup>200-202</sup>. Indeed, data from both mice and nonhuman primates have clearly demonstrated that the priming of T cells in draining lymph nodes is delayed during *M. tuberculosis* infection relative to other infections<sup>164,195,203-205</sup>, although limited antigen availability due to *M. tuberculosis* slow replication rate and low infectious dose may be a confounding factor. Importantly, experimental perturbations that result in more rapid priming of effector T cells, either through BCG vaccination, dendritic cell vaccination, or adoptive transfer, results in more effective control of *M. tuberculosis* infection<sup>206-208</sup>.

**1.6.5 Natural killer cells.** Natural killer (NK) cells are innate lymphocytes present in both lymphoid and nonlymphoid tissues that play a major role in defense against viral infection. In human tuberculosis, a reduction in the number of NK cells or in their expression of activation markers correlates with loss of control and the transition to active disease<sup>209,210</sup>. Furthermore, changes in peripheral blood NK cell levels correlate with disease progression and treatment response, and they inversely correlate with lung inflammation in tuberculosis patients across multiple independent cohorts<sup>210</sup>. However, whether these studies indicate a functional role for NK cells in the immune response is unclear. Although the exact ligands are unknown, NK cells are capable of detecting *M. tuberculosis*-infected macrophages through activating receptors (e.g., NKp46, NKG2D)<sup>211</sup>. Human and mouse NK cells produce perforin and granulysin, are capable of killing *M. tuberculosis*-infected cells through a contact-dependent mechanism<sup>212-214</sup>, and produce IFN- $\gamma$  during infection. *M. tuberculosis*-infected mice show an increase in NK cell numbers in the lungs within 21 days<sup>94,215</sup>. NK cell depletion does not result in an increase in bacterial growth in the lungs in C57BL/6 mice<sup>215</sup>, indicating that these cells are not critical for



restricting the bacterial burden. However, depletion of NK cells or IFN- $\gamma$  in RAG<sup>-/-</sup> mice further increases the susceptibility of these mice to *M. tuberculosis* infection<sup>216</sup>.

**1.6.6 Nonclassical T cells.** Nonclassical T cells, including mucosal-associated invariant T (MAIT) cells and  $\gamma\delta$  T cells, span innate and adaptive immunity. Their T cell receptor repertoire is highly limited, often recognizing PAMPs, and they participate in rapid innate-like effector responses. MAIT and  $\gamma\delta$  T cells have been frequently associated with tuberculosis; however, their role during infection remains unclear. MAIT cells are activated by intermediates of bacterial riboflavin biosynthesis that bind to the highly conserved major histocompatibility complex-related 1 (MR1) molecule<sup>217</sup>. Most bacterial species, including *M. tuberculosis*, synthesize riboflavin and therefore activate MAIT cells. Once activated, individual MAIT cell subsets can produce different combinations of inflammatory/T helper 1 (Th1) cytokines and can kill infected cells through the release of cytotoxic granules<sup>217</sup>. In nonhuman primates, tetramer-restricted MAIT cells accumulate in the airways but not inside granulomas and only show minimal expression of granzyme B or the proliferation marker Ki76, suggesting that MAIT cells are not essential contributors to *M. tuberculosis* restriction in macaques<sup>218,219</sup>. Mice lacking MR1 are susceptible to infection with BCG and *M. tuberculosis*<sup>220</sup>. BCG induces MAIT cell formation in BCG-vaccinated humans and nonhuman primates<sup>221,222</sup>. Furthermore, MAIT cells have activity against BCG-infected macrophages<sup>223</sup>. However, it is unclear whether induction of MAIT cells contributes to the efficacy of BCG and what role MAIT cells play in human *M. tuberculosis* infection.

$\gamma\delta$  T cells expand early during *M. tuberculosis* infection<sup>224,225</sup>. Furthermore, tuberculosis patients have a higher proportion of IL-17-producing  $\gamma\delta$  T cells compared to healthy controls<sup>226</sup>. Human  $\gamma\delta$  T cell clones derived from peripheral blood mononuclear cells respond to live *M. tuberculosis* and to *M. tuberculosis* lysate in vitro<sup>227</sup>. Both AMs and monocytes activate and induce expansion of  $\gamma\delta$  T cells<sup>228</sup>. Activated  $\gamma\delta$  T cells can produce IFN- $\gamma$  in response to *M. tuberculosis* and are cytotoxic to infected monocytes, macrophages, and extracellular bacteria due to release of perforin and granulysin<sup>229,230</sup>. C57BL/6 mice deficient for T cell receptor (TCR)  $\delta$  chain lack  $\gamma\delta$  T cells and show a transient higher bacterial burden early in infection compared to control mice. Interestingly, TcR- $\delta^{-/-}$  mice show control of low-dose infection at later time points but eventually succumb to high-dose infections<sup>231</sup>. The most abundant population of  $\gamma\delta$  T cells in humans are V $\gamma$ 9V $\delta$ 2 T cells that recognize HMBPP, an intermediate of the nonmevalonate pathway of isoprenoid biosynthesis<sup>232-234</sup>. V $\gamma$ 9V $\delta$ 2 T cells activated by BCG are able to protect against *M. tuberculosis* infection in a macaque model<sup>235</sup>. Furthermore, using *Listeria monocytogenes* as a vaccine platform to stimulate V $\gamma$ 9V $\delta$ 2 T cells effectively protects against *M. tuberculosis* infection in primates<sup>236</sup>, demonstrating the potential of  $\gamma\delta$  T cells for vaccine-elicited control of infection. However, whether they play an important role in containing natural human infection remains unclear.

## 1.7 Harnessing the innate immune response.

**1.7.1 Innate immunity and adjuvant development for protein subunit vaccines.** One of the most important practical applications of understanding innate immunity to *M. tuberculosis* is the rational design of novel vaccines. The current vaccine strain BCG is widely administered due to its efficacy in preventing severe manifestations of childhood tuberculosis; however, it has limited efficacy against adult pulmonary tuberculosis. Recently, the M72/AS01<sub>E</sub> protein subunit vaccine demonstrated 50% efficacy in preventing reactivation disease in previously BCG-vaccinated

adults, providing some of the first concrete evidence that vaccines other than BCG can enhance naturally acquired immunity to tuberculosis<sup>237</sup>. Formulating novel vaccines with optimized adjuvant and antigen combinations could improve upon this efficacy, raising the exciting possibility of a truly effective vaccine for tuberculosis. Recent years have witnessed a major leap forward in the development of novel adjuvant systems, including alum and emulsions, TLR agonists, STING agonists, and several lipids derived from *M. tuberculosis*<sup>238,239</sup>. Although these adjuvants all elicit inflammatory responses, the balance of specific cytokines produced can be adjuvant specific, suggesting that adjuvant selection may be important for fine-tuning the innate, and therefore adaptive, response to vaccination. In the context of *M. tuberculosis*, adjuvants under development that have shown efficacy in preclinical animal studies include agonists of TLR2, TLR3, TLR4, TLR7/8, Mincle, and the inflammasome (reviewed in<sup>238</sup>). Thus far, the development of vaccines and selection of specific adjuvants have been largely empirical, due to the lack of immune correlates of protection to guide tuberculosis vaccine design. However, several key lessons have emerged from vaccine development. First, whereas traditional vaccination strategies have sought to maximize the development of IFN- $\gamma$ -producing Th1 and polyfunctional T cells, it is now appreciated that excessive Th1 development may inhibit the development of other (as yet unidentified) protective T cell subsets<sup>240,241</sup>. Furthermore, mucosal delivery of vaccines for tuberculosis can promote enhanced protective immunity relative to parenteral immunization, promoting the development of antigen-specific Th17 cells<sup>242,243</sup>. Therefore, it is crucial that adjuvants for tuberculosis vaccines be selected not purely for their ability to elicit strong inflammatory responses but also for their capacity to elicit balanced Th1/Th17 immunity and for mucosal efficacy. Finally, because the effect of adjuvants can differ based on genetic and epigenetic factors, care must be taken in the selection of the appropriate adjuvant for tuberculosis vaccination in the target population (e.g., infant versus adult)<sup>239</sup>.

**1.7.2 Trained immunity.** Soon after the introduction of the BCG vaccine in Europe in the early twentieth century, it was noted that BCG reduces childhood mortality in a manner that could not be explained by a reduction in tuberculosis incidence. Subsequent studies have confirmed this phenomenon and have attributed the efficacy to a reduction in mortality from childhood respiratory diseases (reviewed in<sup>244</sup>). The ability of BCG to protect against nonmycobacterial infections is attributed to trained immunity—the long-term functional reprogramming of innate immune cells resulting in enhanced responses to other pathogens. BCG vaccination protects mice from viral infections including influenza and herpes simplex virus 2 via nonspecific trained immunity<sup>245,246</sup>. Intriguingly, the observation that coronavirus disease 2019 (COVID-19) cases and fatalities are fewer in regions of the world with universal BCG vaccination has prompted speculation that BCG vaccination may be protective against COVID-19<sup>247</sup>. However, this has not been established through rigorous clinical trials. Intravenously injected BCG elicits an expansion and reprogramming of hematopoietic stem cells in the bone marrow that promote the production of macrophages primed to respond to *M. tuberculosis* infection. This trained immunity is induced via epigenetic changes that result in enhanced responsiveness of innate immunity genes in macrophages and other innate cells. In the mouse model this results in a modest reduction in bacterial titers after infection with *M. tuberculosis* of ~0.5–1 log—comparable to standard vaccination with BCG<sup>248</sup>. BCG infection of bone marrow results in changes that persist for many weeks after eradication of BCG using antibiotics. However, as the timing of infection in the mouse model is necessarily compressed due to a short life span, it is unclear how long-lived trained immunity can be in humans. Importantly, intravenous BCG results in almost complete protection against *M. tuberculosis* infection in macaques<sup>249,250</sup>;

however, there is no evidence of a contribution of trained immunity to this remarkable protective efficacy<sup>249</sup>. Although early exposure to *M. tuberculosis* in humans induced a protective state in circulating monocytes that limited *M. tuberculosis* outgrowth, this effect was modest in BCG-vaccinated individuals<sup>251</sup>. Although it is unclear whether innate immunity alone, even when trained, can ever completely protect against *M. tuberculosis* infection, future vaccination strategies should consider eliciting trained immunity as a contributor to other mechanisms.

### **1.8 Conclusions and perspectives.**

The original view of innate immunity to tuberculosis primarily focused on resistance—the ability of the cells and cytokines of the immune system to prevent infection or eliminate infectious microbes. Thus, much of the first few decades of tuberculosis research focused on identifying mechanisms by which activated macrophages kill or prevent the proliferation of *M. tuberculosis* bacilli in a cell-intrinsic manner and inflammatory cytokines that are important for control of disease. However, there are still major gaps in our understanding of resistance mechanisms. It remains unclear exactly how macrophages control infection with *M. tuberculosis* at the cell-intrinsic level. Furthermore, we lack an understanding of how cytokines like IL-1 contribute to control of infection. The roles of many innate cells, including NK cells and nonclassical T cells, remain enigmatic. The idea that tolerance—limiting the collateral damage caused by the immune response to infection—determines the outcome of infection has more recently become a major focus of research. In the mouse model of infection, it appears that disturbing tolerance may be a major pathway to host susceptibility. This corresponds with our understanding that death from human tuberculosis results from inflammatory destruction of host lung tissue. However, in most susceptible strains of mice rescued by neutrophil depletion, there is an increase in bacterial burden in the lungs, leaving open the question of whether a failure of resistance drives the excessive inflammation that results in death. Furthermore, simply suppressing the immune response using nonspecific anti-inflammatory drugs does not clearly benefit patients with active pulmonary tuberculosis<sup>252</sup>. Human tuberculosis is a remarkably heterogeneous disease, both during different stages of disease within an individual patient and from patient to patient. The design of novel therapeutics that modulate inflammation appropriately for individual patients, or that enhance resistance mechanisms, will require a deeper understanding of the innate pathways that contribute to progression of disease.

## **Chapter 2**

**Variation in immune responses and tuberculosis susceptibility in a novel cohort of genetically diverse mice.**

## 2.1 Summary of results.

The majority of individuals infected with *M. tuberculosis* never develop active disease, yet the immune responses that contribute to successful control of *M. tuberculosis* infections are only partially understood. Mechanisms underlying susceptibility to infection have been studied in a handful of different mouse strains, limiting our understanding of the heterogeneity of disease. In order to identify novel antimicrobial responses that confer resistance or susceptibility to infection, a cohort of 17 wild-derived mouse lines with natural genetic diversity were infected with *M. tuberculosis* and assessed for their capacity to control infection. The median bacterial burden varied over 100-fold between different mouse lines with several lines showing increased susceptibility to infection and others that controlled the infection equally well as B6 mice. This strongly suggests that genetic heterogeneity within the closely related lines can influence the outcome of infection. Furthermore, the underlying immune responses in these mice are diverse, with larger proportions of T cells and B cells that correlated with a lower bacterial burden in the lung. In contrast, influx of neutrophils in the lung correlates with increased susceptibility to infection as has been shown previously for other susceptible mouse lines. Indeed, a susceptible mouse line from Manaus, Brazil (MAN) also shows high neutrophilic influx in the lungs revealing a connection between neutrophil numbers and bacterial burden in this line. Depletion of these neutrophils during infection reduces the bacterial burden, indicating that the increased numbers of these cells are detrimental for the host. Furthermore, cytokine expression analysis in the lungs show slightly enhanced expression of the gene product *Il1rn* in these susceptible mice, suggesting that blocking IL-1 signaling by enhanced *Il1rn* expression could be the driver of susceptibility in these mice. The SARA mouse line also deviates from the classical immunological responses studied in B6 mice that are known to be required for control of infection. The SARA line is resistant to *M. tuberculosis* infection and shows a low number of total CD4<sup>+</sup>IFN- $\gamma$ <sup>+</sup> T cells getting recruited to the lung compared to B6 mice. However, the number of CD4<sup>+</sup>IFN- $\gamma$ <sup>+</sup> T cells inside the *M. tuberculosis* lesions is similar between both mouse lines, suggesting that the T cells from SARA mice are efficient in accessing the lesion. Overall, the data shows that the wild-derived mouse cohort show a wide variety of responses to infection that are distinct from the responses required for control of infection in B6 mice.

**2.2 Introduction.** *Mycobacterium tuberculosis* infection causes a wide range of disease outcomes in humans. Whereas the majority of infected individuals never develop active disease and are able to control infection for their lifetimes, some individuals are highly susceptible to infection and develop active tuberculosis. Patients with active disease show heterogeneity in disease progression. Additionally, the timing of disease onset after initial infection and disease outcome varies from individual to individual<sup>253</sup>. This heterogeneity in human responses suggests that tuberculosis (TB) is a complex genetic disease. Surprisingly, there is only a limited understanding of the genetic factors that contribute to disease progression or control of infection. Indeed, GWAS studies have identified a small number of genetic factors that underlie the variability of responses to *M. tuberculosis* in humans including interferon- $\gamma$  (*IFNG*), interferon- $\gamma$  receptor (*IFNGR1*), interleukin-12 subunit p40 (*IL12B*) and interleukin-12 receptor b-1 chain (*IL12RB1*)<sup>254</sup>. However, many questions remain regarding what factors determine susceptibility to infection.

The murine model of TB infection is a useful tool for analysis of host immune responses to infection, due to the abundance of available reagents, ability to precisely control experimental conditions, and ease of genetic manipulation. Importantly, the mouse model recapitulates much of what is known about human immune responses to *M. tuberculosis*, including the importance of CD4 T cells and IFN- $\gamma$  for control of infection<sup>7,255–258</sup>. However, current mouse models fail to recapitulate several aspects of *M. tuberculosis* infection in humans, including spontaneous resolution of infection as well as the widely varying susceptibility and patterns of disease seen in humans. Although there are minor differences in susceptibility to infection, the majority of commonly used mouse strains all exhibit similar infection dynamics and characteristics. Despite the limited diversity of common laboratory strains, comparison of divergent phenotypes in these strains followed by genetic mapping has identified loci that contribute to susceptibility to mycobacterial infection, including *sst1*<sup>259,260</sup>. The *Sst1* locus regulates type I IFN signaling through a loss of function mutation of the gene *Sp140*, a repressor of type I IFN<sup>32,261</sup>. Excessive expression of type I IFN in *Sst1* susceptible mice elicits increased IL-1 receptor antagonist (IL-1Ra) expression which competes with IL-1 for binding to the IL-1R. IL-1 is crucial for control of infection and the functional deficiency in IL-1 signaling in *Sst1<sup>s</sup>* mice results in increased susceptibility to *M. tuberculosis*<sup>32,262</sup>. These studies suggest that increased genetic diversity in mouse models will lead to the discovery of additional genetic loci that are important for modulating the outcome of *M. tuberculosis* infection.

Historically, the vast majority of *M. tuberculosis* infectious studies in the mouse model have been conducted using only a handful of strains; C57BL/6 (B6), BALB/C and C3Heb/FeJ. In order to increase genetic diversity, new collections of mice have been established. The Collaborative Cross (CC) model was founded by crossing 5 common laboratory strains and 3 wild-derived strains<sup>263</sup>. Further breeding of the CC lines created the Diversity Outbred (DO) mouse collection, which is maintained as outbred population through random crossings. This is currently the most diverse mouse resource available<sup>264</sup>. Both cohorts have been used for the study of *M. tuberculosis* infection and display a range of disease phenotypes, including enhanced control or susceptibility to infection compared to standard laboratory strains<sup>174,265,266</sup>. Infection of the DO cohort with *M. tuberculosis* revealed correlations between disease pathology and neutrophil influx, recapitulating features seen in human lung infections, in addition to identifying new inflammatory biomarkers that correlate with active human disease<sup>266,267</sup>. Furthermore, these cohorts have been used to identify the genetic basis of disease responses. For example, the susceptibility of CC042 strain is associated with the loss of *Itgal* expression, an integrin required

for T cell trafficking to the lung, resulting in decreased T cell trafficking and IFN- $\gamma$  production in the lungs of infected animals.

Studies using CC and DO mice demonstrate the power of using genetically diverse mice for identifying novel host regulators of immunity to *M. tuberculosis*<sup>268</sup>. However, it is unclear that these collections capture the full spectrum of genetic diversity that exists in house mouse populations. To increase the genetic diversity of house mouse available for the analysis of complex phenotypes, researchers recently created a set of 40 new inbred lines derived from wild mice collected across 5 different geographic regions. These mice are all the *Mus musculus domesticus* subspecies of house mouse. The use of a single subspecies to establish this cohort is beneficial, as it limits allelic conflicts that can arise after crossing different subspecies. This allows for the maintenance of natural genetic heterogeneity and makes the presence of genomic “blind spots” – regions of the genome that are the same in all the lines – less likely<sup>269,270</sup>. The heterogeneity in this cohort comes from mice that were originally collected across a latitudinal gradient from Brazil to Canada and show significant phenotypic diversity, including size, body mass index and lipid and glucose metabolism<sup>271</sup>. Each line has been backcrossed for at least 10 generations, providing the benefit of the genetic reproducibility of laboratory derived strains.

This new collection of wild derived mice represents a unique resource for identifying both 1) lines of genetically diverse mice with enhanced or diminished susceptibility to *M. tuberculosis* infection and 2) genes that control the host response to *M. tuberculosis* infection. Here we characterize 17 lines from this collection for enhanced or diminished control of *M. tuberculosis* infection and the accompanying immune responses. This is the first report of the use of this collection of mice for infectious disease or immunology related phenotypes. Infection of the genetically diverse mouse lines reveals a range of responses with several lines showing higher susceptibility to infection compared with standard B6 mice. The immunological responses required for control of infection seem to deviate from responses studied in classic B6 mice, with mouse lines from Manaus showing high neutrophilic influx to the lungs without correlation to bacterial burden. In addition, the SARA line is resistant to *M. tuberculosis* infection and relies on an antimicrobial mechanism that requires very few CD4<sup>+</sup>IFN- $\gamma$ <sup>+</sup> T cells. Characterization of these pathways that are unique from the responses in B6 mice will expand our understanding of the different aspects that contribute to a successful immune response to *M. tuberculosis* infection.

## 2.3 Results.

**2.3.1 Mouse lines collected from different latitudes display variability in immune responses and susceptibility to *M. tuberculosis* infection.** The cohort of wild-derived mice used in this study was established using outbred mice originally collected from 5 different latitudes across the Americas: Edmonton (EDM), Alberta, Canada; Saratoga Springs (SAR), New York, United States of America; Gainesville (GAI), Florida, United States of America; Tucson (TUC), Arizona, United States of America and Manaus (MAN), Amazonas, Brazil (Figure. 2.1 A). These mice exhibit a variety of phenotypic differences, including body weight, body length, body mass index (BMI) and glucose and lipid metabolism<sup>271</sup>. Although there is within group heterogeneity, separate lines of mice collected from a single location are in general more closely related genetically than mice collected from different locales<sup>272</sup>. We hypothesized that the genetic diversity of these mouse lines would contribute to enhanced or diminished capacity to control *M. tuberculosis* infection. Mice were challenged with aerosolized *M. tuberculosis* and the

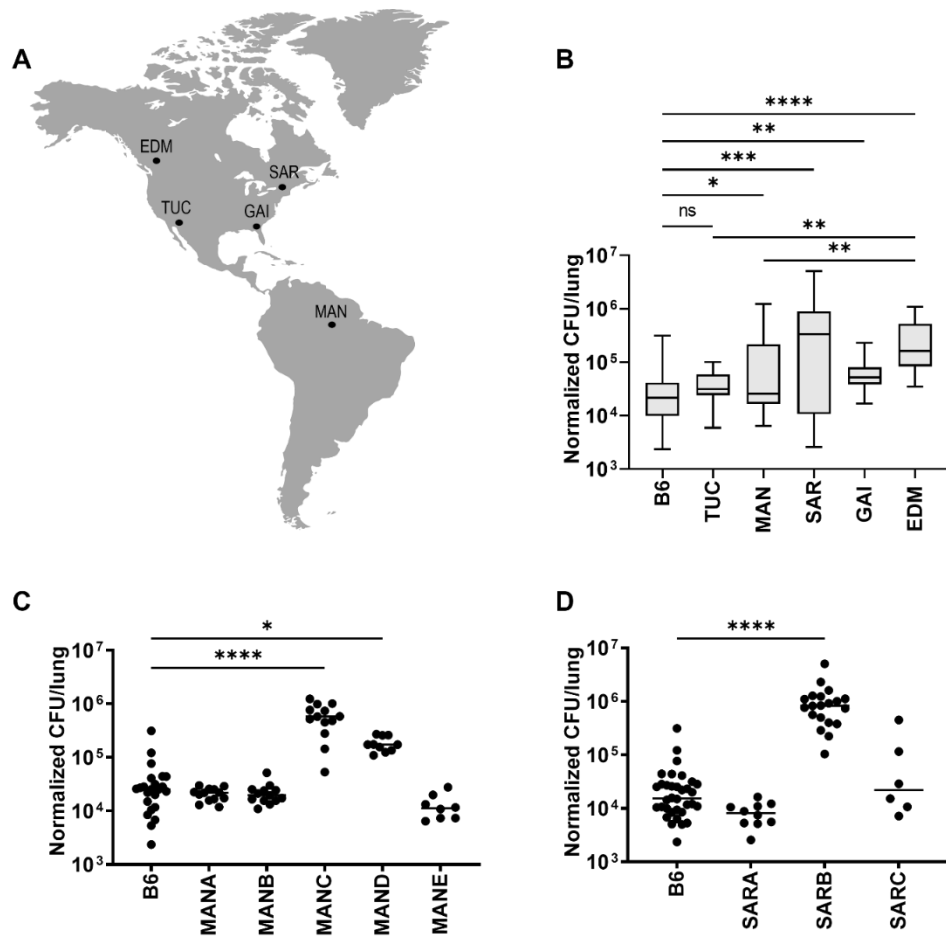


**Figure 2.1 Mouse lines from different latitudes show variable susceptibility to *M. tuberculosis* infection.**

(A) Mice were collected from five different sites across the Americas and inbred to generate individual lines from each location. (B) Overview of the bacterial burden in the lungs of the mice derived from the different location at 21 days post infection with aerosolized *M. tuberculosis* strain Erdman. Comparison of the susceptibility among Manaus lines (C) or Saratoga lines (D) infected with aerosolized *M. tuberculosis*. The average inoculum dose is 400 cfu/mouse. EDM: Edmonton, SAR: Saratoga Springs, TUC: Tucson, GAI: Gainesville, MAN: Manaus. The  $p$  values were determined using a Kruskal-Wallis ANOVA. \* $p < 0.05$ , \*\* $p < 0.005$ , \*\*\* $p < 0.0001$ , \*\*\*\* $p < 0.0001$ .

bacterial burden was assessed by colony-forming units (CFU) after 3 weeks of infection. CFU was normalized to inoculation dose day 1 post infection to correct for any variability in inhaled bacterial load between mouse lines with different activity levels, males and females, and different days of infection. The median bacterial burden varied over 100-fold between mice from different locales when the mean bacterial burden from each group was compared (Figure 2.1 B). Surprisingly, mouse lines that that originated from the same locale also demonstrated a wide variation in susceptibility, suggesting that genetic heterogeneity within the closely related lines can influence the outcome of infection. The bacterial burden in the lungs of the MANC line is significantly higher compared to the closely related MANA, MANB and MANE lines which are approximately as resistant as the standard B6 (Figure 2.1 C). Mice from the MAND line show an intermediate phenotype. We also observed significant variability in bacterial burdens in mice from Saratoga Spring. Whereas SARA mice are similarly resistant to infection as the standard B6, both the SARB and SARC lines harbor significantly more bacteria in the lungs at 3 weeks



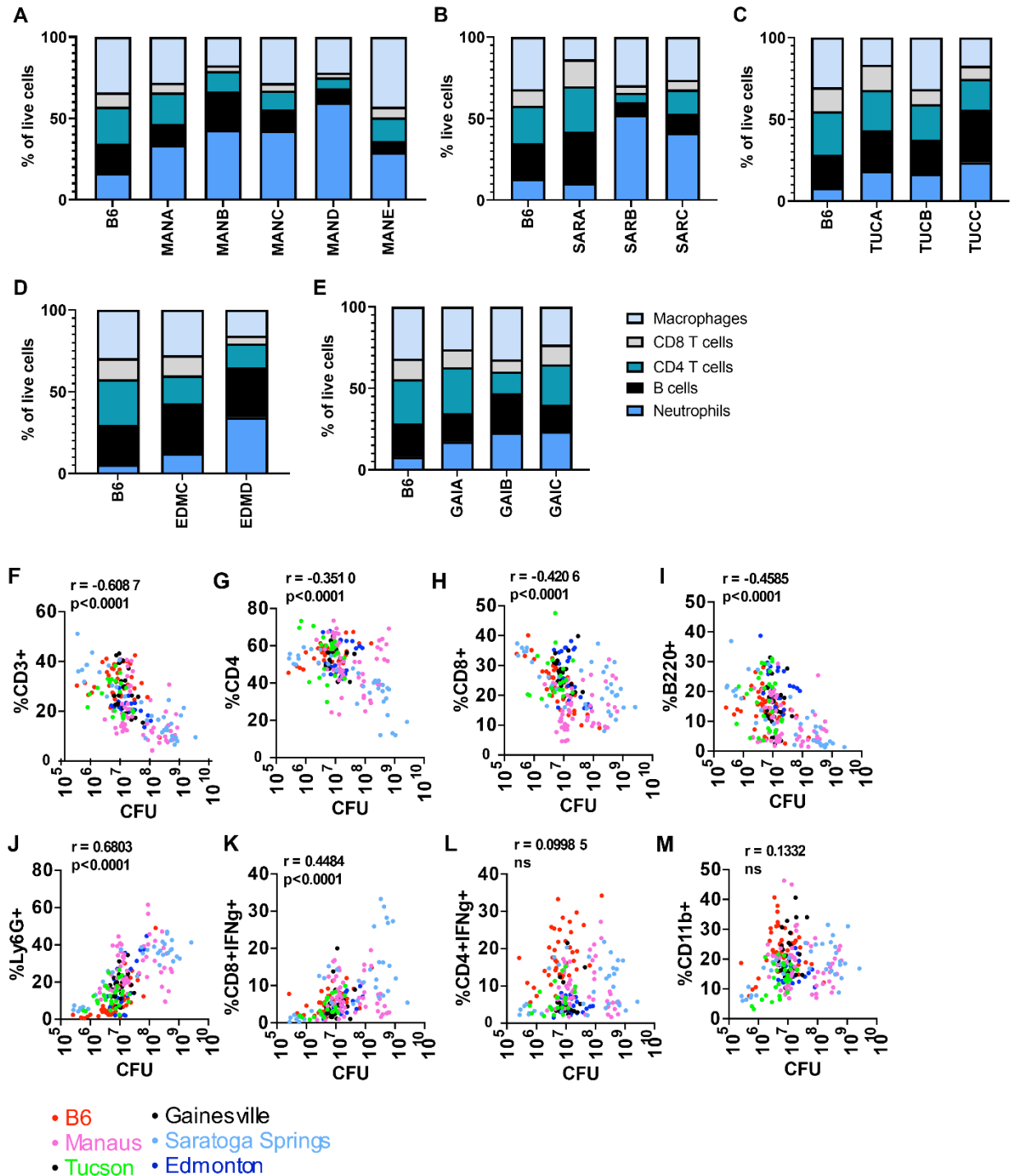


**Figure 2.2 Variation in bacterial burden and immune cells present in the lung between locales.**

The proportions of different cell types in the lung were quantified with flow cytometry at 21 days post infection with aerosolized *M. tuberculosis* strain Erdman (A). The correlation between cell types and CFU is depicted for individual mice (B). The  $p$  value was determined on a two-tailed Spearman correlation.

post infection (Figure 2.1 D). Smaller differences in susceptibility are found in the lines from Tucson, Gainesville and Edmonton (Supplemental Figure 2.1 A-C). A low body mass index (BMI) has been shown to be a risk factor for tuberculosis in humans, possibly associated with

malnutrition<sup>273</sup>. We there for examined body weight to determine whether differences in size could account for differences in the ability to control infection. Although there were significant differences in the body weight of the individual mouse lines from the Manaus and Saratoga Spring groups, we did not find a correlation between body weight and TB control (Supplemental Figure 2.1 D).

To identify immune cell correlates of bacterial burden in the lungs of the infected wild mouse lines, immune responses were analyzed in parallel with CFU counts. We first analyzed immune cell infiltrates in the lungs as a function of the proportion of live cells in each line. We found that across all of the lines we observed the greatest variability in the percentage of CD11b<sup>+</sup>Ly6G<sup>+</sup> neutrophils found in infected mouse lungs. In general, the standard B6 line had the lowest proportion of neutrophils, with other lines with either equivalent or higher (Figure 2.2 A-E). Neutrophil influx often correlates with increased lung pathology and bacterial growth. Interestingly, the majority the Manaus lines show high neutrophilic influx to the lungs compared to B6 mice, despite the strong variability in bacterial burden (Figure 2.2 A). We also observed differences in the total proportion of CD4 T cells as well as CD11b<sup>+</sup>Ly6G<sup>-</sup> cells across the lines (Figure 2.2 A-E). Differences in the proportions in CD8 T cells and B cells were modest (Figure 2.2 A-E).

In order to determine whether observed differences in the proportions of immune correlate with the outcome of infection, we performed correlation analysis between cell types and bacterial burden. We found significant correlations between the proportion of CD3<sup>+</sup>, CD4<sup>+</sup>, CD8<sup>+</sup> and B220<sup>+</sup> cells with control of infection, with larger proportions of these cells corresponding to lower CFU in the lung (Figure 2.2 F-I). In contrast, we found that the proportion of neutrophils in the lung could explain approximately 60% of the variation seen in the wild-derived mice, with higher neutrophil burden associated with higher CFU in the lungs (Figure 2.2 J). This is consistent with numerous studies of susceptible mice on the B6 background that have pointed to a role for excessive infiltration of neutrophil in driving lung pathology and susceptibility to *M. tuberculosis* infection<sup>124,145,182,183</sup>. Production of IFN- $\gamma$  by CD4<sup>+</sup> T cells is known to be important for control of infection<sup>116,117,216,255,274</sup>. Surprisingly, we found that production of IFN- $\gamma$  by CD8 T cells negatively correlates with control of infection, with lower proportions of these cells observed in mice that have lower CFU in the lungs (Figure 2.2 K). Surprisingly the wild-derived mouse lines do not show any significant correlation between the proportion of CD4 T cells or IFN- $\gamma$  in the lung with CFU. This is in contrast to the B6 mice which show a protective effect between the proportion of IFN- $\gamma$  producing T cells in the lung and the bacterial burden (Supplemental Figure 2.2). The overall variation in bacterial burden and immune cells present in the lung among and between the locales indicates the heterogeneity in underlying inflammatory responses to *M. tuberculosis* infection. The notable differences between the wild-derived mouse lines and B6 mice shows the potential for identifying novel mechanisms of susceptibility to infection in these mice.

**2.3.2 Macrophages from Manaus lines respond to IFN- $\gamma$  stimulation during *M. tuberculosis* infection.** Despite being closely genetically related, the Manaus lines show distinct susceptibilities to *M. tuberculosis*; whereas most of the tested lines control infection in the lungs as well as B6, the MANC line is significantly more susceptible to infection (Figure 2.1 C). We therefore focused on these lines for an in-depth immunological analysis. First, we tested whether impaired bacterial restriction in the MANC line can be explained by cell intrinsic differences.

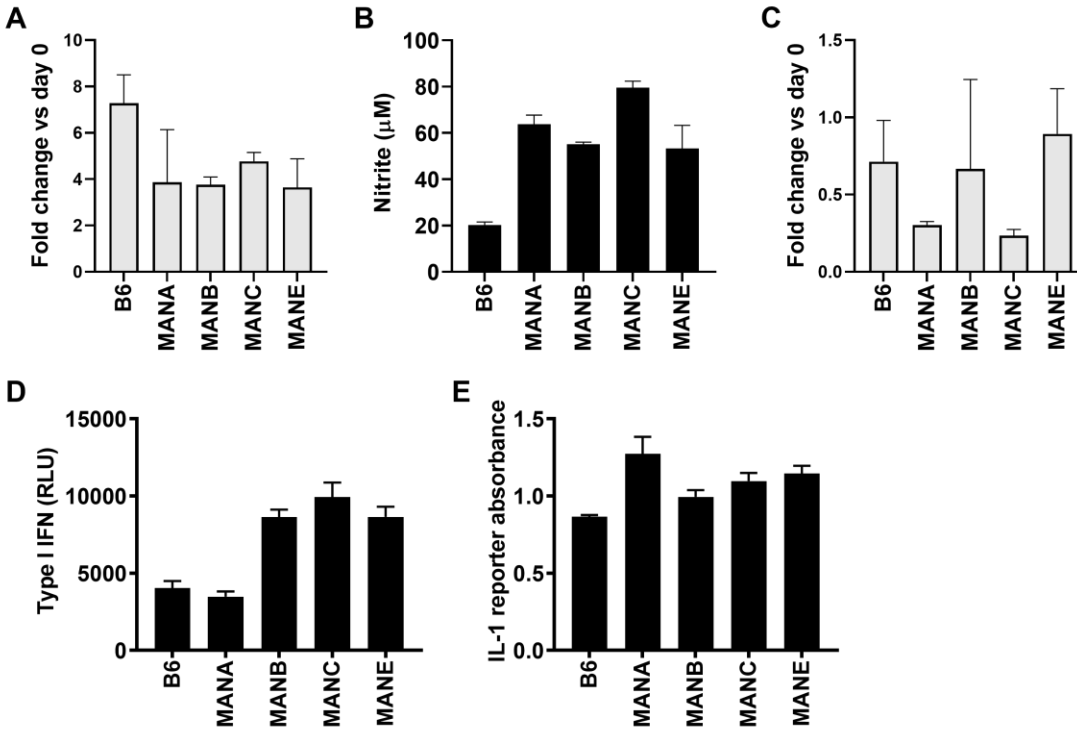


**Figure 2.3 The MANC line does not show obvious defects in intrinsic control of infection.**

BMDM isolated from the indicated mouse lines were infected with *M. tuberculosis* strain Erdman and bacterial growth was determined at 4 days post infection by enumerating CFU (A). The presence of nitrite was determined by Griess assay at 48 hours post infection (B). IFN- $\gamma$  activated macrophages were infected with *M. tuberculosis* and CFU were measured on day 4 post infection (C). Production of type I IFN or IL-1 at 24 hours post infection (D, E).

Macrophages are central to *M. tuberculosis* infection, serving both as the host cell, the cell responsible for killing the bacteria, and an important source of cytokines that regulate infection. Bone marrow-derived macrophages from four Manaus lines were prepared and infected with *M. tuberculosis* followed by quantification of bacterial burden and cytokine production. Macrophages from all the tested lines, including B6, allow the growth of *M. tuberculosis* in the absence of exogenous cytokine stimulation (Figure 2.3 A), with none of the lines exhibiting a loss of control relative to B6. Additionally, all macrophages responded similarly to IFN- $\gamma$  stimulation, producing significantly more NO upon infection than is observed with B6. (Figure 2.3 B). Similarly, we did not observe any defects in IFN- $\gamma$  based control of infection at the macrophage level as all MAN lines controlled infection as well or better than the standard B6 (Figure 2.3 C). Thus, differences in cell intrinsic control of infection do not obviously play a role in the susceptibility of the MANC line to *M. tuberculosis* infection.

Macrophages from Sp140<sup>-/-</sup> mice produce excessive type I IFN upon immune stimulation, recapitulating the high type I IFN/low IL-1 signaling phenotype of these animals *in vivo*. We next tested whether impaired IL-1 signaling could underly the high bacterial burden and neutrophil influx in MANC mice. Macrophages were infected with *M. tuberculosis* and levels of type I IFN were assessed at 24h post infecting using HEK293-ISRE reporter cells. We found that macrophages isolated from three MAN lines (MANC, MANB, MANE) produced significantly more type I IFN than B6 or MANA (Figure 2.3 D), however these findings did not correlate

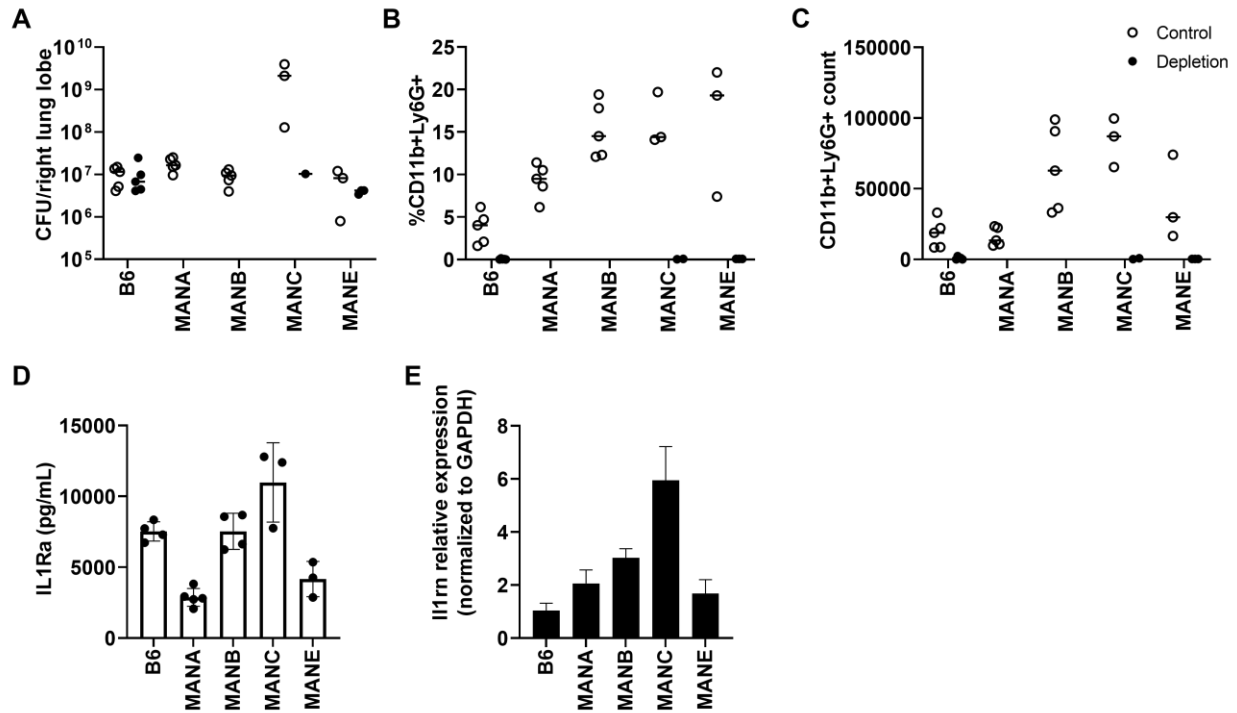


**Figure 2.4. In vivo signaling of IL-1 is not correlated to high neutrophil influx in the Manaus lines.**

(A) CFU in the lungs at 25 days post aerosol infection in mice in control mice and mice depleted for Ly6G<sup>+</sup> cells. Proportion (A) and counts (B) of Ly6G<sup>+</sup> cells in the lung with and without depletion of neutrophils. Production of secreted IL1Ra in lung homogenates of infected mice measured with ELISA (D). *Il1rn* mRNA expression in the lungs of infected mice (E).

with the ability to control infection *in vivo*. We also measured IL-1 bioactivity in the supernatants of infected macrophages using the IL-1 reporter bioassay found that *in vitro* production of IL-1 was comparable to other Manaus genotypes and to B6. Taken together, none of the Manaus lines appear to have major macrophage intrinsic defects that would explain the observed differences in control of infection *in vivo*.

### 3.3.3 High bacterial burden correlates with high neutrophil influx in MANC lines.

Neutrophils possess potent antimicrobial mechanisms, yet their role in host defense during *M. tuberculosis* infection is not well defined. In human tuberculosis, neutrophils are generally associated with active disease and pathogenesis. Mouse models with excessive accumulation of neutrophils in the lung have been correlated with destructive inflammation and a high bacterial burden. Interestingly, MANB and MANC Manaus lines show levels of neutrophil influx in the lungs that are higher than B6, whereas only MANC mice show higher susceptibility to infection (Figure 2.4 A-C). Recently, studies have suggested that neutrophils are heterogenous populations of cells and can participate to the inflammatory response in a protective role as well as an inflammatory role. This prompted us to investigate the phenotypes of neutrophils in the Manaus lines during infection. Due to limitations with mouse breeding, we selected two lines with distinct susceptibility to infection (MANC and MANE), to test the contribution of neutrophils to host susceptibility. Depletion of neutrophils in these lines during infection resulted in a drop in bacterial burden in the MANC line, indicating that high neutrophil influx in this line benefits *M.*

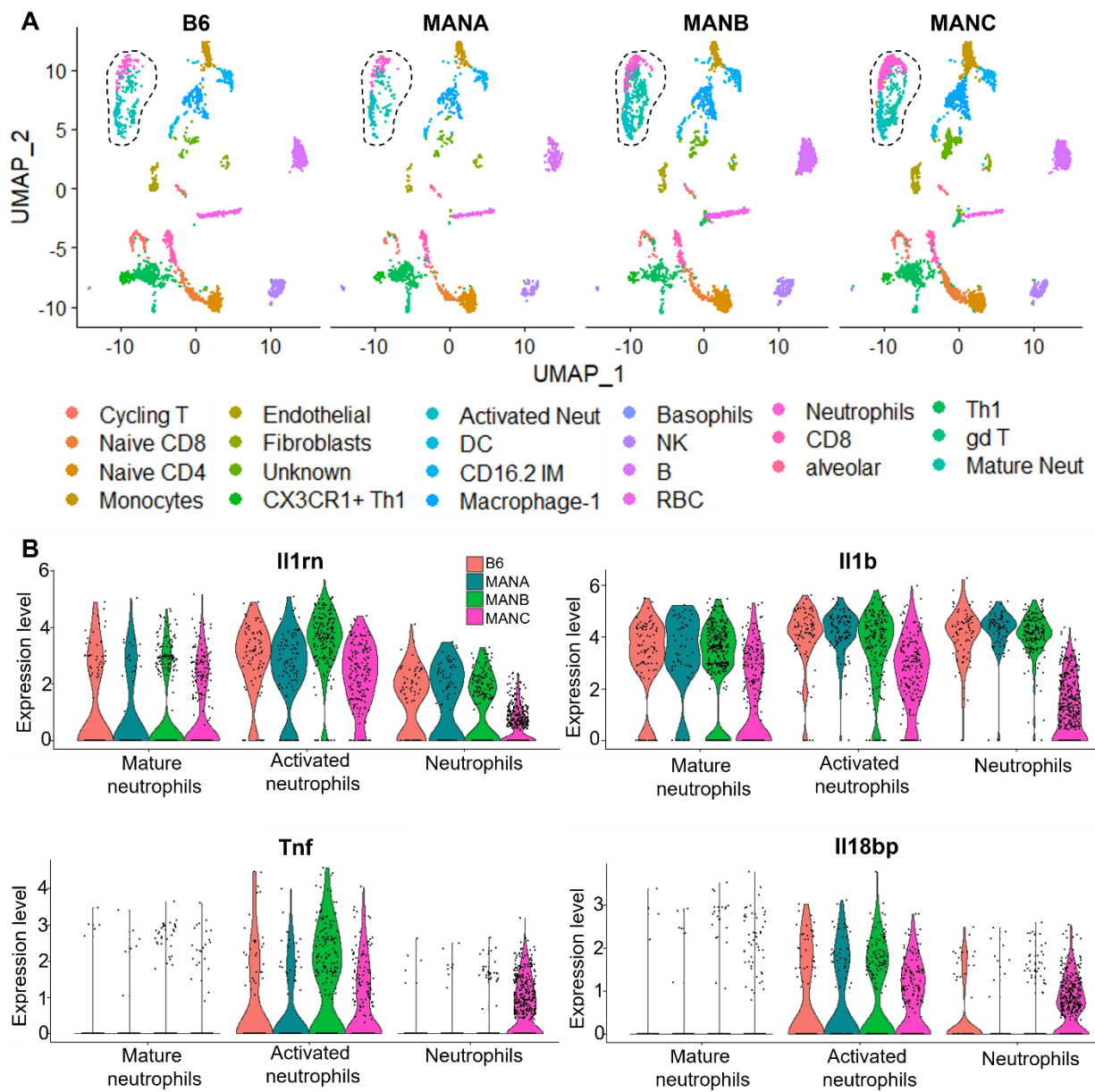


**Figure 2.5** scRNAseq analysis of infected mouse lungs reveals a lower expression of inflammatory cytokines in neutrophils from MANC mice.

Clusters of lung cells were manually annotated based on expression of signature genes, cytokines and cell surface markers (A). Comparison of gene expression levels among neutrophil subsets (B).

*tuberculosis* growth (Figure 2.4 A). Depletion of neutrophils in the resistant MANE and B6 lines does not further reduce bacterial growth, suggesting that low numbers of neutrophils during infection are not detrimental to the host. An increased influx of neutrophils has been linked to impaired IL-1 signaling in susceptible mouse models, which is in part regulated by IL-1Ra. Cytokine expression analysis in the lungs revealed a trend towards increased IL-1Ra protein production in MANC mice, and showed an increase in expression of the IL-1Ra-encoding gene

*Il1rn* (Figure 2.4 D, E), indicating that blocking IL-1 signaling might be the driver of susceptibility in these mice.

In order to identify which cell types contribute to the differences seen in susceptibility seen among Manaus lines, single cell RNAseq was performed on the lungs of *M. tuberculosis* infected mice. As shown in Figure 2.5 A, encircled are 3 unique clusters of neutrophils that were identified in all the mouse lines (Figure 2.5 A). The ‘Neutrophil’ cluster shows high levels of adhesion molecule L-selection (CD62L, *Sell*), indicating younger circulating neutrophils. The second cluster shows a lower expression of L-selectin and increase of activation molecule CD63 and PD-L1 (CD274), indicating the presence of activated neutrophils (‘Activated neutrophils’). The third cluster expresses lower levels of L-selectin and no CD63, suggesting more mature but unactivated neutrophil cluster (‘Mature neutrophils’). Cytokine analysis at the individual cell level indicates similar expression levels of *Il1rn* across clusters and mouse lines, except for the younger ‘Neutrophil’ cluster in the MANC line (Figure 2.5 B). Interestingly, all three neutrophil clusters show slightly lower *Il1b* expression in the MANC lines. IL-1 $\beta$  production in macrophages is in part regulated through NO production by iNOS. NO can dampen excessive IL-1 $\beta$  production by the inflammasome<sup>83</sup> and has therefore been attributed protective immune responses *in vivo*. Furthermore, NO production contributes to intrinsic control of infection in macrophages through stimulation of transcription factor HIF-1 $\alpha$ . Surprisingly, ‘Activated neutrophils’ from the MANC line show significantly increased iNOS expression (Supplemental figure 2.3), showing a disconnect between NO production and enhanced bacterial control in this line. Furthermore, the neutrophils show decreased *Hif1a* expression. Other cytokines that are differentially expressed in the MANC ‘Neutrophil’ are *Tnf* and *Il18bp* (Figure 2.5 B).

**3.3.4 SARA mice show low numbers of CD4<sup>+</sup>IFN- $\gamma$ <sup>+</sup> T cells in the lung.** Infection of the Saratoga lines revealed resistance to infection in the SARA line and loss of control in the SARB line compared to B6 mice (Figure 2.6 A). As the disease progresses, SARA mice do not show enhanced control of infection (Figure 2.6 B). Interestingly, SARA and SARB mice show lower total CD4<sup>+</sup> T cells numbers the lung during infection (Figure 2.6 C). In contrast to B6 mice, SARA mice do not depend on the presence of high IFN- $\gamma$ -expressing T cells in the lung for control of *M. tuberculosis* infection (Figure 2.6 D). Furthermore, CD4<sup>+</sup> T cells from SARA and B6 mice express similar levels of IFN- $\gamma$  (Supplemental Figure 2.4 A). In order to determine whether other T cell subsets contribute to bacterial restriction in these mice, flow cytometry was used to assess the influx of CD8<sup>+</sup>, IL17<sup>+</sup> or TCR $\gamma\delta$  T cells to the lungs. However, no significant differences were found among these cell types that could contribute to IFN- $\gamma$  independent control of infection (Supplemental Figure 2.4 B-D). Interestingly, although B6 show increased numbers of CD4<sup>+</sup>IFN $\gamma$ <sup>+</sup> T cells, most of these cells seem to be derived from the vasculature<sup>275</sup>, based on KLRG1 expression (Figure 2.6 E). In contrast, the numbers of CD4<sup>+</sup>IFN $\gamma$ <sup>+</sup> T cells in the lung parenchyma (CXCR3<sup>+</sup>) are similar between B6 and SARA mice (Figure 2.6 F), suggesting that the T cells in SARA mice are more efficient in exiting the vasculature and are capable of accomplishing the antimicrobial effect as T cells in B6 mice with smaller total numbers.

## 2.4 Discussion.

In order to better understand the variability in immune responses that result in control *M. tuberculosis* infection in human patients, we studied the underlying mechanisms of *M.*

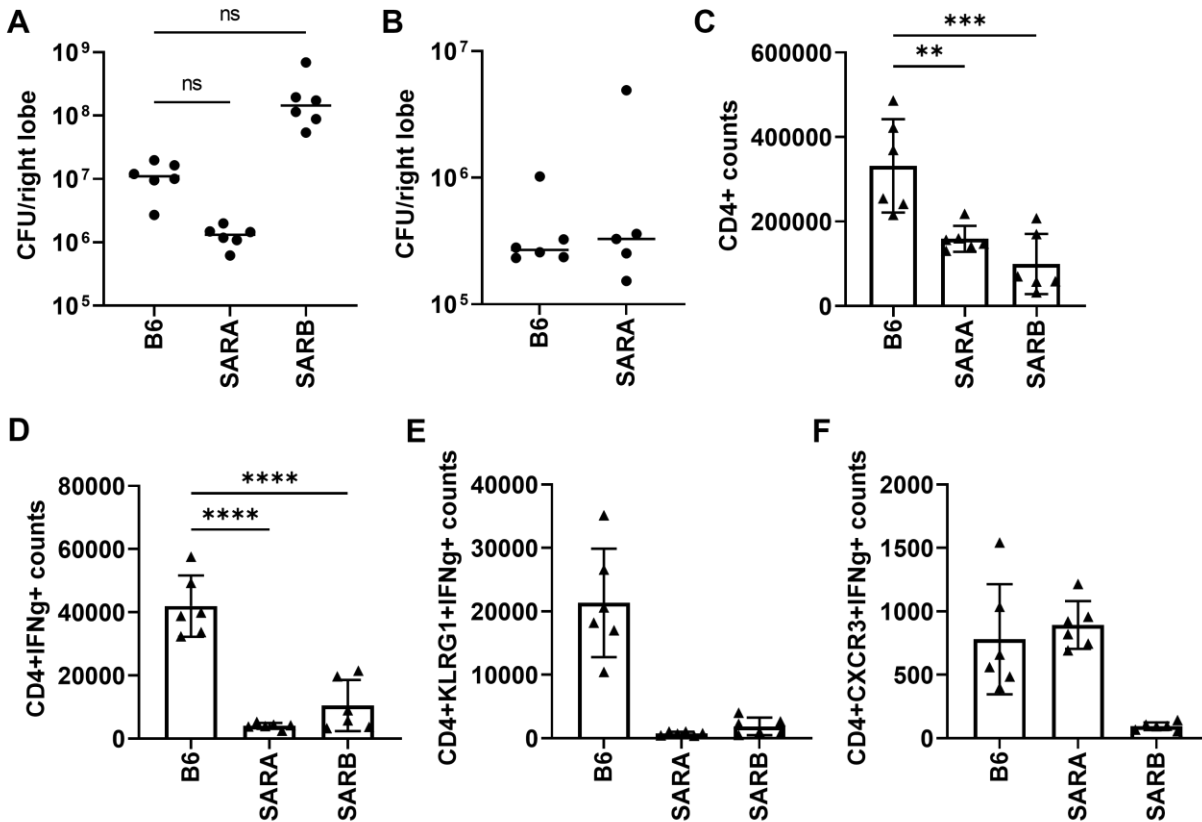


**Figure 2.6 SARA mice show increased bacterial restriction in the absence of high numbers of total CD4<sup>+</sup>IFN $\gamma$ <sup>+</sup> cells.**

Bacterial burden in the lung of B6 and Saratoga mice at 21 (A) and 61 (B) days post aerosol infection. CD4<sup>+</sup> (C) and CD4<sup>+</sup>IFN $\gamma$ <sup>+</sup> (D) cell counts in the lung determined by flow cytometry on day 21 post infection. The number of KLRG1<sup>+</sup> (E) and CXCR3<sup>+</sup> (F) CD4<sup>+</sup>T cells that express IFN- $\gamma$  at 21 days post infection.

*tuberculosis* restriction in a cohort of genetically diverse mice. This cohort exhibited a range in susceptibilities at early timepoints during infection as well as diversity in the immune responses that benefit control of infection. First, it showed that neutrophils are highly abundant during infection of the MANC line, which benefits *M. tuberculosis* growth. Depletion of neutrophils in the resistant MANE line does not result in a further decrease of bacterial numbers, suggesting that low numbers of neutrophils are not detrimental to the host. Similarly to the susceptible Sp140<sup>-/-</sup> mouse line, the MANC line shows increased *Il1rn* expression. Infection of Sp140<sup>-/-</sup> mice demonstrated that blocking IL-1 $\beta$  signaling through excessive IL-1Ra production drives neutrophil recruitment and results in an increased bacterial burden. Furthermore, increased IL-1Ra production is driven by increased levels of type I IFN. Quantification of type I IFN in the lungs of MANC mice and depletion of the type I IFN receptor (IFNAR) in these mice is necessary to determine if neutrophil recruitment depends on this signaling pathway. Interestingly, scRNAseq expression data shows that neutrophil clusters from MANC mice show slightly decreased IL-1 $\beta$  expression at a single cell level, but an increase in neutrophil-specific *Il1rn* expression is not observed. This suggests that other cell types contribute to increased *Il1rn* levels. In order to confirm the role of IL-1 in neutrophil recruitment and the susceptibility of the MANC line, the total amount of IL-1 $\beta$  present in the lung should be determined by ELISA.

ScRNAseq on mouse lungs revealed the presence of the same immune cell clusters among the susceptible and resistant mice, including similar neutrophil, macrophage and T cell clusters. There was no obvious presence or absence of unique cell clusters that could explain the susceptibility of the MANC mice. However, more research is needed to identify specific gene signatures within the clusters that can underlie the differences in the bacterial burden among the Manaus lines. Another mechanism of control that deviates from the immune responses seen in B6 mice is the absence of high levels of IFN- $\gamma$ -expressing T cells in the lung of resistant SARA mice. We hypothesize that this could be due to enhanced targeting of IFN- $\gamma$  to the bacteria in the lesion, since most of CD4<sup>+</sup>IFN $\gamma$ <sup>+</sup> T cells seem to extravasate from the vasculature into the tissue. In addition, it is possible that these mice depend on an IFN- $\gamma$ -independent mechanism of control. In order to determine whether localization of these cells differs between B6 and SARA mice, fluorescent microscopy can be used to quantify number of T cells in the tissue and determine if T cells are in closer proximity to the bacteria in the lesion and to the macrophage that will respond to IFN- $\gamma$  production. Furthermore, to confirm whether control of infection relies on IFN- $\gamma$  production in these mice, IFN- $\gamma$  receptor depletion experiments should be performed during infection followed by quantification of bacterial burden in the lungs. Taken together, the data show a wide variety of immune responses and susceptibility to infection among the lines from the wild-derived mouse cohort and compared to responses in the classical B6 mouse model. This makes this novel mouse cohort a promising resource for studying immune responses to pathogens in genetically diverse backgrounds with the potential to identify genetic loci responsible for these phenotypes.



## **2.5 Materials and Methods.**

### **Mice**

C57BL/6J (no. 000664), mice were obtained from The Jackson Laboratory (Bar Harbor, ME) and bred in-house. Wild-derived mouse lines were obtained from the Nachman laboratory (UC, Berkeley). Mice were sex and age matched for all experiments.

### **Bacterial culture**

*M. tuberculosis* strain Erdman was grown in Middlebrook 7H9 liquid medium supplemented with 10% albumin-dextrose-saline 0.4% glycerol; and 0.05% Tween 80 or on solid 7H10 agar plates supplemented with 10% Middlebrook OADC (BD Biosciences) and 0.4% glycerol. Frozen stocks of *M. tuberculosis* were made from single cultures and used for all experiments.

### **Cell preparation for bacterial enumeration and flow cytometry**

For bacterial enumeration, the largest lung lobe was homogenized in PBS plus 0.05% Tween 80, and serial dilutions were plated on 7H10 plates. CFU were counted 21 days after plating. The three smallest lung lobes were harvested into complete RPMI 1640, dissociated, and strained through a 40-mm strainer. Cells were washed, stained with antibodies used for cytokine and surface marker staining: live/dead (L34970; ThermoFisher), CD4, CD3, CD8a, CD11b, B220, Ly-6G, CXCR3 and TCRg/d (100509, 100219, 100707, 101237, 103233, 127627, 126522, and 118124 respectively; BioLegend) or CD4, Ly6G and KLRG1 (564933, 551460 and 740279 respectively, BD Biosciences) and fixed/permeabilized with BD Cytotfix/Cytoperm Fixation/Permeabilization Solution Kit (554714; Thermo Fisher Scientific) before staining with antibody specific for IFN- $\gamma$  and IL-17 (505816 and 506904; BioLegend) and IL-17. Data were collected using a BD LSR Fortessa flow cytometer and analyzed using FlowJo Software (Tree Star, Ashland, OR).

### **IL-1 bioactivity reporter assay**

The second largest lung lobe from infected mice was harvested into complete RPMI 1640, dissociated, and strained through a 40-mm strainer to form a single cell suspension. Samples were assayed using HEK-Blue IL-1R cells (InvivoGen). Cells were authenticated and tested for mycoplasma by the manufacturer. A total of  $3.75 \times 10^4$  cells per well were plated in 96-well plates, and allowed to adhere overnight in DMEM supplemented with 10% FBS, 2 mM glutamine. Reporter cells were treated overnight with 100  $\mu$ l of sample (consisting of 50  $\mu$ l of cell-free lung homogenates and 50  $\mu$ l of media), or recombinant mouse IL-1 $\beta$  (R&D systems 401-ML-005) mixed with 100  $\mu$ l of media (to generate a standard curve). Assays were developed using QUANTI-Blue (InvivoGen) according to the manufacturer's protocols.

### **IFN- $\beta$ bioactivity reporter assay**

Interferon responsive ISRE-L929 cells were cultured in ISRE media (DMEM, 2 mM glutamine, 1 mM pyruvate, 10% heat inactivated FBS, and penicillin-streptomycin). Induction of type-I interferon was assessed using lung homogenate as described previously. Homogenates were applied in various dilutions to the interferon responsive ISRE-L929 cells ( $5 \times 10^4$  cells/well) in white, 96-well, tissue culture treated plates (Thermo Scientific Nunc). Cells were incubated for 4 hours, media aspirated, and cells were lysed with 30  $\mu$ l Luciferase cell culture lysis reagent

(Promega). Finally, 100  $\mu$ L of luciferase substrate solution (Promega) was added to each well and luminescence was measured using a M3 luminometer (Spectramax).

### **qRT-PCR**

For q-RT-PCR, the second largest lung lobe from infected mice was harvested into 500  $\mu$ L RNeasy lysis solution (Qiagen) and stored at  $-80^{\circ}\text{C}$ . Tissues were transferred to 500  $\mu$ L TRIzol (Invitrogen Life Technologies) and homogenized. Total RNA was extracted using chloroform (100  $\mu$ l), and the aqueous layer was further purified using RNeasy spin columns (Qiagen). For qPCR, cDNA was generated from 1  $\mu$ g RNA using Superscript III (Invitrogen Life Technologies) and oligo(dT) primers. Select genes were analyzed using Maxima SYBR Green qPCR master mix (Thermo Scientific). Each sample was analyzed in triplicate on a CFX96 real-time PCR detection system (Bio-Rad). C<sub>Q</sub> values were normalized to values obtained for GAPDH, and relative changes in gene expression were calculated using the  $\Delta\Delta\text{C}_Q$  method.

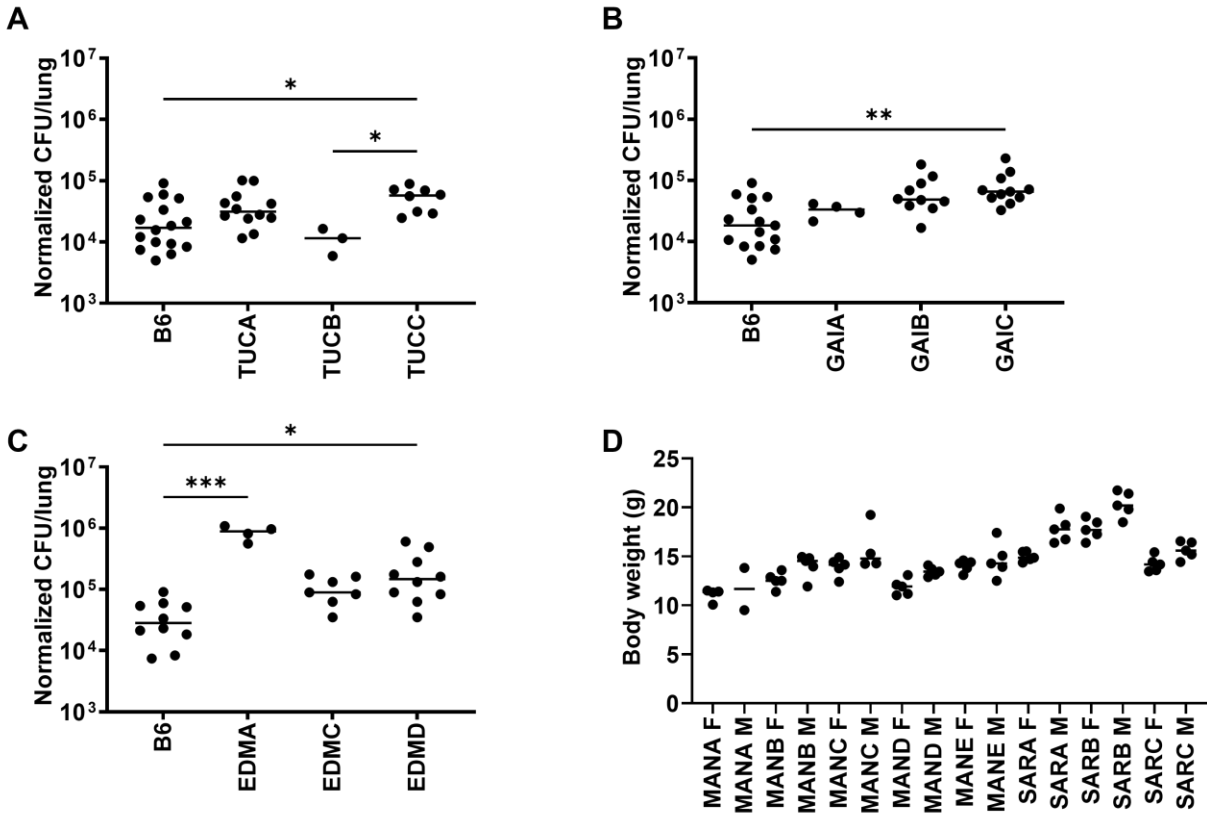
### ***In vitro* infections**

BMDM were plated into 96-well or 24-well plates with  $5 \times 10^4$  and  $3 \times 10^5$  macrophages/well, respectively, and were allowed to adhere and rest for 24 h. BMDM were then treated with vehicle or IFN- $\gamma$  (6.25 ng/ml) overnight and then infected in DMEM supplemented with 5% horse serum and 5% FBS with *M. tuberculosis* Erdman strain at a multiplicity of infection of 5, unless otherwise noted. After a 4-h phagocytosis period, media was replaced with DMEM supplemented with 10% FBS, 2 mM glutamine and 10% M-CSF. For IFN- $\gamma$ -pretreated wells, IFN- $\gamma$  was also added post infection at the same concentration. For enumeration of CFU, infected BMDM were washed with PBS and lysed in water with 0.1% Triton X-100 for 10 min; and serial dilutions were prepared in PBS with 0.05% Tween 80 and were plated onto 7H10 plates.

### **scRNA-seq**

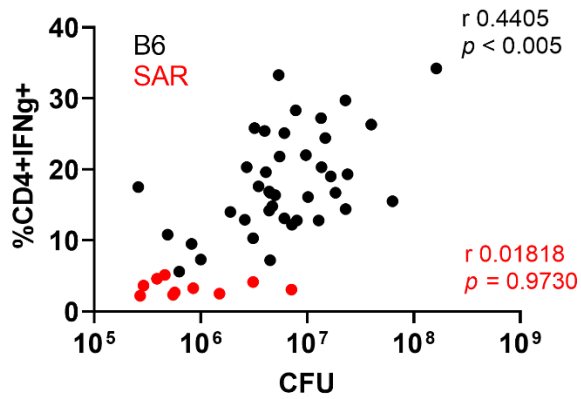
The second largest lung lobes were pooled from five infected mice, tissue dissociated in RPMI 1640 containing liberase and DNase I in gentleMACS C tubes using the gentleMACS dissociator and strained through a 70- $\mu$ m filter in RPMI 1640 and counted. A total of 10,000 cells per sample were used for scRNAseq according to the 10 Genomics protocol. Briefly, single-cell suspensions were partitioned into Gel Beads in emulsion using the Chromium Next GEM Single Cell v3.1 system. The 10 barcoded primers were used to reverse-transcribe poly-adenylated mRNA to produce barcoded, full-length cDNA. Purified DNA was amplified, fragmented, and amplified again to attach Illumina adapter sequences by the Functional Genomics Laboratory at UC, Berkeley. Libraries were sequenced on an Illumina NovaSeq S1 demultiplexed by the Vincent J. Coates Genomics Sequencing Laboratory at UC, Berkeley. Reads were aligned to the mouse transcriptome mm10 with the 10 Cell Ranger analysis pipeline using the Savio computational cluster at UC, Berkeley. After filtering, barcode counting, and unique molecular identifier counting, the Seurat 4.0.6 toolkit (Satija lab) was used to preprocess the data. The filtered data were manually annotated using signature genes and gene expression and visualization was explored using Seurat.

## 2.6 Supplemental figures.



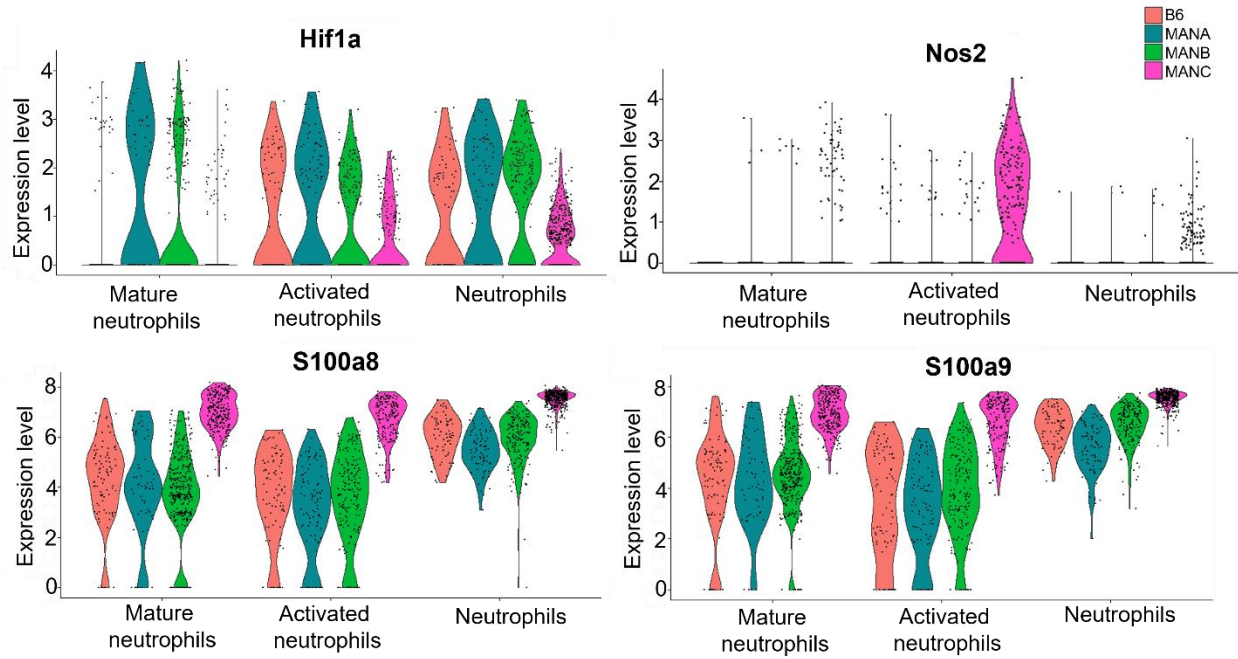
### Supplemental Figure 2.1 Mouse lines from within and among different locations show variability in *M. tuberculosis* susceptibility.

(A-C) Bacterial burden in mouse lines from Tucson (TUC), Gainesville (GAI), or Edmonton (EDM) infected with aerosolized *M. tuberculosis* strain Erdman. (D) Body weights of female (F) and male (M) mice from the MAN and SAR lines determined at 7 weeks after birth. The  $p$  values were determined using a Kruskal-Wallis ANOVA. \* $p < 0.05$ , \*\* $p < 0.005$ , \*\*\* $p < 0.0001$ .



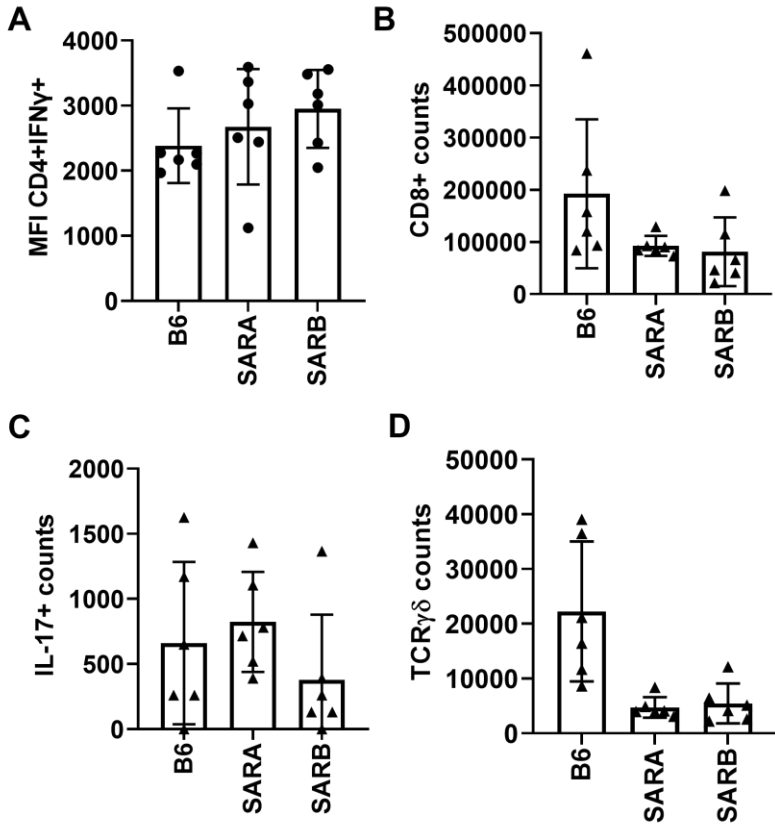
**Supplemental Figure 2.2 Correlation between CFU and the proportion CD4<sup>+</sup>IFN $\gamma$ <sup>+</sup> cells in the lung of B6 and Saratoga mice.**

The bacterial burden in the lung and the percentage CD4<sup>+</sup>IFN $\gamma$ <sup>+</sup> T cells was determined at 21 days post infection. Correlations were calculated as Spearman correlations.



**Supplemental Figure 2.3 Expression of genes involved in intrinsic control of infection are differentially expressed in MANC mice.**

Gene expression from scRNAseq dataset among different neutrophil subsets at 25 days post aerosol infection.



**Supplemental Figure 2.4 Differences in abundance of T cell subsets do not explain the underlying mechanism for bacterial restriction in SARA mice.**

(A) Mean fluorescent intensity of IFN- $\gamma$  expressing CD4<sup>+</sup> T cells. Lung cell counts of CD8<sup>+</sup>, CD4<sup>+</sup>IL17<sup>+</sup> or TCR $\gamma\delta$  T cells (B-D). Data from 21 days post infection.

## **Chapter 3**

### **Intrinsic effects of interferon- $\gamma$ signaling**

### 3.1 Summary of results.

Intrinsic control of *M. tuberculosis* infection in macrophages depends on IFN- $\gamma$  signaling. HIF-1 $\alpha$  is a crucial transcriptional activator of IFN- $\gamma$ -dependent immunity. However, HIF-1 $\alpha$  protein levels are regulated by constitutive degradation in the absence of IFN- $\gamma$ . Although HIF-1 $\alpha$  has been extensively described as target for proteasomal degradation, this study indicates the existence of a lysosomal-dependent degradation pathway in resting macrophages. Furthermore, our data shows that E3 ubiquitin ligase VHL is required for HIF-1 $\alpha$  protein turnover, despite previous work that associates VHL with proteasomal degradation of proteins. Deletion of *Vhl* in macrophages results in increased HIF-1 $\alpha$  stabilization. Furthermore, the lack of VHL induces nitric oxide (NO) production in macrophages. Together, this results in increased cell-intrinsic control of *M. tuberculosis* infection.

HIF-1 $\alpha$  is both a regulator of metabolic genes as well as pro-inflammatory responses. Mass spectrometry was used to identify differentially expressed proteins in the presence or absence of IFN- $\gamma$  and HIF-1 $\alpha$ . This was followed by a targeted CRISPR approach to identify which genes contribute to control of infection. Knockout of individual kinases, guanylate binding proteins (GBP) or metabolite transporters did not reveal IFN- $\gamma$ -dependent control mediated through these genes. However, the development of a flow cytometry-based CRISPR screen will be used to identify the contribution of solute carrier (SLC) metabolite transporters to cell-intrinsic control of *M. tuberculosis* infection in macrophages.



## 3.2 Introduction.

### 3.2.1 IFN- $\gamma$ signaling is essential for induction of antimicrobial pathways in macrophages.

The potent immune activating cytokine interferon- $\gamma$  (IFN- $\gamma$ ) plays an essential role in the control of *M. tuberculosis* infection<sup>7</sup>. Indeed, people with mutations in the IFN- $\gamma$  signaling pathway can suffer from mendelian susceptibility to mycobacterial disease (MSMD) and are more susceptible to weakly virulent mycobacteria. Mutations in *IFNGR1*, *IFNGR2*, and *STAT1* are among the genes that have been identified as causing MSMD<sup>276,277</sup>. The importance of IFN- $\gamma$  for control of infection is recapitulated in mouse models of *M. tuberculosis* infection where mice defective in IFN- $\gamma$  signaling succumb quickly to *M. tuberculosis* infection<sup>7,151,255</sup>. Although IFN- $\gamma$  is produced by several cell types, including NK cells and CD8<sup>+</sup> T cells, the most important source of IFN- $\gamma$  during *M. tuberculosis* infection is derived from CD4<sup>+</sup> T cells<sup>116,117,216,255,274</sup>. One of the main cell types that responds to IFN- $\gamma$  stimulation are macrophages. During infection with *M. tuberculosis* macrophages populations are abundant cells within the lung<sup>191</sup> and phagocytose the bacteria upon contact. After phagocytosis, the bacteria remain within the phagosome, but gain access to the macrophage cytosol by use of their type seven secretion system<sup>33</sup>. *M. tuberculosis* can then grow unrestricted inside macrophages, until the cells become activated in the presence of IFN- $\gamma$ . IFN- $\gamma$  signaling results in the upregulation of a microbicidal program that results in the killing and growth restriction of the bacteria<sup>7</sup>. However, the direct effectors of IFN- $\gamma$ -dependent antimicrobial responses remain largely unknown.

In addition to activating antimicrobial pathways, IFN- $\gamma$  signaling induces a switch in macrophage metabolism that is essential for control of infection. The metabolic adaptation that occurs results in a metabolic switch from oxidative phosphorylation to aerobic glycolysis and glutaminolysis and is associated with the differentiation of macrophages into the pro-inflammatory M1 polarized phenotype<sup>156,278</sup>. Macrophages in this state rely on aerobic glycolysis for the generation of metabolic intermediates to support amino acid and fatty acid synthesis. Interestingly, aerobic glycolysis is not only important for maintenance of biosynthetic pathways and ATP production. Instead, changes in metabolites also impact inflammatory gene expression, including expression of IL-1 $\beta$ , which are essential for control of *M. tuberculosis* infection. Additionally, the TCA cycle is interrupted at several points in glycolytic cells, resulting in the build-up of metabolites that are essential for the regulation of inflammatory responses. Changes in metabolites impact protein expression and function through regulation of transcription factor activity, mRNA translation, histone acetylation and post-translational modifications including succinylation and glycosylation<sup>156,279,280</sup>. The accumulation of succinate is of particular interest, since it benefits the protein stability of the metabolically critical transcription factor hypoxia-inducible factor 1 $\alpha$  (HIF-1 $\alpha$ )<sup>156</sup>. In turn, HIF-1 $\alpha$  induces the expression of glycolytic genes, thereby stimulating glycolytic metabolism<sup>281</sup>.

### 3.2.2 HIF-1 $\alpha$ activity is regulated through a constitutively active degradation pathway.

HIF-1 $\alpha$  binds to hypoxia responsive elements (HRE) in the promoter region of target genes and is essential for expression of inflammatory cytokines, production of host-protective eicosanoids, and cell-intrinsic control of bacterial replication (154). Despite its clear role in the macrophage antimicrobial program, no studies have successfully investigated how HIF-1 $\alpha$  promotes cell-intrinsic control of *M. tuberculosis* infection. HIF-1 $\alpha$  functions as master regulator in infected IFN- $\gamma$  activated macrophages, making it challenging to identify individual pathways that contribute to cell-intrinsic control. Furthermore, the factors that regulate HIF-1 $\alpha$  levels in the cell during *M. tuberculosis* infection are still unclear. HIF-1 $\alpha$  is constitutively transcribed and

translated in macrophages, but also quickly degraded with a half-life of less than five minutes. Degradation of HIF-1 $\alpha$  is mediated through the activity of the HIF-1 $\alpha$  negative regulators prolyl hydroxylases (PHD) (Supplemental Figure 3.1). In the presence of oxygen, PHD proteins are active and hydroxylate HIF-1 $\alpha$ , thereby marking it for recognition by the E3 ubiquitin ligase complex containing von Hippel-Lindau (VHL). Subsequent ubiquitylation of HIF-1 $\alpha$  results in recognition and degradation by the proteasome. Interestingly, HIF-1 $\alpha$  escapes degradation and is “stabilized” upon *M. tuberculosis* infection in the presence of IFN- $\gamma$  at normal oxygen levels<sup>155</sup>, indicating the presence of oxygen-independent regulatory pathways in macrophages. Recently, it was shown that HIF1 $\alpha$  contains a chaperone-mediated autophagy (CMA) targeting motif that identifies CMA substrates<sup>282</sup>. The CMA pathway of protein degradation also relies on ubiquitylation for protein recognition and transports proteins to the lysosome where they are degraded by proteases. Identification of the proteins involved in this regulatory pathway in macrophages will also identify potential target proteins downstream of IFN- $\gamma$  signaling that mediate HIF-1 $\alpha$  stabilization during infection.

**3.2.3 IFN- $\gamma$  regulates the expression of metabolite transporters.** IFN- $\gamma$  dependent changes in macrophage metabolism requires solute carrier (SLC) transporters to mediate metabolite transport across membranes. Mammalian cells express over 300 individual SLC transporters with overlapping functions<sup>283</sup>. They are found on different cellular membranes, including the plasma membrane, phagosome, Golgi and ER and are required for a multitude of different cell processes. In contrast to ABC transporters, the majority of SLC transporters utilize electrochemical or ion gradients for transport and do not depend on adenosine triphosphate (ATP)<sup>283</sup>. An example that illustrates how SLC transporters are involved in macrophage metabolism is the transport of glucose by SLC2a1. Glucose import is essential for upregulation of glycolytic genes<sup>284</sup> and maintenance of the glycolytic flux in pro-inflammatory macrophages. Furthermore, succinate production during glycolytic flux results in stabilization of HIF-1 $\alpha$  protein levels, which in turn upregulates *Slc2a1* expression and further stimulates glycolytic metabolism<sup>281</sup>. Interestingly, SLC transporters have not been well studied in the context of macrophage metabolism in response to infection. This study aims to identify the SLC transporters that are regulated by IFN- $\gamma$  signaling and are required for cell-intrinsic control. We hypothesize that there are several IFN- $\gamma$  dependent processes in which SLC transporters contribute to the cell intrinsic control of *M. tuberculosis*. First, macrophages rely on metabolite import by SLC transporters to support their metabolic needs during infection and perform antimicrobial functions. Second, SLC transporters might restrict essential nutrients from *M. tuberculosis* in the phagosome by efflux of metabolites from the phagosome into the cytosol. Third, SLC transporters might have an antimicrobial function by creating a toxic environment for *M. tuberculosis* within the phagosome. Evidence for the latter was shown in a study with *S. aureus* that demonstrated that the lack of SLC4a7 on the macrophage plasma membrane resulted in the impaired influx of bicarbonate and inability of the cell to maintain the cytoplasmic pH. The subsequent loss of the pH gradient between the cell cytosol and the phagosome leads to impaired phagosome acidification and resulted in the survival of the pathogen<sup>285</sup>. This chapter focuses on the contribution of macrophage metabolism to the control of *M. tuberculosis* infection. It investigates the possible pathways involved in HIF-1 $\alpha$  regulation in macrophages and aims to make a connection between IFN- $\gamma$ -dependent control of infection and the metabolic requirements in activated macrophages. We hypothesize that metabolic changes in IFN- $\gamma$  activated macrophages can directly impact bacterial growth. In order to identify the

metabolite transporters that are required for bacterial restriction, mass spectrometry and RNAseq datasets were used to characterize IFN- $\gamma$  and HIF-1 $\alpha$  signaling in macrophages, followed by the generation of a CRISPR knockout library targeting all macrophage-expressed *Slc* genes.

### 3.3 Results

**3.3.1 HIF-1 $\alpha$  protein levels are stabilized by inhibition of lysosomal acidification.** IFN- $\gamma$  signaling is essential for control of *M. tuberculosis* infection in macrophages (Figure 3.1 A). Over the course of several days, *M. tuberculosis* grows unrestricted inside macrophages. However, bacterial growth is completely inhibited in the presence of IFN- $\gamma$ . IFN- $\gamma$ -dependent intrinsic control of infection is partially dependent on HIF-1 $\alpha$  expression<sup>155</sup>. HIF-1 $\alpha$  protein levels are stabilized during *M. tuberculosis* infection in the presence of exogenous IFN- $\gamma$  (Figure 3.1 B). HIF-1 $\alpha$  stabilization is also dependent on nitric oxide (NO) production, since inhibition of inducible nitric oxide synthase (iNOS) reduces HIF-1 $\alpha$  levels in a dose-dependent manner (Figure 3.1 B)<sup>146</sup>. However, it is unclear how low HIF-1 $\alpha$  protein levels are maintained in resting macrophages. Previously established models of HIF-1 $\alpha$  regulation in human and murine cell lines show that HIF-1 $\alpha$  is first hydroxylated by PHDs and subsequently degraded by the proteasome. To determine if HIF-1 $\alpha$  degradation depends on proteasome activity in macrophages, bone marrow-derived macrophages were treated with several proteasome inhibitors with varying affinities and HIF-1 $\alpha$  protein levels were assessed by Western blot. MG132 is a potent and widely used reversible proteasome inhibitor, but it inhibits calpains and lysosomal cathepsins at higher concentrations. Lactacystin is an irreversible and more specific inhibitor of the proteasome, targeting the threonines in the proteasomal active site as well as some serine proteases, including cathepsin A. Epoxomicin is one of the most selective proteasome inhibitors and does not affect other proteolytic enzymes. As shown in Figure 3.2 A, HIF-1 $\alpha$  protein is present at baseline levels in resting macrophages. As expected, HIF-1 $\alpha$  stabilization is increased during TLR2 stimulation by PAM3CSK4 in combination with exogenous IFN- $\gamma$  stimulation. Macrophages incubated with MG132 show a dose-dependent increase in HIF-1 $\alpha$  stabilization, whereas more specific proteasome inhibitors epoxomicin or lactacystin do not increase HIF-1 $\alpha$  levels (Figure 3.2A, D). This suggests that HIF-1 $\alpha$  degradation is not dependent on the proteasome in resting macrophage and instead involves the activity of proteases that could be present within lysosomes. Indeed, inhibition of lysosomal acidification by Bafilomycin A, a pharmacological inhibitor of the lysosomal V-ATPase, results in a dose-dependent increase of HIF-1 $\alpha$  protein levels, suggesting that HIF-1 $\alpha$  is degraded through a lysosomal pathway in these cells (Figure 3.2B). Stabilization of HIF-1 $\alpha$  protein levels was also observed when autophagosome-lysosome fusion was inhibited by chloroquine (Figure 3.2 C).

Classically, proteasome-dependent HIF-1 $\alpha$  degradation has been shown to require PHD function. However, the presence of DMOG, a direct inhibitor of PHD, also results in increased HIF-1 $\alpha$  protein levels in bone marrow derived macrophages (Figure 3.2 B), suggesting that PHD are required for proteasome-independent HIF-1 $\alpha$  regulation. Interestingly, a combination of DMOG and lysosomal inhibitor bafilomycin A or chloroquine resulted in higher HIF-1 $\alpha$  protein levels compared to the individual compounds, supporting that PHDs as well as the lysosome are both actively involved in HIF-1 $\alpha$  degradation in macrophages (Figure 3.2C). Indeed, inhibiting PHD or the lysosome results in increased expression of HIF-1 $\alpha$  target genes *Bnip3*, *Pfkfb3* and *Il1b*,

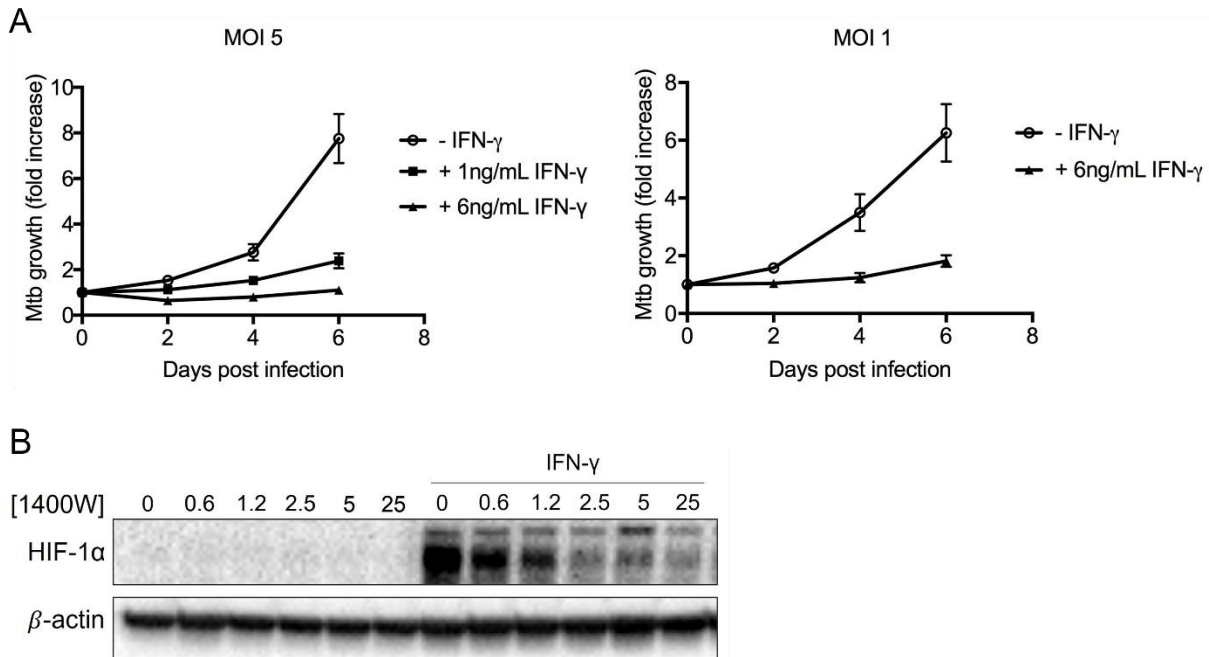


**Figure 3.1. Interferon- $\gamma$  signaling restricts *M. tuberculosis* growth in macrophages.**

(A) BMDM were infected with luciferase-expressing *M. tuberculosis* and bacterial growth was determined by relative light units over the course of several days in the presence or absence of IFN- $\gamma$ . Bacterial growth was normalized to the initial infectious dose. (B) HIF-1 $\alpha$  Western blot of lysates prepared from PAM3CSK4 and IFN- $\gamma$ -activated BMDM with a dose response of 1400W ( $\mu$ M).

whereas epoxomicin treatment does not result in HIF-1 $\alpha$ -dependent gene expression (Figure 3.2 E). Surprisingly, proteasome inhibition through epoxomicin seems to prevent up HIF-1 $\alpha$  accumulation in the presence of PHD inhibitors (Figure 3.2 C) and in TLR2 with IFN- $\gamma$  stimulated cells (Figure 3.2 D). Blocking proteasome activity can lead to an acute increase of CMA-dependent protein turnover<sup>286</sup>, which could explain the increased HIF-1 $\alpha$  degradation.

### 3.3.2 Ubiquitin ligase VHL is involved in an uncanonical HIF-1 $\alpha$ degradation pathway.

Proteins that are targeted for degradation by the ubiquitin-proteasome system are canonically post-translationally modified with lysine 48 (K48)-conjugated ubiquitin chains. In contrast, lysine 63 (K63) ubiquitin chains mainly provide signals for trafficking to lysosomal compartments<sup>287</sup>. To identify which ubiquitin linkages are present on HIF-1 $\alpha$ , immunoprecipitation of HIF-1 $\alpha$  was performed on cell lysates of resting macrophages followed by probing for the presence of K48 and K63 linkages. As shown in Supplemental Figure 3.2, the input fraction shows clear build-up of K48-labeled proteins when the proteasome was inhibited by epoxomicin. Nevertheless, HIF-1 $\alpha$  levels were not specifically enriched in epoxomicin-treated cells, confirming that proteasome inhibition does not prevent degradation of HIF-1 $\alpha$ . Unfortunately, neither K48 nor K63 HIF-1 $\alpha$ -specific labeling was detected in resting macrophages, possibly due to quick turnover of ubiquitin-labeled proteins. One of the E3 ubiquitin ligases that has been described to recognize and ubiquitylate HIF-1 $\alpha$  upstream of proteasomal degradation is VHL. To determine if HIF-1 $\alpha$  regulation in macrophages occurs independently of VHL, BMDM lacking VHL were generated by CRISPR knockout. Surprisingly, resting BMDM lacking VHL show a significant increase in HIF-1 $\alpha$  protein levels

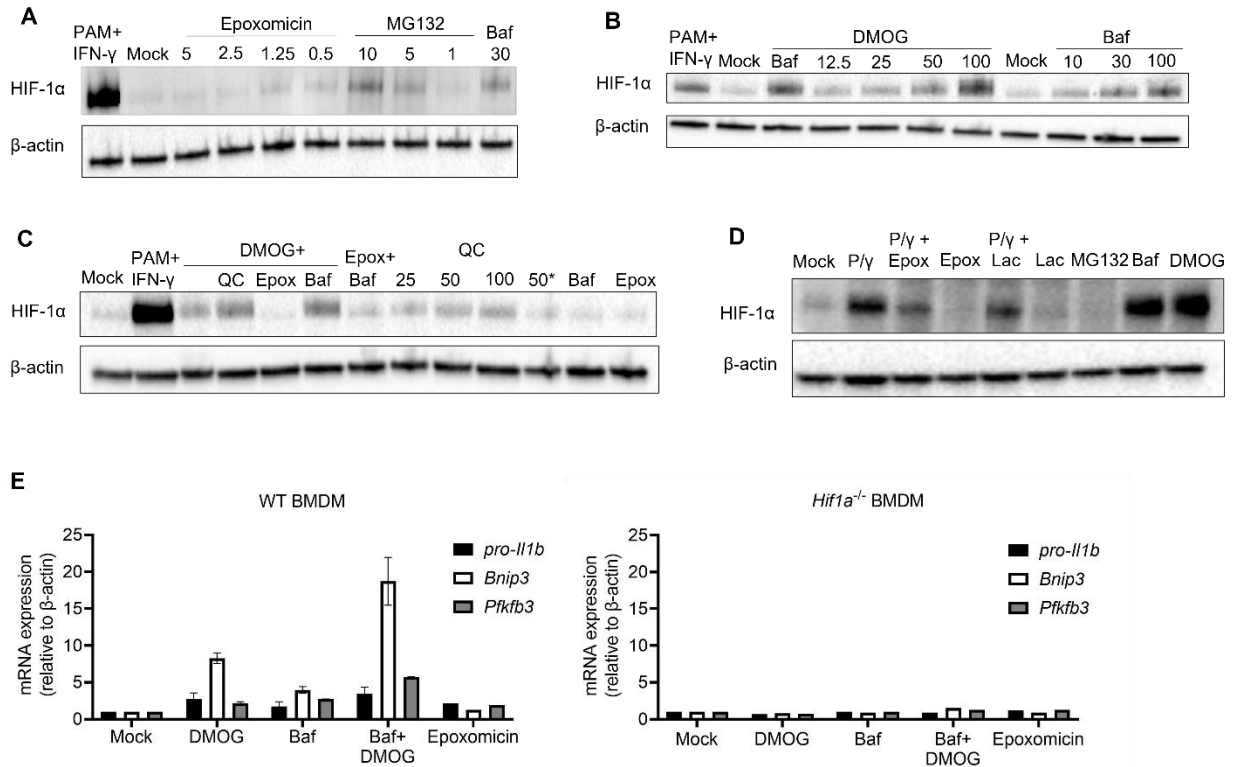


**Figure 3.2. HIF-1 $\alpha$  degradation in macrophages is inhibited by lysosomal inhibitors.**

Western blot for HIF-1 $\alpha$  in resting BMDM (mock) or BMDM treated with Pam3CSK4 and interferon- $\gamma$  (PAM+IFN- $\gamma$ ), DMOG, lysosomal inhibitors bafilomycin (Baf) and chloroquine (CQ) or proteasomal inhibitors epoxomicin (Epo), MG132 and Lactacystin (Lac) for 8 hours (A-D). Gene expression fold change of the indicated genes after treatment of wildtype and HIF-1 $\alpha$ <sup>-/-</sup> BMDM with inhibitors for 8h (E).

(Figure 3.3 A), indicating that VHL is involved in constant turn-over of the protein in a proteasome-independent manner.

### 3.3.3 Enhanced HIF-1 $\alpha$ -dependent NO production results in increased bacterial restriction.

HIF-1 $\alpha$  stabilization and signaling results in increased NO production by (iNOS), which is essential for IFN- $\gamma$ -dependent intrinsic control. To determine if increased HIF-1 $\alpha$  levels in *Vhl* knockout cells have an impact on NO production, NO levels were quantified in the supernatant of *Vhl* knockout cells through measurement of nitrite, a stable and nonvolatile breakdown product of NO. *Vhl* knockout cells produced more NO compared to wildtype cells when they are infected with *M. tuberculosis* and activated with IFN- $\gamma$  (Figure 3.3 B). Furthermore, *Vhl* knockout cells require higher concentrations of iNOS inhibitor 1400W to block NO production compared to wildtype cells. To determine whether intrinsic control of infection is enhanced by increased basal levels of HIF-1 $\alpha$  and NO, *Vhl* knockout BMDM were infected with *M. tuberculosis* and bacterial growth was quantified over the course of several days. In resting macrophages, *M. tuberculosis* grows significantly more in VHL-expressing control cells compared to *Vhl* knockout cells (Figure 3.3 C), most likely due to the increased basal level of HIF-1 $\alpha$  and NO in the *Vhl* knockout cells. There is no further increase in growth when NO synthesis is inhibited. Furthermore, the presence of exogenous IFN- $\gamma$  results in bacterial restriction in both cell types, with enhanced restriction in the *Vhl* knockout cells. This restriction

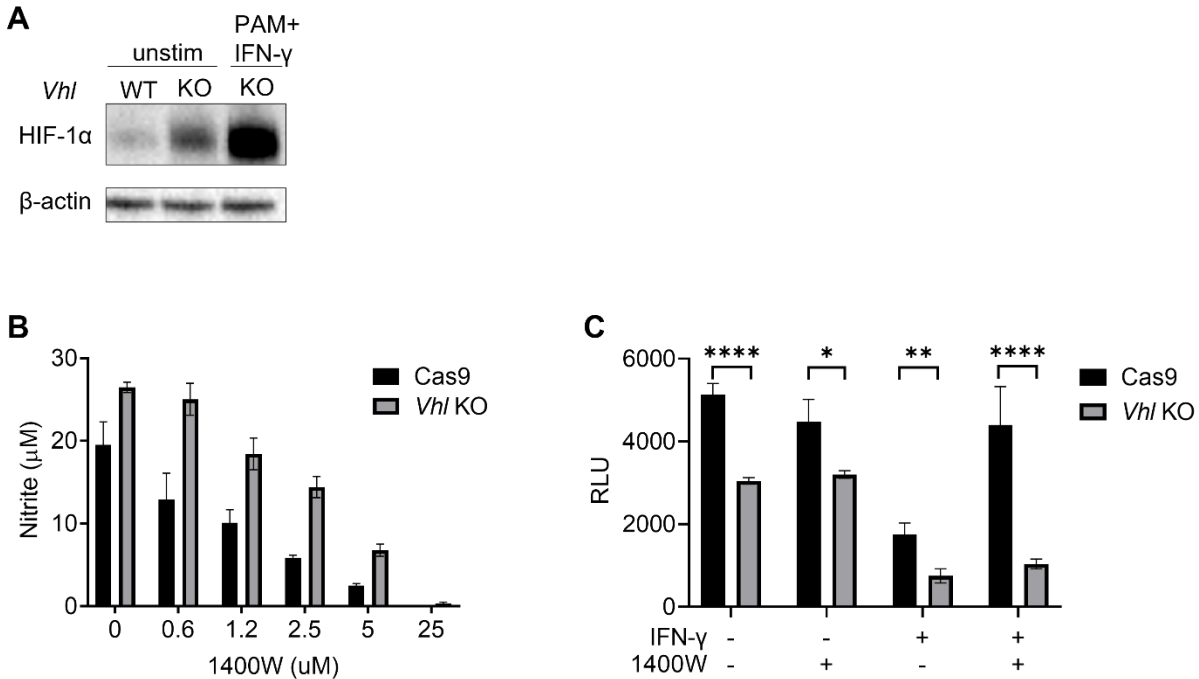


**Figure 3.3. VHL is required for HIF-1 $\alpha$  degradation and control of infection.**

Western blot for HIF-1 $\alpha$  in Cas9-expressing BMDM or *Vhl* CRISPR knockout BMDM in the presence or absence of IFN- $\gamma$  (A). BMDM were grown in 200ul in 96-well plates and infected with *M. tuberculosis* strain Erdman expressing the *luc* operon at MOI 5. BMDM were incubated with indicated concentrations of 1400W through infection and nitrite levels were quantified in the supernatant at 24hr by Griess assay (B). Growth of *M. tuberculosis* was assessed at 72hr by relative light units (RLU). The *p* values were determined using a one-way ANOVA. \**p* < 0.05, \*\**p* < 0.005, \*\*\*\**p* < 0.0001.

depends on NO production, since blocking iNOS results in loss of control in the wildtype cells, whereas the *Vhl* knockout cells still restrict bacterial growth at these inhibitor concentrations.

**3.3.4 HIF-1 $\alpha$  regulates expression of metabolite transporters.** In order to identify changes in the macrophage proteome that are required to mount an IFN- $\gamma$  and HIF-1 $\alpha$  dependent antimicrobial response to *M. tuberculosis* infection, wildtype and *Hif1 $\alpha$ <sup>-/-</sup>* bone marrow-derived macrophages were infected with *M. tuberculosis* in the presence or absence of IFN- $\gamma$  and protein expression was assessed by mass spectrometry. As predicted, iNOS (*Nos2*) is one of the significantly enriched proteins downstream of IFN- $\gamma$  signaling and protein levels depend on expression of HIF-1 $\alpha$  (Figure 3.4 A,B). To identify pathways under the control of IFN- $\gamma$  signaling, functional pathway enrichment analysis was performed with the bioinformatics pipeline Metascape. As expected, highly enriched pathways include metabolic responses, including gluconeogenesis, IL-1 regulation and detoxification of reactive oxygen species (Figure 3.4 C). The proteomics measurements were compared with an existing transcriptomics dataset from previous experiments (Braverman et al. 2016)<sup>155</sup>. Indeed, many of the enriched proteins that were found in the mass spectrometry analysis show increased expression levels in the presence of IFN- $\gamma$  (Figure 3.4 D) and several genes depend on HIF-1 $\alpha$  expression. Interestingly, mass spectrometry revealed that multiple transporters, including SLCs and chloride intracellular channels (CLICs), and guanylate binding proteins (GBPs) are enriched in IFN- $\gamma$  activated macrophages.

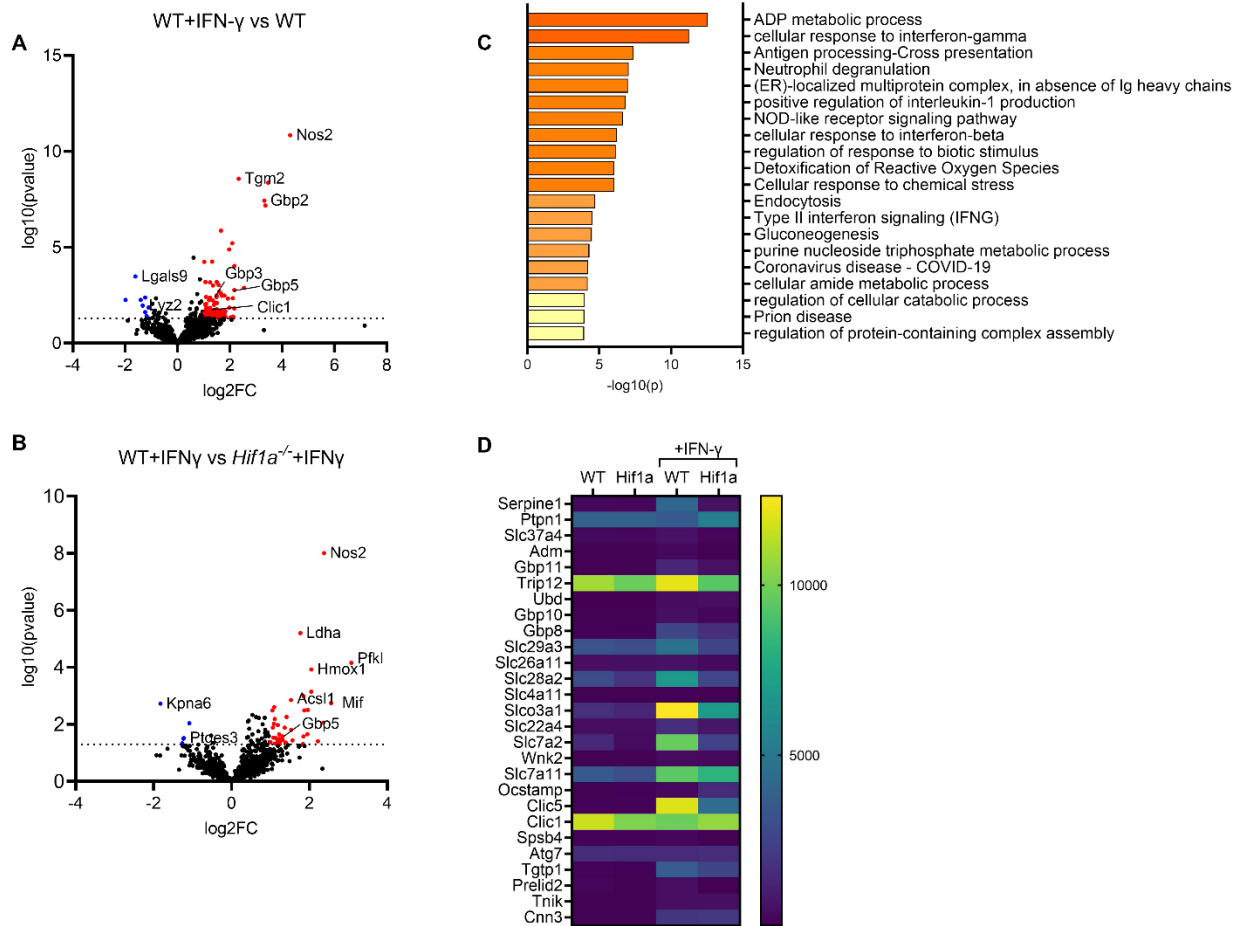


**Figure 3.4. HIF-1 $\alpha$  regulates expression of metabolite transporters downstream of IFN- $\gamma$  signaling.**

Wildtype and HIF-1 $\alpha$ <sup>-/-</sup> BMDM were infected with *M. tuberculosis* at MOI 5 in the presence or absence of IFN- $\gamma$  for 72 hours. Cell lysates were prepared for mass spectrometry. Protein abundance is plotted comparing wildtype infected cells in the presence or absence IFN- $\gamma$  (A) or infected IFN- $\gamma$ -activated wildtype and HIF-1 $\alpha$ <sup>-/-</sup> cells (A). Proteins with a log<sub>2</sub> fold change greater than 1 are colored red. Proteins with a log<sub>2</sub> fold change less than -1 are colored blue. Proteins with a *p* value less than 0.05 (or -log<sub>10</sub>(*p* value) greater than 1.3) are above the horizontal dotted line. (C) Enriched pathways based on protein abundance in WT BMDM in the presence or absence of IFN- $\gamma$ . (D) Relative gene expression in resting or IFN- $\gamma$ -activated BMDM infected with *M. tuberculosis* derived from wildtype or *Hif1 $\alpha$ <sup>-/-</sup>* mice.

**3.3.5 GBP activity does not benefit the host during *M. tuberculosis* infection.** GBPs have been implicated in mycobacterial infections in both mice and humans. Control of *Mycobacterium bovis* BCG infection in mice requires *Gbp1* expression<sup>148</sup>. Furthermore, latently infected human patients that transition to active disease show a gene expression signature containing *GBP1*. The highly enriched genes in the mass spectrometry dataset included *Gbp2*, *Gbp4*, *Gbp6* and *Gbp10*. To study the role of GBPs in intrinsic control of infection, BMDM from several *Gbp* knockout mice were infected *M. tuberculosis* and additional GBPs were knocked out *in vitro* with CRISPR. A lack of *Gbp2* results in a slight increase in bacterial growth, but IFN- $\gamma$  induced control of infection is not affected. Absence of *Gbp6* also does not result in loss of control (Figure 3.5 A). Furthermore, CRISPR deletion of *Gbp10* or *Gbp4* did not result in differences in

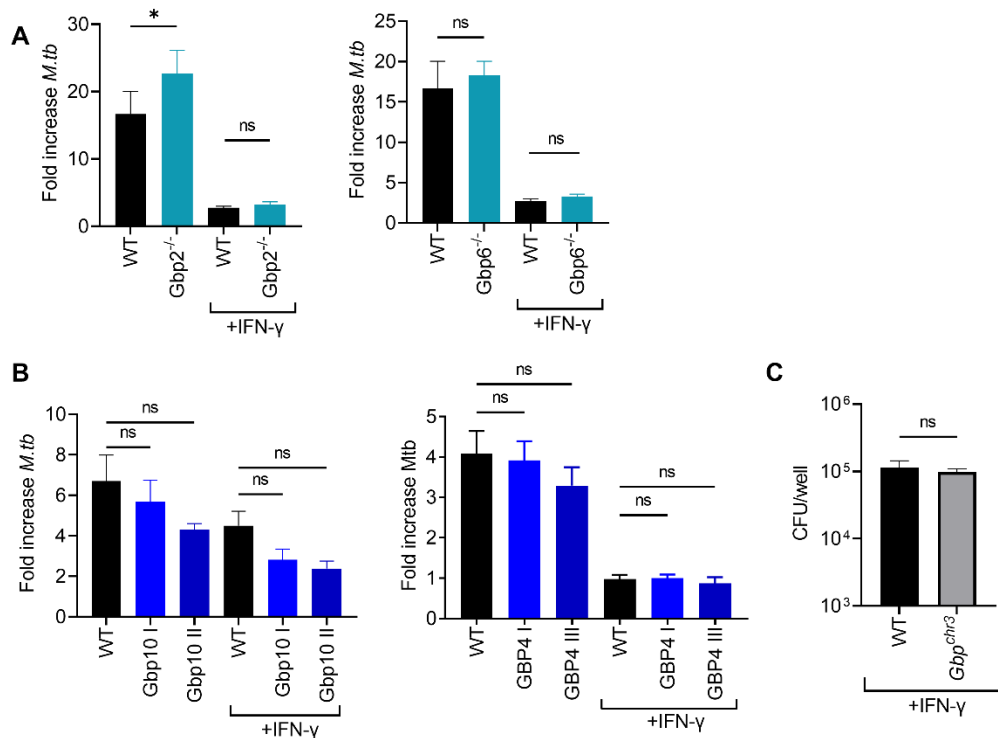


**Figure 3.5. Lack of individual GBPs does not impair intrinsic control of *M. tuberculosis* infection in macrophages.**

(A) BMDM from mice lacking *Gbp2* or *Gbp6* were harvested, differentiated and infected with *M. tuberculosis* strain Erdman expressing the *luciferase* (*luc*) operon in the presence or absence of IFN- $\gamma$  for 4 to 6 days, respectively. Fold increase in growth was determined based on infection levels on the day of infection. (B) Resting or IFN- $\gamma$ -activated BMDM were infected with *luc*-expressing Erdman. CRISPR was used to knockout *Gbp10* or *Gbp4* in BMDM with two independent sgRNA. (C) BMDM from *Gbp3<sup>Chr3</sup>* knockout mice were infected with *M. tuberculosis* strain Erdman at MOI 5 in the presence of IFN- $\gamma$  and bacterial growth was assessed after 3 days by preparing macrophage cell lysates and plating for counting colony forming units (CFU). Statistical significance was determined using a Mann-Whitney U test (A, C) or Kruskal Wallis ANOVA (B),  $p$  value < 0.05.

bacterial growth (Figure 3.5 B), indicating that these genes are not important for restriction of *M. tuberculosis* infection or that other GBPs have redundant functions and can compensate for individual deletions. To address potential functional redundancy among GBPs, BMDM lacking all GBPs on chromosome 3, namely GBP1, 2, 3, 5 and 7, were challenged with *M. tuberculosis* and bacterial growth was enumerated by colony forming units (CFU). Nevertheless, deletion of multiple GBPs did not result in increased susceptibility in the presence of IFN-g (Figure 3.5 C), suggesting that these genes might carry out a different function during *M. tuberculosis* infection, compared to *M. bovis* infection.

### 3.3.6 Identifying the role of SLC transporters in IFN- $\gamma$ dependent cell-intrinsic control.

Another family of genes that was enriched in the mass spectrometry data included *Slc* transporters. In particular, the arginine transporter gene *Slc7a2* is highly dependent on IFN- $\gamma$  signaling and HIF-1 $\alpha$  expression. SLC7a2 functions by importing arginine, a substrate required for NO production by iNOS. As a proof of concept, *Slc7a2* was deleted by CRISPR, and knockout cells show a trend towards loss of intrinsic control of infection in the presence and absence of IFN- $\gamma$  (Figure 3.6 A). Deletion of other genes encoding SLC, kinases or transporters



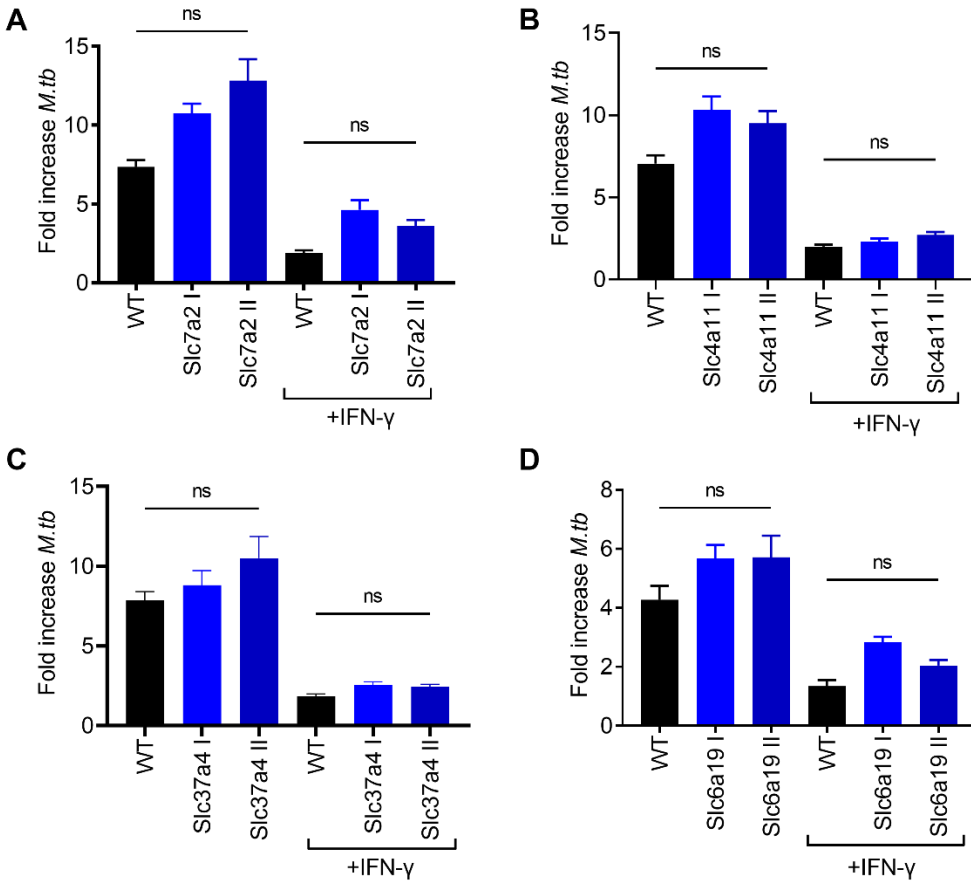


**Figure 3.6. Slc gene expression do not contribute to IFN- $\gamma$  dependent control of infection.**

Relative growth of luciferase-operon expressing *M. tuberculosis* determined by RLU in resting or IFN- $\gamma$ -activated BMDM at 4 days post infection (A-D). Statistical significance was determined using a Kruskal Wallis ANOVA, *p* value < 0.05.

resulted in minimal to no difference in bacterial growth, suggesting that these genes are not involved in IFN- $\gamma$  dependent control of infection (Figure 3.6 B-D and Supplemental Figure 3.3). However, the lack of involvement of each gene might be obscured by functional redundancy among SLC as well as incomplete mutation of the gene introduced by Cas9 across the population of cells. Nevertheless, the obvious IFN- $\gamma$  dependent regulation of this family of genes indicates that they may contribute somehow to antimicrobial responses. To determine which transporters are essential during infection, an unbiased CRISPR approach was developed in Cas9-expressing conditionally immortalized macrophages (CIM), a gift from Gregory Barton at UC Berkeley<sup>288</sup>. The advantage of this cell type over primary cells is the ability to generate a CRISPR knockout macrophage library that can be propagated, sequenced and repeatedly used for large-scale assays. Comparing the lentiviral transduction efficiency in CIM with BMDM and THP-1 cells revealed that CIM had the lowest transduction efficiency out of the three cell types, indicating the need for a stringent antibiotic knockout selection and subsequent outgrowth of knockout cells (Supplemental Figure 3.4). The RNAseq dataset was used to determine which *Slc* genes are expressed in BMDM, generating a list of 196 *Slc* genes. A CRISPR deletion library containing 10 unique sgRNA targeting each *Slc* gene was created using sgRNA sequences from the publicly available dataset from Morgens *et al.*, 2017<sup>289</sup>. In addition to the *Slc*-targeting sgRNAs, the library also contains known IFN- $\gamma$  regulated control genes (*Ifngr1*, *Hif1a*, *Nos2*, *Stat1*, *Jak1* and

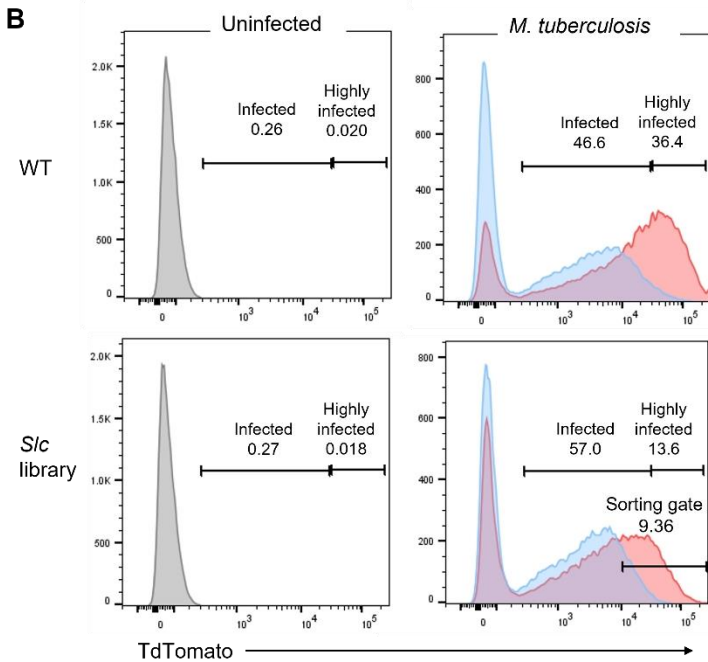
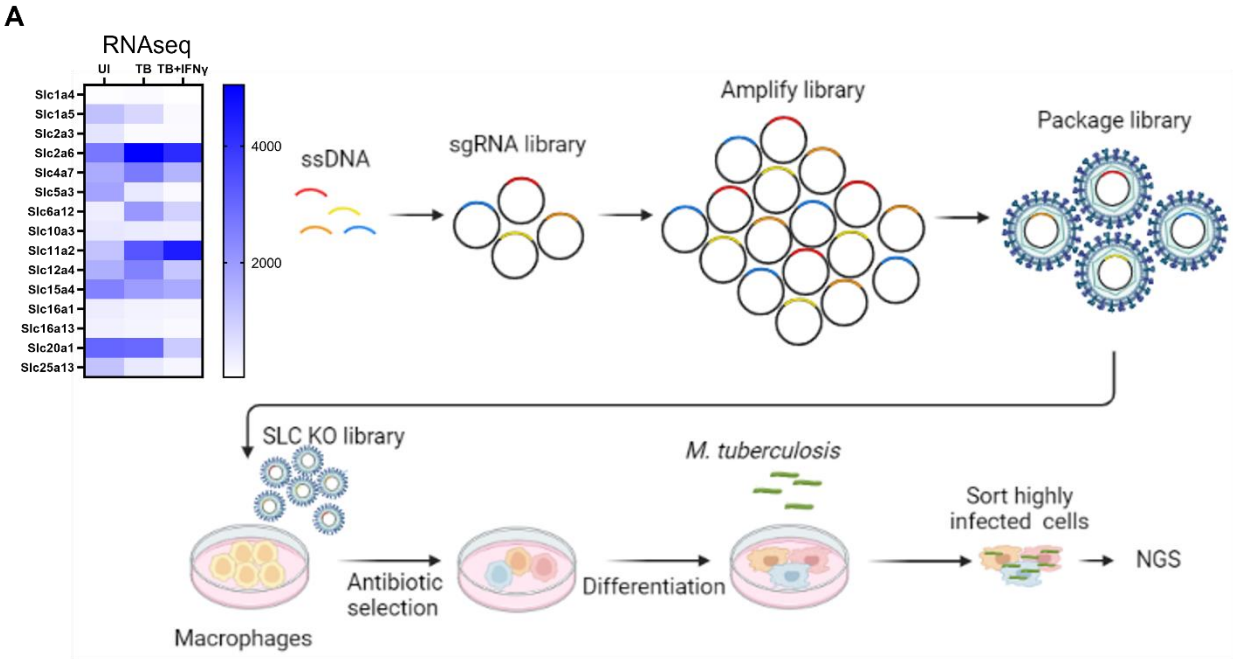


**Figure 3.7. Model of forward genetics screen to identify *Slc* genes that are required for IFN- $\gamma$  dependent control of infection.**

(A) A sgRNA library was generated based on all *Slc* genes expressed in BMDM. ssDNA molecules encoding the sgRNA sequences were cloned into a lentiviral expression vector and amplified for packaging into lentivirus particles. CIM were transduced with lentivirus and selection for successful viral delivery was performed by antibiotic selection. Differentiation of the cells into a M1 macrophage like state and subsequent infection with tdTomato-expressing *M. tuberculosis* allows for the sorting for highly infected IFN- $\gamma$ -activated CIM and the identification of *Slc* gene that contribute to restriction of bacterial growth. (B) Representation of uninfected CIM (grey) or *M. tuberculosis*-infected resting (red) and IFN- $\gamma$ -activated (blue) CIM at 5 days post infection. Cells were

infected with tdTomato-expressing strain Erdman at MOI 5. The sorting gate indicates ~10% most highly infected cells in IFN- $\gamma$ -activated CIM.

*Jak2*), 1000 non-targeting controls and 1000 sgRNA targeting non-functional, non-genic regions to minimize any off-target and non-specific effects. The sgRNA were cloned into the pLentiGuidePuro expression vector packaged into lentivirus particles for transduction of CIM. The CIM knockout library was then amplified and can be used for macrophage differentiation followed by *M. tuberculosis* infection with a fluorescent strain in the presence of IFN- $\gamma$  (Figure 3.7 A). The goal of this study is to sort the 10% most highly infected cells, assuming that these knockout cells are no longer capable of controlling the infection. Sequencing of the sorted cells will indicate which genes are required for restriction of bacterial growth and will be confirmed by further screening assays. As shown in Figure 3.7 B, cells contain a very high bacterial burden after 5 days of infection in the absence of IFN- $\gamma$ . In contrast, the presence of IFN- $\gamma$  results in a clear restriction of bacterial growth and greater proportion of cells with a low bacterial burden, indicating that bacterial growth is efficiently inhibited. The *Slc* knockout library shows fewer highly infected cells in the absence of IFN- $\gamma$  (13.6% vs 36.4%), suggesting that the lack of certain *Slc* might contribute to control of infection. Together these data suggest that this approach can discriminate between wildtype cells and cells that can no longer respond to IFN- $\gamma$  and will be a valuable tool to investigate host genetics during *M. tuberculosis* infection.

**3.4 Discussion.** The current study demonstrates that HIF-1 $\alpha$  is degraded by a pathway that requires lysosome acidification. Furthermore, this pathway solely depends on lysosomal-dependent protein degradation since inhibition of the proteasome with various inhibitors fails to induce HIF-1 $\alpha$  protein stabilization. In addition, this degradation pathway requires the activity of VHL and PHD proteins, which are classically associated with proteasome-degradation. Taken together, these data suggest the presence of a non-canonical regulatory process of HIF-1 $\alpha$  protein expression in resting macrophages.

The involvement of VHL in lysosomal-dependent degradation is surprising and suggest the participation of additional ubiquitin ligases that can target HIF-1 $\alpha$  to the lysosome. VHL forms a complex that includes scaffold Cullin-2 and E3 ubiquitin RING ligase Rbx1<sup>290</sup>, resulting in the addition of K48-linked ubiquitin chains to proteins that require targeting to the proteasome. However, it is possible that VHL interacts with another E3 ubiquitin ligase that adds K63 linkages that targets HIF-1 $\alpha$  for lysosomal degradation. In addition, another ubiquitin ligase that has been implicated in CMA-dependent degradation of HIF-1 $\alpha$  is CHIP (C-terminus of Hsc70-interacting protein)<sup>282,291,292</sup>. CHIP has a broad substrate range and can target proteins to the ubiquitin-proteasome system as well as to autophagy due to its ability to bind different chaperones<sup>293</sup>. CHIP is expressed in BMDM (data not shown) and could act in conjunction with VHL to add mixed K48 and K63 ubiquitin chains onto HIF-1 $\alpha$  that target it for degradation to the lysosome. There is precedent for the cooperation of E3 ubiquitin ligases for the formation of mixed ubiquitin chains in yeast<sup>287</sup>. Identifying which factors are required for HIF-1 $\alpha$  degradation could reveal potential targets downstream of IFN- $\gamma$  signaling that are modified to allow for HIF-1 $\alpha$  protein stabilization during infection, including deubiquitylation enzymes that could reverse the ubiquitin chains added to HIF-1 $\alpha$  by VHL.

Consistent with previous studies, we found that HIF-1 $\alpha$  expression depends on the presence of NO. Furthermore, increased levels of NO induced HIF-1 $\alpha$  stabilization and enhanced the capacity of macrophages to restrict *M. tuberculosis* growth. We hypothesize that NO mediates the increase in HIF-1 $\alpha$  stabilization through protein S-nitrosylation. Protein S-

nitrosylation occurs through covalent addition of an NO group to a thiol group on protein cysteine residues and this modification can either activate or inactivate proteins<sup>294</sup>. It has been demonstrated that S-nitrosylation can occur on HIF-1 $\alpha$  directly, enhancing its binding to transcriptional coactivator p300 and resulting in increased target gene expression<sup>295,296</sup>. Other S-nitrosylation candidates include PHDs and VHL. It has been shown that iNOS blocks PHD function in vitro, thereby stabilizing HIF-1 $\alpha$  in normoxic conditions<sup>297</sup>. Another study showed that PHD2 is nitrosylated after stimulation of the RAW macrophage cell-line with LPS and IFN- $\gamma$ <sup>298</sup>, indicating that PHDs could become inactivated by S-nitrosylation. A direct effect of iNOS on VHL has not been studied but it has been shown that the E3 ubiquitin ligase Parkin can be S-nitrosylated and subsequently inactivated<sup>294</sup>.

This study confirms that HIF-1 $\alpha$  regulates the expression of many proteins, including proteins from the GBP and SLC families. Loss of *Gbp* expression in macrophages did not result in loss of intrinsic control of infection, indicating that GBPs are not essential for mediating bacterial restriction. Indeed, recent studies in mice lacking several *Gbp* genes (*Gbp1*, *Gbp2*, *Gbp3*, *Gbp5* and *Gbp7*) are only mildly more susceptible to *M. tuberculosis* infection<sup>149</sup>. In addition, targeted deletion of several kinases, ubiquitin ligases and individual metabolite transporters did not have a significant impact on bacterial growth. There are several possible explanations for these results. First, these proteins might not have an antimicrobial function during *M. tuberculosis* infection. Second, there might be functional redundancy among proteins, which seems likely for the SLC transporters. Third, the luciferase assay is not sensitive enough to detect small phenotypes downstream of HIF-1 $\alpha$  signaling. Nevertheless, the clear enrichment of SLC genes in mass spectrometry assays and RNAseq data, as well as their essential function in macrophage metabolism makes these interesting candidates to investigate further with alternative approaches. We decided to study their role in IFN- $\gamma$  dependent control of infection with a forward genetic approach based on a sensitive flow cytometry sorting method. As our preliminary data demonstrates, there is a clear distinction in bacterial burden between resting CIM and IFN- $\gamma$ -activated CIM after five days of infection, showing promise for the identification of gene knockouts that result in loss of bacterial control.

### 3.5 Materials and Methods.

#### **Bacterial culture**

The *M. tuberculosis* strain Erdman was used for all experiments. *M. tuberculosis* was grown in Middlebrook 7H9 liquid media supplemented with 10% albumin-dextrose-saline, 0.4% glycerol, and 0.05% Tween 80 or on solid 7H10 agar plates supplemented with 10% Middlebrook OADC (BD Biosciences) and 0.4% glycerol. The luciferase expressing strain of *M. tuberculosis* used for measuring bacterial growth was derived from an Erdman strain and was cultured as described above.

#### **In vitro infections**

BMDM were plated into 96-well or 24-well plates with  $5 \times 10^4$  and  $3 \times 10^5$  macrophages/well, respectively, and were allowed to adhere and rest for 24 h. BMDM were then treated with vehicle or IFN- $\gamma$  (6.25 ng/ml) overnight and infected in DMEM supplemented with 5% horse serum and 5% FBS at a multiplicity of infection of 5, unless otherwise noted. After a 4h phagocytosis period, infected BMDM were washed with PBS before replacing with BMDM media. For experiments with DMOG, Bafilomycin, Epoxomicin, Lactacystin and MG132, these reagents were added to the BMDM media after the 4 h phagocytosis. For IFN- $\gamma$ -pretreated wells, IFN- $\gamma$  was also added post-infection at the same concentration. To measure intracellular growth of *M. tuberculosis*, cells were infected with an Erdman strain expressing the luciferase operon and luminescence was measured at 32°C immediately following the 4 h phagocytosis, PBS wash, and media replacement. Luminescence was then read again at the noted time points. All growth was normalized to day 0 luminescence readings for each infected well and is presented as fold change in luminescence compared with day 0. For enumeration of CFU, *M. tuberculosis* Erdman strain was used; infected BMDM were washed with PBS and lysed in water with 0.1% Triton X-100 for 10 min; and serial dilutions were prepared in PBS with 0.05% Tween 80 and were plated onto 7H10 plates.

#### **Griess assays**

The Griess reaction was used to detect nitrite in the supernatants of BMDM as a proxy for NO production. Briefly, a solution of 0.2% naphthylethylenediamine dihydrochloride was mixed 1:1 with a 2% sulfanilamide, 4% phosphoric acid solution. Supernatant from cultured cells was added to this mixture in a 1:1 ratio, and absorbance was measured at 546 nm. Concentrations were determined by comparing to a standard curve of nitrite in BMDM media.

#### **Western blots**

Infected BMDM were washed with PBS, lysed in SDS-PAGE buffer on ice, and heat sterilized for 10 min at 100°C. Total protein lysates were analyzed by SDS-PAGE using precast Tris-HCl criterion gels (Bio-Rad). The following primary Abs were used: rabbit IgG against HIF-1 $\alpha$  (NB100-479, Novus Biologicals, Littleton, CO and D2U3T, Cell Signaling Technology), rabbit IgG against K48-polyubiquitin (D9D5, Cell Signaling Technology) and rabbit IgG against K63-polyubiquitin (D7a11, Cell Signaling Technologies). HRP-conjugated secondary Abs were used. Western Lightning Plus-ECL chemiluminescence substrate (Perkin-Elmer) was used, and blots were developed on film or using a ChemiDoc MP System (Bio-Rad). Blots were stripped using 0.2 M NaOH and then washed in ddH<sub>2</sub>O and TBST before blocking and reprobing for

actin as a loading control, using a HRP-conjugated rabbit Ab against b-actin (13E5; Cell Signaling Technology).

### **qRT-PCR**

For q-RT-PCR,  $3 \times 10^5$  BMDM were seeded in 24-well dishes and infected, as described. At 24h post infection, cells were washed with room temperature PBS and lysed in 500  $\mu$ L TRIzol (Invitrogen Life Technologies). Total RNA was extracted using chloroform (100 ml), and the aqueous layer was further purified using RNeasy spin columns (Qiagen). For qPCR, cDNA was generated from 1 mg RNA using Superscript III (Invitrogen Life Technologies) and oligo(dT) primers. Select genes were analyzed using Maxima SYBR Green qPCR master mix (Thermo Scientific). Each sample was analyzed in triplicate on a CFX96 real-time PCR detection system (Bio-Rad). CQ values were normalized to values obtained for GAPDH, and relative changes in gene expression were calculated using the  $\Delta\Delta C_Q$  method.

### **CRISPR knockout of BMDM**

CRISPR guide sequences targeting genes of interest were selected from the murine Brie guide library. Oligonucleotides encoding the chosen gRNAs were cloned into pLentiGuide-Puro (Addgene #52963) and verified by sequencing using the human U6 sequencing primer. 293T cells were co-transfected with pLentiGuide-Puro, psPAX2, and pMD2.G using Lipofectamine and Optimem according to manufacturer's guidelines to generate lentiviral particles for transduction into freshly harvested Cas9-expressing BMDM. Two days post transduction, 4 $\mu$ g/ml puromycin was added to cells, and cells were selected in puromycin for 2 days. Cells were infected 8 days post transduction.

### **Creating *Slc* knockout library in CIM**

CRISPR guide sequences targeting genes of interest were selected from the Bassik lab guide RNA library<sup>289</sup>. A library of single stranded oligonucleotides encoding the chosen gRNAs was ordered from Twist Biosciences and was cloned into pLentiGuide-Puro (Addgene #52963), and verified by sequencing using the human U6 sequencing primer. 293T cells were co-transfected with pLentiGuide-Puro, psPAX2, and pMD2.G using Lipofectamine and Optimem according to manufacturer's guidelines to generate lentiviral particles for transduction into Cas9-expressing CIM progenitors. For optimal transduction of Cas9-expressing CIM progenitors,  $5.0 \times 10^5$  cells/well in a 6-well plate were spininfected at 1000xg for 2 h at 32°C in the presence of 10  $\mu$ g/ml protamine sulfate. Two days post-transduction, 12  $\mu$ g/ml puromycin was added to cells, and cells were selected in puromycin for 4 days. Puromycin-resistant cells were maintained as polyclonal populations.

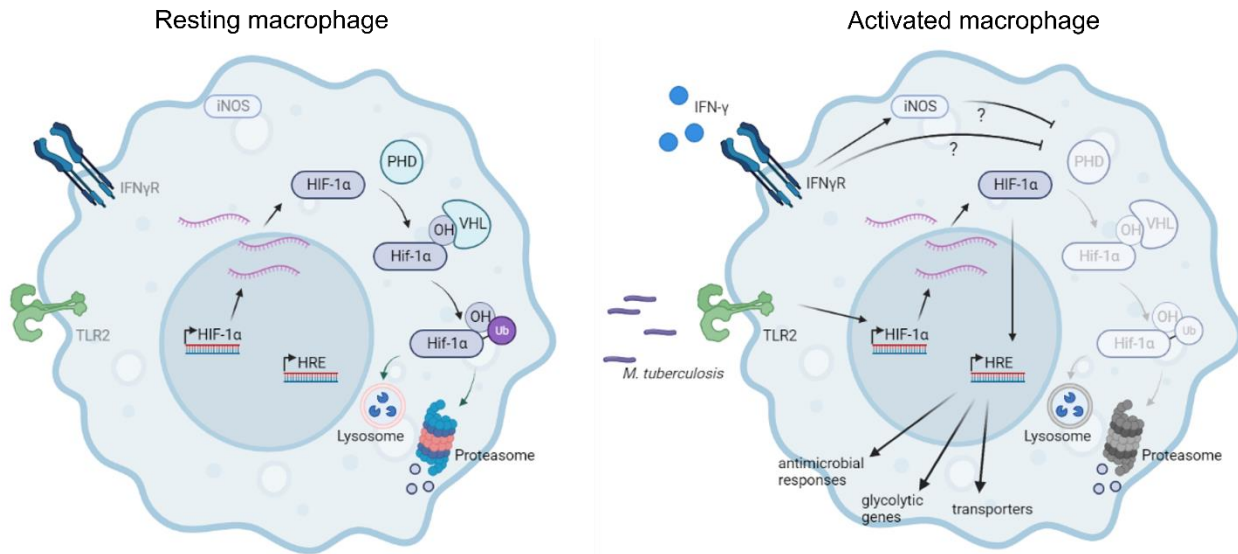
Progenitor CIM prior to differentiation were maintained in RPMI (Gibco) supplemented with 10% FBS, 2% GM-CSF supernatant produced by a B16 murine melanoma cell line, 2 mM L-glutamine, 1 mM sodium pyruvate, 10 mM HEPES, 43  $\mu$ M  $\beta$ -mercaptoethanol, and 2  $\mu$ M  $\beta$ -estradiol (Sigma #E2758). Progenitor CIM were maintained in suspension in non-treated tissue culture treated flasks at densities below 500,000 cells/ml before removal of  $\beta$ -estradiol and differentiation. BMMs and differentiated CIM macrophages were cultured in macrophage media: DMEM (Gibco) supplemented with 10% FBS, 10% M-CSF supernatant produced by 3T3-MCSF cells as previously described, 2 mM L-glutamine (Gibco), and 1 mM sodium pyruvate (Gibco). RAW 264.7 cells were cultured in DMEM (Gibco) supplemented with 10% FBS, 2 mM L-glutamine (Gibco), and 20 mM HEPES. To differentiate progenitor CIMs into macrophages,

cells were washed twice in PBS +1% FBS to fully remove  $\beta$ -estradiol, resuspended in complete macrophage media, and seeded onto non-treated 15 cm tissue culture plates at  $5.0 \times 10^6$  cells/plate in 20 ml of media. Differentiating CIM macrophages were given an additional 10 ml of macrophage media on days 3 and 6 post-differentiation, and infection occurred on day 9 post differentiation.

#### **Detection of bacteria with flow cytometry**

$3 \times 10^5$  BMDM were seeded in 24-well dishes and infected with tdTomato-expressing Erdman, as described. At five days post-infection, cells were washed with room temperature PBS and harvested in cold PBS. Cells were fixed with BD Cytfix/Cytoperm Fixation/Permeabilization Solution Kit (554714; Thermo Fisher Scientific) and data were collected using a BD LSR Fortessa flow cytometer and analyzed using FlowJo Software (Tree Star, Ashland, OR).

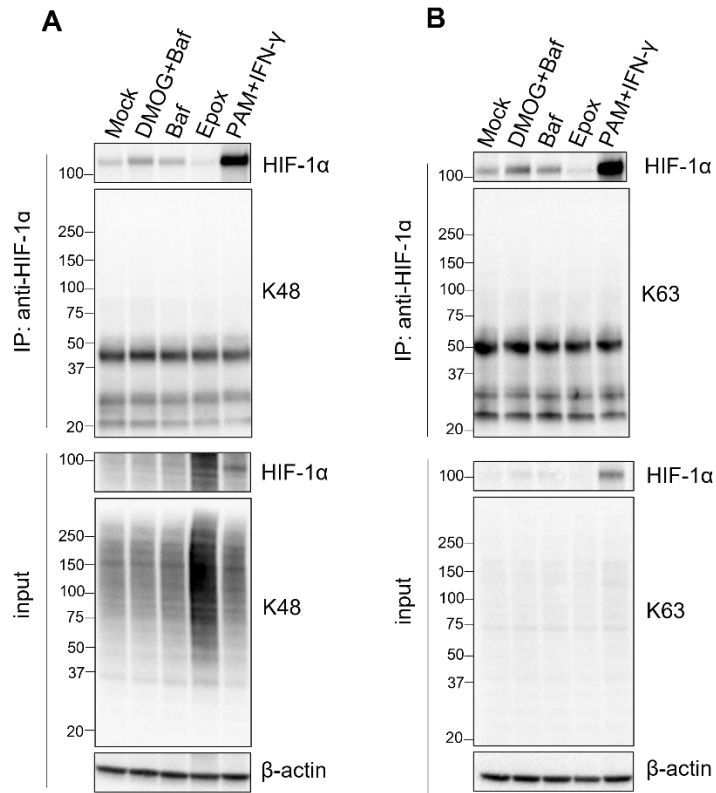
### 3.6 Supplemental Figures.



#### Supplemental Figure 3.1. Model of HIF-1 $\alpha$ expression and protein degradation.

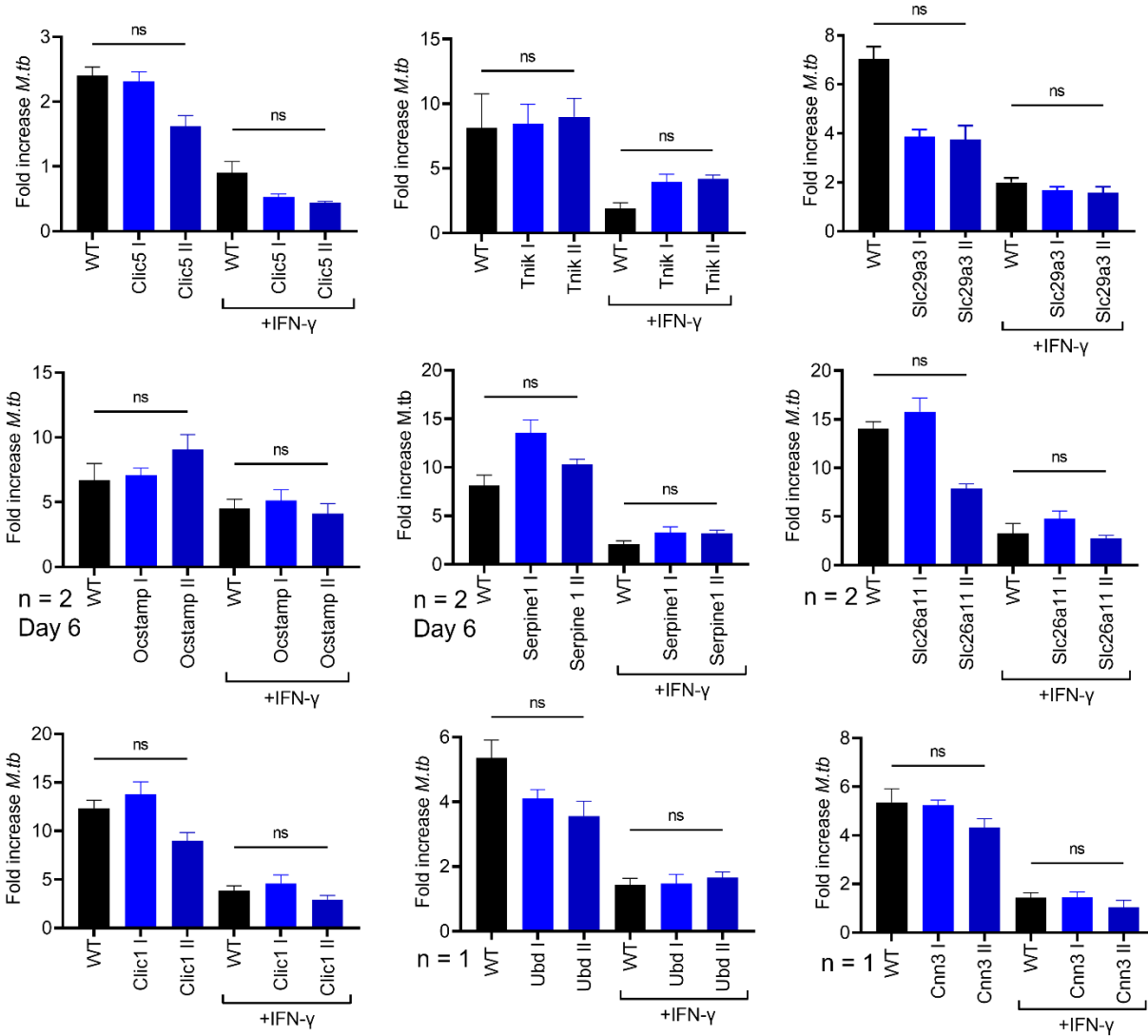
In resting macrophages, HIF-1 $\alpha$  is constitutively expressed and translated into protein. HIF-1 $\alpha$  is quickly recognized by PHD proteins followed by hydroxylation. Hydroxylated HIF-1 $\alpha$  is then recognized by E3 ubiquitin ligase VHL which adds ubiquitin moieties to HIF-1 $\alpha$ , targeting it for degradation by the lysosome. IFN- $\gamma$ -activated macrophages show increased *Hif1a* expression through TLR2 signaling which leads to modest increases in HIF-1 $\alpha$  protein levels. IFN- $\gamma$  signaling increases iNOS activity that results in inhibition of the HIF-1 $\alpha$  degradation pathway through an uncharacterized mechanism. Additionally, there might be other pathways downstream of IFN $\gamma$ R signaling that contribute to HIF-1 $\alpha$  stabilization. HIF-1 $\alpha$  then translocates to the nucleus and acts as transcription factor for HRE-containing genes, including transporters, glycolytic genes and genes involved in antimicrobial responses.





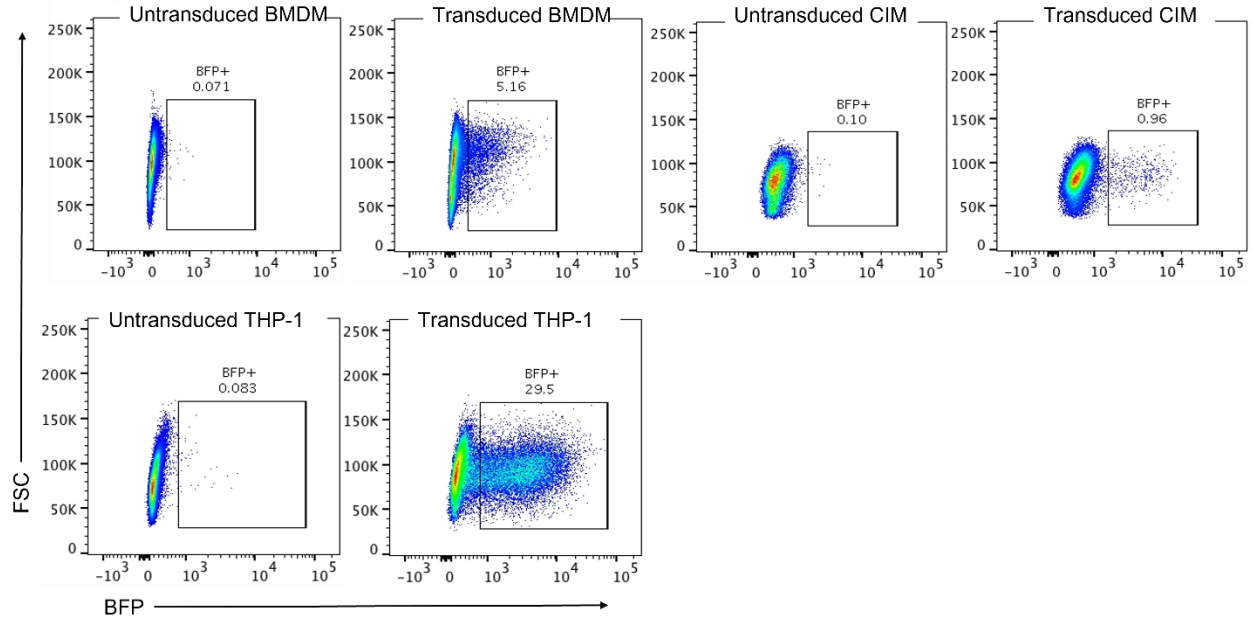
**Supplemental Figure 2. Absence of HIF-1 $\alpha$  specific K48 and K63 ubiquitin staining.**

BMDM were stimulated with indicated proteasomal or lysosomal inhibitors or Pam3CSK4 and interferon- $\gamma$  for 8 hours. Cell lysates were prepared for immunoprecipitation of HIF-1 $\alpha$  followed by staining for the presence of K48 (A) or K63 (B) ubiquitin linkages on HIF-1 $\alpha$ .



**Supplemental Figure 3. Loss of various individual genes in BMDM does not result in enhanced bacterial growth in the presence of IFN- $\gamma$ .**

BMDM were knocked out for various genes by CRISPR. Resting and IFN- $\gamma$  activated cells were then infected with luciferase-expressing *M. tuberculosis* strain Erdman at MOI 5 and bacterial growth was determined by relative light units (RLU). Fold increases in growth are normalized to the RLU of the phagocytosed bacteria on the day of infection.



**Supplemental Figure 4. Transduction efficiency varies among cell types.**

BMDM, CIM or THP-1 cells were transduced with equal volumes of lentivirus containing a blue fluorescent protein (BFP)-expressing plasmid. Flow cytometry was performed 1 day after transduction to determine transduction efficiency based on the number of BFP+ cells.

## **Chapter 4**

### **Conclusions and future directions**

#### 4.1 Summary of results.

The *M. tuberculosis* specific innate and adaptive immune responses are both crucial for control of infection, as highlighted in chapter 1 and 2. Neutrophils are an important determinant for susceptibility to infection in wild-derived mice, similarly to what has been described in infection of the classical B6 model. The MANC line has a similar phenotype, showing high neutrophilic influx into the lung resulting in an increased bacterial burden. The role of neutrophils in these mice needs to be further investigated since known factors for susceptibility, including excessive *Il1rn* production, are only slightly upregulated in these mice. Furthermore, depletion of neutrophils in resistant mice did not affect the bacterial burden, indicating that low numbers of neutrophils recruited to the lung do not play a detrimental role for the host.

Another mechanism that has been described as essential for control of infection in B6 mice is the production of IFN- $\gamma$  by CD4<sup>+</sup> T cells. However, we identified that SARA mice maintain low bacterial burdens in the lung, despite a low influx of CD4<sup>+</sup>IFN- $\gamma$ <sup>+</sup> T cells to the lung and without relying on the presence of other T cell subsets.

In order to identify the contribution of individual cell types to control of infection, scRNAseq was performed comparing cells from the lungs of infected B6, MANA, MANB and MANC mice. Further characterization into differential gene expression between the mouse lines is necessary to identify which mechanism underly bacterial control or lack of control in these mice. Nevertheless, the identification of global immune responses that deviate from the responses that have been classically described as important for control of infection confirms the interesting resource that this genetically diverse mouse cohort provides for investigating novel mechanism of control of infection.

In order to define the determinants of intrinsic control of infection, the degradation pathway of transcription factor HIF-1 $\alpha$  was studied. Inhibition of proteasomal and lysosomal activity in resting macrophages revealed that HIF-1 $\alpha$  is degraded by a non-canonical pathway. In contrast to previous studies, we found that this pathway requires the function of PHD proteins and ubiquitin ligase VHL, but acts independently of the proteasome. In addition, we confirmed the requirement for NO production to inhibit HIF-1 $\alpha$  degradation and the dependence on HIF-1 $\alpha$  stabilization to increase NO synthesis. Both factors are essential for IFN- $\gamma$ -dependent intrinsic control *M. tuberculosis* infection.

Furthermore, infection of IFN- $\gamma$ -activated macrophages revealed that several GBP proteins are highly abundant in these cells. Despite their dependence on IFN- $\gamma$  signaling for expression, GBP do not contribute to intrinsic bacterial restriction early in infection, since knockout of these genes in BMDM does no results in enhanced bacterial growth in activated macrophages. In our mass spectrometry assays on infected BMDM we also found enrichment of metabolite transporters, including SLC proteins. We confirmed that expression of a majority of *Slc* genes is dependent on IFN- $\gamma$  and many show dependence on the presence of HIF-1 $\alpha$ . A targeted approach using CRISPR knockout to delete several *Slc* genes in BMDM did not result in identifying genes that contribute to bacterial killing in an assay relying on bacterial luciferase expression to determine growth. However, the development of a flow cytometry-based screen with a small CRISPR knockout sublibrary of *Slc* genes shows increased sensitivity for the detection bacterial growth, indicating a promising resource to identify the SLC proteins that play a role in *M. tuberculosis* infection.

## 4.2 Remaining questions and future directions.

### 4.2.1 Chapter 2 and the abundance of neutrophils in the Manaus lines.

In the context of human *M. tuberculosis* infections, one of the biggest remaining questions is why a small percentage of people are incapable of eliciting an immune response that controls infection and progress to active disease at some point in their life. It is crucial to understand the immune requirements for a successful response that controls *M. tuberculosis* growth. Flow cytometry data show an increased influx of neutrophils to the lungs of susceptible Manaus mice, indicating a detrimental role for excessive neutrophils during infection, as has been shown by previous studies in susceptible mice. Studying the role of neutrophils during *M. tuberculosis* infection has been challenging, due to the short lifespan and the subsequent difficulties of culturing neutrophils *ex vivo*. Previous studies have reported both intrinsic killing of *M. tuberculosis* by neutrophils as well as bacterial growth inside neutrophils. In addition, it has not been studied whether *Hif1a* expression contributes to the function of infected neutrophils. The scRNAseq data suggest a potential role for HIF-1 $\alpha$  during infection, which we are currently investigating through breeding of mice with *Hif1a* floxed alleles under the control of neutrophil-specific Mrp8-cre promoter. Bone marrow derived neutrophils from these mice can be assessed for their antimicrobial capacity against *M. tuberculosis*. Furthermore, *in vivo* infections of these mice will elucidate whether *Hif1a* expression by neutrophil contributes to susceptibility to infection. In addition, preliminary histology data from the lungs of these mice show an increase of neutrophils within the lesions of MANC mice, whereas highly abundant neutrophils in MANB mice as localized throughout the tissue (data not shown). Further studies are required to determine if this difference in localization contributes the differences in susceptibility in these mice. Furthermore, it is important to characterize the presence of different immune cell type in naïve animals, to determine if baseline levels can predict susceptibility to infection.

The scRNAseq data set from the Manaus mice is an essential tool to determine the contribution of individual cell types to infection as opposed to bulk RNAseq which depicts the immune state of the whole lung. However, both techniques lack information on the location of where essential cytokine production or cell-interactions occur. Therefore, we are currently processing spatial transcriptomics data from the lesions of B6, MANA, MANB and MANC mice to identify potential immune signature from cells within the lesions versus cells surrounding the lesions. The presence of lesion-specific expression profiles can inform analysis of our scRNAseq dataset by identifying whether these expression profiles are enriched in susceptible or resistant mouse lines.

### 4.2.2 Chapter 3 and HIF-1 $\alpha$ regulation.

A surprising observation in the study of the HIF-1 $\alpha$  degradation pathway was the finding of VHL-dependent lysosomal degradation of HIF-1 $\alpha$ . In order to determine the function of VHL in this pathway, the ubiquitin linkages on HIF-1 $\alpha$  can be further investigated with more sensitive detection methods, including TUBE (Tandem Ubiquitin Binding Entities) staining to detect polyubiquitin K48 or K63 linkages. An unbiased approach to identify additional ubiquitin ligases that could cooperate with VHL is challenging due to the potentially short interaction times with HIF-1 $\alpha$ . However, the flow cytometry based CRISPR screen from this study could be adapted to detect fluorescent HIF-1 $\alpha$  expression in CIM with a knockout sublibrary of known ubiquitin ligases. The main goal for this project is to determine how IFN- $\gamma$  regulates HIF-1 $\alpha$  stabilization and as well as other pathways that result in *M. tuberculosis* restriction. We hypothesize that this regulation mediated through S-nitrosylation. We propose to identify all S-nitrosylated proteins in

IFN- $\gamma$ -activated macrophages by using a biotin switch assay to label all S-nitrosylated cytosolic proteins with biotin followed by identification of biotinylated proteins by mass spectrometry<sup>299</sup>. This would address with proteins in the HIF-1 $\alpha$ -degradation pathway are S-nitrosylated as well as protein that contribute to bacterial control directly and independent of HIF-1 $\alpha$  activity. Although HIF-1 $\alpha$  degradation clearly depends on lysosomal acidification in macrophages, further research is necessary to confirm whether HIF-1 $\alpha$  is degraded through chaperone-mediated autophagy. HIF-1 $\alpha$  interacts and colocalizes with CMA components heat shock protein 70 (HSC70) and lysosome-associated membrane protein type 2A (LAMP2A) in several human cell lines<sup>282,300</sup>. To confirm the presence of this pathway in macrophages with a genetic approach, LAMP-2A could be knocked out with CRISPR by targeting unique sequences in exon 9 that are not present in other isoforms. The effect of CMA interruption on HIF-1 $\alpha$  protein levels in resting cells can then be compared to the levels of proteins which are exclusively degraded by the proteasome or lysosome, including SerpinB (serpin peptidase inhibitor, clade B) and RNase1 (RNase A family 1), respectively. Following the fate of these specific proteins during proteasome and lysosome inhibition will also reveal whether shunting between these pathways occurs and could explain the increase in HIF-1 $\alpha$  degradation in the presence of epoxomicin.

#### **4.2.3 Chapter 3 and the function of SLC.**

The results from the *Slc* screen will be used to either identify pathways that support maintenance of macrophage glycolytic metabolism or the restriction of essential metals or metabolites from *M. tuberculosis* in the phagosome. It is currently unclear which nutrients *M. tuberculosis* requires for growth in the phagosome and we hypothesize that IFN- $\gamma$  activation of SLC transporters could contribute to creating a nutrient-poor environment in which *M. tuberculosis* growth is inhibited. This screen could reveal genes important for host antimicrobial mechanisms and give more insight into bacterial metabolic requirements.

#### **Final thoughts and speculation into the future.**

It is a humbling feeling that after decades of research we know so little about the drivers of TB disease, despite the fact that *M. tuberculosis* has been the deadliest infectious pathogen for years. The study of immune responses in a single mouse model has been compared to studying TB disease in a single human, thereby limiting our knowledge on the responses that are beneficial for bacterial clearance. The development of novel mouse models that can mimic successful immune responses to infection or reveal the weaknesses that *M. tuberculosis* is able to exploit is an incredibly exciting progression in the field. I'm highly optimistic that we can increase our knowledge of the requirements for *M. tuberculosis* killing by broadening our approach to infection. For example, the presence or absence of IFN- $\gamma$  signaling has historically been a major research focus for explaining the susceptibility of mice. However, novel techniques including spatial transcriptomics can shift the focus towards the importance of localization of these immune responses and highlight the requirement of IFN- $\gamma$  production at the correct sites of infection. The study of spatial and temporal parameters of the immune response can pinpoint which aspects of a global immune response are important for control of infection. The development of new techniques combined with the availability of new mouse models to confirm susceptibility or resistance phenotypes will be a promising new approach to identify additional dimensions that are required for a successful immune response to *M. tuberculosis*. Hopefully, the development of new mouse models will also translate into the development of much-needed *M. tuberculosis* vaccines. First, by understanding which immune responses are

essential for clearance of infection that should be enhanced by vaccination. Second, by understanding and minimizing adverse effects caused by exacerbated immune responses that should be avoided with vaccination. It is exciting to imagine that the development of these new resources will accelerate our gain of knowledge about this pathogen, and I hope for the successful translation of these findings into benefiting tuberculosis patients.



## References

1. Geneva. *Global tuberculosis report 2018*. (World Health Organization, 2018).
2. Reiling, N. *et al.* Cutting edge: Toll-like receptor (TLR)2- and TLR4-mediated pathogen recognition in resistance to airborne infection with *Mycobacterium tuberculosis*. *J. Immunol.* **169**, 3480–3484 (2002).
3. Sugawara, I. *et al.* Mycobacterial infection in TLR2 and TLR6 knockout mice. *Microbiol. Immunol.* **47**, 327–336 (2003).
4. Feng, C. G. *et al.* Mice lacking myeloid differentiation factor 88 display profound defects in host resistance and immune responses to *Mycobacterium avium* infection not exhibited by Toll-like receptor 2 (TLR2)- and TLR4-deficient animals. *J. Immunol.* **171**, 4758–4764 (2003).
5. Bafica, A. *et al.* TLR9 regulates Th1 responses and cooperates with TLR2 in mediating optimal resistance to *Mycobacterium tuberculosis*. *J. Exp. Med.* **202**, 1715–1724 (2005).
6. Scanga, C. A. *et al.* MyD88-deficient mice display a profound loss in resistance to *Mycobacterium tuberculosis* associated with partially impaired Th1 cytokine and nitric oxide synthase 2 expression. *Infect. Immun.* **72**, 2400–2404 (2004).
7. Flynn, J. L. *et al.* An essential role for interferon gamma in resistance to *Mycobacterium tuberculosis* infection. *J. Exp. Med.* **178**, 2249–2254 (1993).
8. Maeda, N. *et al.* The cell surface receptor DC-SIGN discriminates between *Mycobacterium* species through selective recognition of the mannose caps on lipoarabinomannan. *J. Biol. Chem.* **278**, 5513–5516 (2003).
9. Kang, P. B. *et al.* The human macrophage mannose receptor directs *Mycobacterium tuberculosis* lipoarabinomannan-mediated phagosome biogenesis. *J. Exp. Med.* **202**, 987–999 (2005).
10. Doz, E. *et al.* Acylation determines the toll-like receptor (TLR)-dependent positive versus TLR2-, mannose receptor-, and SIGNR1-independent negative regulation of pro-inflammatory cytokines by mycobacterial lipomannan. *J. Biol. Chem.* **282**, 26014–26025 (2007).
11. Yonekawa, A. *et al.* Dectin-2 is a direct receptor for mannose-capped lipoarabinomannan of mycobacteria. *Immunity* **41**, 402–413 (2014).
12. Bowdish, D. M. E. *et al.* MARCO, TLR2, and CD14 are required for macrophage cytokine responses to mycobacterial trehalose dimycolate and *Mycobacterium tuberculosis*. *PLoS Pathog.* **5**, e1000474 (2009).
13. Marakalala, M. J. *et al.* The Syk/CARD9-coupled receptor Dectin-1 is not required for host resistance to *Mycobacterium tuberculosis* in mice. *Microbes Infect.* **13**, 198–201 (2011).
14. Heitmann, L., Schoenen, H., Ehlers, S., Lang, R. & Hölscher, C. Mincle is not essential for controlling *Mycobacterium tuberculosis* infection. *Immunobiology* **218**, 506–516 (2013).
15. Court, N. *et al.* Partial redundancy of the pattern recognition receptors, scavenger receptors, and C-type lectins for the long-term control of *Mycobacterium tuberculosis* infection. *J. Immunol.* **184**, 7057–7070 (2010).
16. Yang, Y. *et al.* NOD2 pathway activation by MDP or *Mycobacterium tuberculosis* infection involves the stable polyubiquitination of Rip2. *J. Biol. Chem.* **282**, 36223–36229 (2007).
17. Coulombe, F. *et al.* Increased NOD2-mediated recognition of N-glycolyl muramyl dipeptide. *J. Exp. Med.* **206**, 1709–1716 (2009).
18. Pandey, A. K. *et al.* NOD2, RIP2 and IRF5 play a critical role in the type I interferon response to *Mycobacterium tuberculosis*. *PLoS Pathog.* **5**, e1000500 (2009).
19. Juárez, E. *et al.* NOD2 enhances the innate response of alveolar macrophages to *Mycobacterium tuberculosis* in humans. *Eur. J. Immunol.* **42**, 880–889 (2012).
20. Gandotra, S., Jang, S., Murray, P. J., Salgame, P. & Ehrt, S. Nucleotide-binding oligomerization domain protein 2-deficient mice control infection with *Mycobacterium tuberculosis*. *Infect. Immun.* **75**, 5127–5134 (2007).

21. Ferwerda, G. *et al.* NOD2 and toll-like receptors are nonredundant recognition systems of *Mycobacterium tuberculosis*. *PLoS Pathog.* **1**, 279–285 (2005).
22. Girardin, S. E. *et al.* Nod2 is a general sensor of peptidoglycan through muramyl dipeptide (MDP) detection. *J. Biol. Chem.* **278**, 8869–8872 (2003).
23. Divangahi, M. *et al.* NOD2-deficient mice have impaired resistance to *Mycobacterium tuberculosis* infection through defective innate and adaptive immunity. *J. Immunol.* **181**, 7157–7165 (2008).
24. Wu, J. *et al.* Cyclic GMP-AMP is an endogenous second messenger in innate immune signaling by cytosolic DNA. *Science* **339**, 826–830 (2013).
25. Ablasser, A. *et al.* cGAS produces a 2'-5'-linked cyclic dinucleotide second messenger that activates STING. *Nature* **498**, 380–384 (2013).
26. Burdette, D. L. *et al.* STING is a direct innate immune sensor of cyclic di-GMP. *Nature* **478**, 515–518 (2011).
27. Diner, E. J. *et al.* The innate immune DNA sensor cGAS produces a noncanonical cyclic dinucleotide that activates human STING. *Cell Rep.* **3**, 1355–1361 (2013).
28. Woodward, J. J., Iavarone, A. T. & Portnoy, D. A. c-di-AMP secreted by intracellular *Listeria monocytogenes* activates a host type I interferon response. *Science* **328**, 1703–1705 (2010).
29. Stanley, S. A., Johndrow, J. E., Manzanillo, P. & Cox, J. S. The Type I IFN response to infection with *Mycobacterium tuberculosis* requires ESX-1-mediated secretion and contributes to pathogenesis. *J. Immunol.* **178**, 3143–3152 (2007).
30. Manca, C. *et al.* Hypervirulent *M. tuberculosis* W/Beijing strains upregulate type I IFNs and increase expression of negative regulators of the Jak-Stat pathway. *J. Interferon Cytokine Res.* **25**, 694–701 (2005).
31. Mayer-Barber, K. D. *et al.* Innate and adaptive interferons suppress IL-1 $\alpha$  and IL-1 $\beta$  production by distinct pulmonary myeloid subsets during *Mycobacterium tuberculosis* infection. *Immunity* **35**, 1023–1034 (2011).
32. Ji, D. X. *et al.* Type I interferon-driven susceptibility to *Mycobacterium tuberculosis* is mediated by IL-1Ra. *Nat. Microbiol.* **4**, 2128–2135 (2019).
33. Manzanillo, P. S., Shiloh, M. U., Portnoy, D. A. & Cox, J. S. *Mycobacterium tuberculosis* activates the DNA-dependent cytosolic surveillance pathway within macrophages. *Cell Host Microbe* **11**, 469–480 (2012).
34. Watson, R. O. *et al.* The Cytosolic Sensor cGAS Detects *Mycobacterium tuberculosis* DNA to Induce Type I Interferons and Activate Autophagy. *Cell Host Microbe* **17**, 811–819 (2015).
35. Collins, A. C. *et al.* Cyclic GMP-AMP Synthase Is an Innate Immune DNA Sensor for *Mycobacterium tuberculosis*. *Cell Host Microbe* **17**, 820–828 (2015).
36. Wassermann, R. *et al.* *Mycobacterium tuberculosis* Differentially Activates cGAS- and Inflammasome-Dependent Intracellular Immune Responses through ESX-1. *Cell Host Microbe* **17**, 799–810 (2015).
37. Dey, B. *et al.* A bacterial cyclic dinucleotide activates the cytosolic surveillance pathway and mediates innate resistance to tuberculosis. *Nat. Med.* **21**, 401–406 (2015).
38. Dorhoi, A. & Kaufmann, S. H. E. Tumor necrosis factor alpha in mycobacterial infection. *Semin. Immunol.* **26**, 203–209 (2014).
39. Roach, D. R. *et al.* TNF regulates chemokine induction essential for cell recruitment, granuloma formation, and clearance of mycobacterial infection. *J. Immunol.* **168**, 4620–4627 (2002).
40. Flynn, J. L. *et al.* Tumor necrosis factor-alpha is required in the protective immune response against *Mycobacterium tuberculosis* in mice. *Immunity* **2**, 561–572 (1995).
41. Bean, A. G. *et al.* Structural deficiencies in granuloma formation in TNF gene-targeted mice underlie the heightened susceptibility to aerosol *Mycobacterium tuberculosis* infection, which is not compensated for by lymphotoxin. *J. Immunol.* **162**, 3504–3511 (1999).

42. Kaneko, H. *et al.* Role of tumor necrosis factor- $\alpha$  in Mycobacterium-induced granuloma formation in tumor necrosis factor- $\alpha$ -deficient mice. *Lab. Invest.* **79**, 379–386 (1999).
43. Keane, J. *et al.* Tuberculosis associated with infliximab, a tumor necrosis factor  $\alpha$ -neutralizing agent. *N. Engl. J. Med.* **345**, 1098–1104 (2001).
44. Xie, X., Li, F., Chen, J.-W. & Wang, J. Risk of tuberculosis infection in anti-TNF- $\alpha$  biological therapy: from bench to bedside. *J Microbiol Immunol Infect* **47**, 268–274 (2014).
45. Galloway, J. B. *et al.* Risk of skin and soft tissue infections (including shingles) in patients exposed to anti-tumour necrosis factor therapy: results from the British Society for Rheumatology Biologics Register. *Ann. Rheum. Dis.* **72**, 229–234 (2013).
46. Kindler, V., Sappino, A. P., Grau, G. E., Piguët, P. F. & Vassalli, P. The inducing role of tumor necrosis factor in the development of bactericidal granulomas during BCG infection. *Cell* **56**, 731–740 (1989).
47. Egen, J. G. *et al.* Macrophage and T cell dynamics during the development and disintegration of mycobacterial granulomas. *Immunity* **28**, 271–284 (2008).
48. Reece, S. T. *et al.* Serine protease activity contributes to control of Mycobacterium tuberculosis in hypoxic lung granulomas in mice. *J. Clin. Invest.* **120**, 3365–3376 (2010).
49. Myllymäki, H., Bäuerlein, C. A. & Rämets, M. The Zebrafish Breathes New Life into the Study of Tuberculosis. *Front. Immunol.* **7**, 196 (2016).
50. Tobin, D. M. *et al.* The *Ita4h* locus modulates susceptibility to mycobacterial infection in zebrafish and humans. *Cell* **140**, 717–730 (2010).
51. Clay, H., Volkman, H. E. & Ramakrishnan, L. Tumor necrosis factor signaling mediates resistance to mycobacteria by inhibiting bacterial growth and macrophage death. *Immunity* **29**, 283–294 (2008).
52. Di Paolo, N. C. *et al.* Interdependence between Interleukin-1 and Tumor Necrosis Factor Regulates TNF-Dependent Control of Mycobacterium tuberculosis Infection. *Immunity* **43**, 1125–1136 (2015).
53. Roca, F. J., Whitworth, L. J., Redmond, S., Jones, A. A. & Ramakrishnan, L. TNF Induces Pathogenic Programmed Macrophage Necrosis in Tuberculosis through a Mitochondrial-Lysosomal-Endoplasmic Reticulum Circuit. *Cell* **178**, 1344–1361.e11 (2019).
54. Roca, F. J. & Ramakrishnan, L. TNF dually mediates resistance and susceptibility to mycobacteria via mitochondrial reactive oxygen species. *Cell* **153**, 521–534 (2013).
55. Guilliams, M. *et al.* Alveolar macrophages develop from fetal monocytes that differentiate into long-lived cells in the first week of life via GM-CSF. *J. Exp. Med.* **210**, 1977–1992 (2013).
56. Dranoff, G. *et al.* Involvement of granulocyte-macrophage colony-stimulating factor in pulmonary homeostasis. *Science* **264**, 713–716 (1994).
57. Gonzalez-Juarrero, M. *et al.* Disruption of granulocyte macrophage-colony stimulating factor production in the lungs severely affects the ability of mice to control Mycobacterium tuberculosis infection. *J. Leukoc. Biol.* **77**, 914–922 (2005).
58. Rothchild, A. C. *et al.* Role of Granulocyte-Macrophage Colony-Stimulating Factor Production by T Cells during Mycobacterium tuberculosis Infection. *MBio* **8**, (2017).
59. Rothchild, A. C., Jayaraman, P., Nunes-Alves, C. & Behar, S. M. iNKT cell production of GM-CSF controls Mycobacterium tuberculosis. *PLoS Pathog.* **10**, e1003805 (2014).
60. Benmerzoug, S. *et al.* GM-CSF targeted immunomodulation affects host response to M. tuberculosis infection. *Sci. Rep.* **8**, 8652 (2018).
61. Chroneos, Z. C., Midde, K., Sever-Chroneos, Z. & Jagannath, C. Pulmonary surfactant and tuberculosis. *Tuberculosis (Edinb)* **89**, S10–S14 (2009).
62. Bryson, B. D. *et al.* Heterogeneous GM-CSF signaling in macrophages is associated with control of Mycobacterium tuberculosis. *Nat. Commun.* **10**, 2329 (2019).

63. Juffermans, N. P. *et al.* Interleukin-1 signaling is essential for host defense during murine pulmonary tuberculosis. *J. Infect. Dis.* **182**, 902–908 (2000).
64. Guler, R. *et al.* Blocking IL-1 $\alpha$  but not IL-1 $\beta$  increases susceptibility to chronic Mycobacterium tuberculosis infection in mice. *Vaccine* **29**, 1339–1346 (2011).
65. Bourigault, M.-L. *et al.* Relative contribution of IL-1 $\alpha$ , IL-1 $\beta$  and TNF to the host response to Mycobacterium tuberculosis and attenuated M. bovis BCG. *Immun. Inflamm. Dis.* **1**, 47–62 (2013).
66. Mayer-Barber, K. D. *et al.* Caspase-1 independent IL-1 $\beta$  production is critical for host resistance to mycobacterium tuberculosis and does not require TLR signaling in vivo. *J. Immunol.* **184**, 3326–3330 (2010).
67. Bohrer, A. C., Tocheny, C., Assmann, M., Ganusov, V. V. & Mayer-Barber, K. D. Cutting Edge: IL-1R1 Mediates Host Resistance to Mycobacterium tuberculosis by Trans-Protection of Infected Cells. *J. Immunol.* **201**, 1645–1650 (2018).
68. Settas, L. D., Tsimirikas, G., Vosvotekas, G., Triantafyllidou, E. & Nicolaidis, P. Reactivation of pulmonary tuberculosis in a patient with rheumatoid arthritis during treatment with IL-1 receptor antagonists (anakinra). *J Clin Rheumatol* **13**, 219–220 (2007).
69. Brassard, P., Kezouh, A. & Suissa, S. Antirheumatic drugs and the risk of tuberculosis. *Clin. Infect. Dis.* **43**, 717–722 (2006).
70. Abdalla, H. *et al.* Mycobacterium tuberculosis infection of dendritic cells leads to partially caspase-1/11-independent IL-1 $\beta$  and IL-18 secretion but not to pyroptosis. *PLoS One* **7**, e40722 (2012).
71. Mishra, B. B. *et al.* Mycobacterium tuberculosis protein ESAT-6 is a potent activator of the NLRP3/ASC inflammasome. *Cell Microbiol.* **12**, 1046–1063 (2010).
72. Wong, K.-W. & Jacobs, W. R. Critical role for NLRP3 in necrotic death triggered by Mycobacterium tuberculosis. *Cell Microbiol.* **13**, 1371–1384 (2011).
73. Dorhoi, A. *et al.* Activation of the NLRP3 inflammasome by Mycobacterium tuberculosis is uncoupled from susceptibility to active tuberculosis. *Eur. J. Immunol.* **42**, 374–384 (2012).
74. Carlsson, F. *et al.* Host-detrimental role of Esx-1-mediated inflammasome activation in mycobacterial infection. *PLoS Pathog.* **6**, e1000895 (2010).
75. McElvania Tekippe, E. *et al.* Granuloma formation and host defense in chronic Mycobacterium tuberculosis infection requires PYCARD/ASC but not NLRP3 or caspase-1. *PLoS One* **5**, e12320 (2010).
76. Fremont, C. M. *et al.* IL-1 receptor-mediated signal is an essential component of MyD88-dependent innate response to Mycobacterium tuberculosis infection. *J. Immunol.* **179**, 1178–1189 (2007).
77. Saiga, H. *et al.* Critical role of AIM2 in Mycobacterium tuberculosis infection. *Int. Immunol.* **24**, 637–644 (2012).
78. Walter, K., Hölscher, C., Tschopp, J. & Ehlers, S. NALP3 is not necessary for early protection against experimental tuberculosis. *Immunobiology* **215**, 804–811 (2010).
79. Joosten, L. A. B. *et al.* Inflammatory arthritis in caspase 1 gene-deficient mice: contribution of proteinase 3 to caspase 1-independent production of bioactive interleukin-1 $\beta$ . *Arthritis Rheum.* **60**, 3651–3662 (2009).
80. Greten, F. R. *et al.* NF-kappaB is a negative regulator of IL-1 $\beta$  secretion as revealed by genetic and pharmacological inhibition of IKK $\beta$ . *Cell* **130**, 918–931 (2007).
81. Guma, M. *et al.* Caspase 1-independent activation of interleukin-1 $\beta$  in neutrophil-predominant inflammation. *Arthritis Rheum.* **60**, 3642–3650 (2009).
82. Karmakar, M., Sun, Y., Hise, A. G., Rietsch, A. & Pearlman, E. Cutting edge: IL-1 $\beta$  processing during Pseudomonas aeruginosa infection is mediated by neutrophil serine proteases and is independent of NLRC4 and caspase-1. *J. Immunol.* **189**, 4231–4235 (2012).

83. Mishra, B. B. *et al.* Nitric oxide controls the immunopathology of tuberculosis by inhibiting NLRP3 inflammasome-dependent processing of IL-1 $\beta$ . *Nat. Immunol.* **14**, 52–60 (2013).
84. Watson, R. O., Manzanillo, P. S. & Cox, J. S. Extracellular M. tuberculosis DNA targets bacteria for autophagy by activating the host DNA-sensing pathway. *Cell* **150**, 803–815 (2012).
85. Maertzdorf, J. *et al.* Human gene expression profiles of susceptibility and resistance in tuberculosis. *Genes Immun.* **12**, 15–22 (2011).
86. Berry, M. P. R. *et al.* An interferon-inducible neutrophil-driven blood transcriptional signature in human tuberculosis. *Nature* **466**, 973–977 (2010).
87. Moreira-Teixeira, L. *et al.* Mouse transcriptome reveals potential signatures of protection and pathogenesis in human tuberculosis. *Nat. Immunol.* **21**, 464–476 (2020).
88. Singhanian, A. *et al.* A modular transcriptional signature identifies phenotypic heterogeneity of human tuberculosis infection. *Nat. Commun.* **9**, 2308 (2018).
89. Scriba, T. J. *et al.* Sequential inflammatory processes define human progression from M. tuberculosis infection to tuberculosis disease. *PLoS Pathog.* **13**, e1006687 (2017).
90. Zak, D. E. *et al.* A blood RNA signature for tuberculosis disease risk: a prospective cohort study. *Lancet* **387**, 2312–2322 (2016).
91. Cooper, A. M., Pearl, J. E., Brooks, J. V., Ehlers, S. & Orme, I. M. Expression of the nitric oxide synthase 2 gene is not essential for early control of Mycobacterium tuberculosis in the murine lung. *Infect. Immun.* **68**, 6879–6882 (2000).
92. Dorhoi, A. *et al.* Type I IFN signaling triggers immunopathology in tuberculosis-susceptible mice by modulating lung phagocyte dynamics. *Eur. J. Immunol.* **44**, 2380–2393 (2014).
93. Yamashiro, L. H. *et al.* Interferon-independent STING signaling promotes resistance to HSV-1 in vivo. *Nat. Commun.* **11**, 3382 (2020).
94. Desvignes, L., Wolf, A. J. & Ernst, J. D. Dynamic roles of type I and type II IFNs in early infection with Mycobacterium tuberculosis. *J. Immunol.* **188**, 6205–6215 (2012).
95. Antonelli, L. R. V. *et al.* Intranasal Poly-IC treatment exacerbates tuberculosis in mice through the pulmonary recruitment of a pathogen-permissive monocyte/macrophage population. *J. Clin. Invest.* **120**, 1674–1682 (2010).
96. Novikov, A. *et al.* Mycobacterium tuberculosis triggers host type I IFN signaling to regulate IL-1 $\beta$  production in human macrophages. *J. Immunol.* **187**, 2540–2547 (2011).
97. McNab, F. W. *et al.* Type I IFN induces IL-10 production in an IL-27-independent manner and blocks responsiveness to IFN- $\gamma$  for production of IL-12 and bacterial killing in Mycobacterium tuberculosis-infected macrophages. *J. Immunol.* **193**, 3600–3612 (2014).
98. Mayer-Barber, K. D. *et al.* Host-directed therapy of tuberculosis based on interleukin-1 and type I interferon crosstalk. *Nature* **511**, 99–103 (2014).
99. Moreira-Teixeira, L., Mayer-Barber, K., Sher, A. & O’Garra, A. Type I interferons in tuberculosis: Foe and occasionally friend. *J. Exp. Med.* **215**, 1273–1285 (2018).
100. Olobo, J. O. *et al.* Circulating TNF-alpha, TGF-beta, and IL-10 in tuberculosis patients and healthy contacts. *Scand. J. Immunol.* **53**, 85–91 (2001).
101. Harling, K. *et al.* Constitutive STAT3 phosphorylation and IL-6/IL-10 co-expression are associated with impaired T-cell function in tuberculosis patients. *Cell Mol Immunol* (2018). doi:10.1038/cmi.2018.5
102. Higgins, D. M. *et al.* Lack of IL-10 alters inflammatory and immune responses during pulmonary Mycobacterium tuberculosis infection. *Tuberculosis (Edinb)* **89**, 149–157 (2009).
103. Redford, P. S. *et al.* Enhanced protection to Mycobacterium tuberculosis infection in IL-10-deficient mice is accompanied by early and enhanced Th1 responses in the lung. *Eur. J. Immunol.* **40**, 2200–2210 (2010).

104. Cyktor, J. C. *et al.* IL-10 inhibits mature fibrotic granuloma formation during Mycobacterium tuberculosis infection. *J. Immunol.* **190**, 2778–2790 (2013).
105. Beamer, G. L. *et al.* Interleukin-10 promotes Mycobacterium tuberculosis disease progression in CBA/J mice. *J. Immunol.* **181**, 5545–5550 (2008).
106. Batlle, E. & Massagué, J. Transforming Growth Factor- $\beta$  Signaling in Immunity and Cancer. *Immunity* **50**, 924–940 (2019).
107. Bonecini-Almeida, M. G. *et al.* Down-modulation of lung immune responses by interleukin-10 and transforming growth factor beta (TGF-beta) and analysis of TGF-beta receptors I and II in active tuberculosis. *Infect. Immun.* **72**, 2628–2634 (2004).
108. Toossi, Z., Gogate, P., Shiratsuchi, H., Young, T. & Ellner, J. J. Enhanced production of TGF-beta by blood monocytes from patients with active tuberculosis and presence of TGF-beta in tuberculous granulomatous lung lesions. *J. Immunol.* **154**, 465–473 (1995).
109. Fiorenza, G., Rateni, L., Farroni, M. A., Bogue, C. & Dlugovitzky, D. G. TNF-alpha, TGF-beta and NO relationship in sera from tuberculosis (TB) patients of different severity. *Immunol. Lett.* **98**, 45–48 (2005).
110. DiFazio, R. M. *et al.* Active transforming growth factor- $\beta$  is associated with phenotypic changes in granulomas after drug treatment in pulmonary tuberculosis. *Fibrogenesis Tissue Repair* **9**, 6 (2016).
111. Rook, G. A. W., Lowrie, D. B. & Hernández-Pando, R. Immunotherapeutics for tuberculosis in experimental animals: is there a common pathway activated by effective protocols? *J. Infect. Dis.* **196**, 191–198 (2007).
112. Hernández-Pando, R. *et al.* A combination of a transforming growth factor-beta antagonist and an inhibitor of cyclooxygenase is an effective treatment for murine pulmonary tuberculosis. *Clin. Exp. Immunol.* **144**, 264–272 (2006).
113. Jayaswal, S. *et al.* Identification of host-dependent survival factors for intracellular Mycobacterium tuberculosis through an siRNA screen. *PLoS Pathog.* **6**, e1000839 (2010).
114. Gern, B. H. *et al.* TGF $\beta$  restricts expansion, survival, and function of T cells within the tuberculous granuloma. *Cell Host Microbe* (2021). doi:10.1016/j.chom.2021.02.005
115. Li, H. *et al.* Latently and uninfected healthcare workers exposed to TB make protective antibodies against Mycobacterium tuberculosis. *Proc. Natl. Acad. Sci. USA* **114**, 5023–5028 (2017).
116. Cadena, A. M., Flynn, J. L. & Fortune, S. M. The Importance of First Impressions: Early Events in Mycobacterium tuberculosis Infection Influence Outcome. *MBio* **7**, e00342–16 (2016).
117. Mogue, T., Goodrich, M. E., Ryan, L., LaCourse, R. & North, R. J. The relative importance of T cell subsets in immunity and immunopathology of airborne Mycobacterium tuberculosis infection in mice. *J. Exp. Med.* **193**, 271–280 (2001).
118. Gallegos, A. M. *et al.* A gamma interferon independent mechanism of CD4 T cell mediated control of M. tuberculosis infection in vivo. *PLoS Pathog.* **7**, e1002052 (2011).
119. Bah, A. & Vergne, I. Macrophage autophagy and bacterial infections. *Front. Immunol.* **8**, 1483 (2017).
120. Gutierrez, M. G. *et al.* Autophagy is a defense mechanism inhibiting BCG and Mycobacterium tuberculosis survival in infected macrophages. *Cell* **119**, 753–766 (2004).
121. Manzanillo, P. S. *et al.* The ubiquitin ligase parkin mediates resistance to intracellular pathogens. *Nature* **501**, 512–516 (2013).
122. Franco, L. H. *et al.* The Ubiquitin Ligase Smurf1 Functions in Selective Autophagy of Mycobacterium tuberculosis and Anti-tuberculous Host Defense. *Cell Host Microbe* **21**, 59–72 (2017).
123. Castillo, E. F. *et al.* Autophagy protects against active tuberculosis by suppressing bacterial burden and inflammation. *Proc. Natl. Acad. Sci. USA* **109**, E3168–76 (2012).

124. Kimmey, J. M. *et al.* Unique role for ATG5 in neutrophil-mediated immunopathology during M. tuberculosis infection. *Nature* **528**, 565–569 (2015).
125. Aibana, O. *et al.* Vitamin D status and risk of incident tuberculosis disease: A nested case-control study, systematic review, and individual-participant data meta-analysis. *PLoS Med.* **16**, e1002907 (2019).
126. Wilkinson, R. J. *et al.* Influence of vitamin D deficiency and vitamin D receptor polymorphisms on tuberculosis among Gujarati Asians in west London: a case-control study. *Lancet* **355**, 618–621 (2000).
127. Wu, H.-X. *et al.* Effects of vitamin D supplementation on the outcomes of patients with pulmonary tuberculosis: a systematic review and meta-analysis. *BMC Pulm Med* **18**, 108 (2018).
128. Jolliffe, D. A. *et al.* Adjunctive vitamin D in tuberculosis treatment: meta-analysis of individual participant data. *Eur. Respir. J.* **53**, (2019).
129. Liu, P. T. *et al.* Toll-like receptor triggering of a vitamin D-mediated human antimicrobial response. *Science* **311**, 1770–1773 (2006).
130. Campbell, G. R. & Spector, S. A. Vitamin D inhibits human immunodeficiency virus type 1 and Mycobacterium tuberculosis infection in macrophages through the induction of autophagy. *PLoS Pathog.* **8**, e1002689 (2012).
131. Rao Muvva, J., Parasa, V. R., Lerm, M., Svensson, M. & Brighenti, S. Polarization of Human Monocyte-Derived Cells With Vitamin D Promotes Control of Mycobacterium tuberculosis Infection. *Front. Immunol.* **10**, 3157 (2019).
132. Rivas-Santiago, B. *et al.* Activity of LL-37, CRAMP and antimicrobial peptide-derived compounds E2, E6 and CP26 against Mycobacterium tuberculosis. *Int. J. Antimicrob. Agents* **41**, 143–148 (2013).
133. Gupta, S., Winglee, K., Gallo, R. & Bishai, W. R. Bacterial subversion of cAMP signalling inhibits cathelicidin expression, which is required for innate resistance to Mycobacterium tuberculosis. *J. Pathol.* **242**, 52–61 (2017).
134. Fabri, M. *et al.* Vitamin D is required for IFN-gamma-mediated antimicrobial activity of human macrophages. *Sci. Transl. Med.* **3**, 104ra102 (2011).
135. Vogt, G. & Nathan, C. In vitro differentiation of human macrophages with enhanced antimycobacterial activity. *J. Clin. Invest.* **121**, 3889–3901 (2011).
136. Bustamante, J. *et al.* Germline CYBB mutations that selectively affect macrophages in kindreds with X-linked predisposition to tuberculous mycobacterial disease. *Nat. Immunol.* **12**, 213–221 (2011).
137. Khan, T. A. *et al.* A novel missense mutation in the NADPH binding domain of CYBB abolishes the NADPH oxidase activity in a male patient with increased susceptibility to infections. *Microb. Pathog.* **100**, 163–169 (2016).
138. Cooper, A. M., Segal, B. H., Frank, A. A., Holland, S. M. & Orme, I. M. Transient loss of resistance to pulmonary tuberculosis in p47(phox-/-) mice. *Infect. Immun.* **68**, 1231–1234 (2000).
139. Olive, A. J., Smith, C. M., Kiritsy, M. C. & Sasseti, C. M. The Phagocyte Oxidase Controls Tolerance to Mycobacterium tuberculosis Infection. *J. Immunol.* **201**, 1705–1716 (2018).
140. MacMicking, J., Xie, Q. W. & Nathan, C. Nitric oxide and macrophage function. *Annu. Rev. Immunol.* **15**, 323–350 (1997).
141. Nicholson, S. *et al.* Inducible nitric oxide synthase in pulmonary alveolar macrophages from patients with tuberculosis. *J. Exp. Med.* **183**, 2293–2302 (1996).
142. Nathan, C. Inducible nitric oxide synthase in the tuberculous human lung. *Am. J. Respir. Crit. Care Med.* **166**, 130–131 (2002).
143. Idh, J. *et al.* Nitric oxide production in the exhaled air of patients with pulmonary tuberculosis in relation to HIV co-infection. *BMC Infect. Dis.* **8**, 146 (2008).

144. MacMicking, J. D. *et al.* Identification of nitric oxide synthase as a protective locus against tuberculosis. *Proc. Natl. Acad. Sci. USA* **94**, 5243–5248 (1997).
145. Mishra, B. B. *et al.* Nitric oxide prevents a pathogen-permissive granulocytic inflammation during tuberculosis. *Nat. Microbiol.* **2**, 17072 (2017).
146. Braverman, J. & Stanley, S. A. Nitric Oxide Modulates Macrophage Responses to Mycobacterium tuberculosis Infection through Activation of HIF-1 $\alpha$  and Repression of NF- $\kappa$ B. *J. Immunol.* **199**, 1805–1816 (2017).
147. Darwin, K. H., Ehrt, S., Gutierrez-Ramos, J.-C., Weich, N. & Nathan, C. F. The proteasome of Mycobacterium tuberculosis is required for resistance to nitric oxide. *Science* **302**, 1963–1966 (2003).
148. Kim, B.-H. *et al.* A family of IFN- $\gamma$ -inducible 65-kD GTPases protects against bacterial infection. *Science* **332**, 717–721 (2011).
149. Ahmed, M. *et al.* Immune correlates of tuberculosis disease and risk translate across species. *Sci. Transl. Med.* **12**, (2020).
150. Plumlee, C. R. *et al.* A blood RNA signature in a novel murine model predicts human tuberculosis risk. *SSRN Journal* (2020). doi:10.2139/ssrn.3541362
151. MacMicking, J. D., Taylor, G. A. & McKinney, J. D. Immune control of tuberculosis by IFN-gamma-inducible LRG-47. *Science* **302**, 654–659 (2003).
152. Hunn, J. P. & Howard, J. C. The mouse resistance protein Irgm1 (LRG-47): a regulator or an effector of pathogen defense? *PLoS Pathog.* **6**, e1001008 (2010).
153. Kim, B.-H., Shenoy, A. R., Kumar, P., Bradfield, C. J. & MacMicking, J. D. IFN-inducible GTPases in host cell defense. *Cell Host Microbe* **12**, 432–444 (2012).
154. Gleeson, L. E. *et al.* Cutting Edge: Mycobacterium tuberculosis Induces Aerobic Glycolysis in Human Alveolar Macrophages That Is Required for Control of Intracellular Bacillary Replication. *J. Immunol.* **196**, 2444–2449 (2016).
155. Braverman, J., Sogi, K. M., Benjamin, D., Nomura, D. K. & Stanley, S. A. HIF-1 $\alpha$  Is an Essential Mediator of IFN- $\gamma$ -Dependent Immunity to Mycobacterium tuberculosis. *J. Immunol.* **197**, 1287–1297 (2016).
156. Tannahill, G. M. *et al.* Succinate is an inflammatory signal that induces IL-1 $\beta$  through HIF-1 $\alpha$ . *Nature* **496**, 238–242 (2013).
157. Lee, J., Repasy, T., Papavinasasundaram, K., Sasseti, C. & Kornfeld, H. Mycobacterium tuberculosis induces an atypical cell death mode to escape from infected macrophages. *PLoS One* **6**, e18367 (2011).
158. Duan, L., Gan, H., Arm, J. & Remold, H. G. Cytosolic phospholipase A2 participates with TNF-alpha in the induction of apoptosis of human macrophages infected with Mycobacterium tuberculosis H37Ra. *J. Immunol.* **166**, 7469–7476 (2001).
159. Chen, M., Gan, H. & Remold, H. G. A mechanism of virulence: virulent Mycobacterium tuberculosis strain H37Rv, but not attenuated H37Ra, causes significant mitochondrial inner membrane disruption in macrophages leading to necrosis. *J. Immunol.* **176**, 3707–3716 (2006).
160. Schaible, U. E. *et al.* Apoptosis facilitates antigen presentation to T lymphocytes through MHC-I and CD1 in tuberculosis. *Nat. Med.* **9**, 1039–1046 (2003).
161. Winau, F. *et al.* Apoptotic vesicles crossprime CD8 T cells and protect against tuberculosis. *Immunity* **24**, 105–117 (2006).
162. Hinchey, J. *et al.* Enhanced priming of adaptive immunity by a proapoptotic mutant of Mycobacterium tuberculosis. *J. Clin. Invest.* **117**, 2279–2288 (2007).
163. Divangahi, M., Desjardins, D., Nunes-Alves, C., Remold, H. G. & Behar, S. M. Eicosanoid pathways regulate adaptive immunity to Mycobacterium tuberculosis. *Nat. Immunol.* **11**, 751–758 (2010).



164. Blomgran, R., Desvignes, L., Briken, V. & Ernst, J. D. Mycobacterium tuberculosis inhibits neutrophil apoptosis, leading to delayed activation of naive CD4 T cells. *Cell Host Microbe* **11**, 81–90 (2012).
165. Martin, C. J. *et al.* Efferocytosis is an innate antibacterial mechanism. *Cell Host Microbe* **12**, 289–300 (2012).
166. Divangahi, M. *et al.* Mycobacterium tuberculosis evades macrophage defenses by inhibiting plasma membrane repair. *Nat. Immunol.* **10**, 899–906 (2009).
167. Chang, D. J., Ringold, G. M. & Heller, R. A. Cell killing and induction of manganous superoxide dismutase by tumor necrosis factor- $\alpha$  is mediated by lipoxygenase metabolites of arachidonic acid. *Biochem. Biophys. Res. Commun.* **188**, 538–546 (1992).
168. Chen, M. *et al.* Lipid mediators in innate immunity against tuberculosis: opposing roles of PGE2 and LXA4 in the induction of macrophage death. *J. Exp. Med.* **205**, 2791–2801 (2008).
169. Ricciotti, E. & FitzGerald, G. A. Prostaglandins and inflammation. *Arterioscler. Thromb. Vasc. Biol.* **31**, 986–1000 (2011).
170. Levy, B. D., Clish, C. B., Schmidt, B., Gronert, K. & Serhan, C. N. Lipid mediator class switching during acute inflammation: signals in resolution. *Nat. Immunol.* **2**, 612–619 (2001).
171. Tobin, D. M. *et al.* Host genotype-specific therapies can optimize the inflammatory response to mycobacterial infections. *Cell* **148**, 434–446 (2012).
172. Thuong, N. T. T. *et al.* Leukotriene A4 hydrolase genotype and HIV infection influence intracerebral inflammation and survival from tuberculous meningitis. *J. Infect. Dis.* **215**, 1020–1028 (2017).
173. Segal, A. W. How neutrophils kill microbes. *Annu. Rev. Immunol.* **23**, 197–223 (2005).
174. Gopal, R. *et al.* S100A8/A9 proteins mediate neutrophilic inflammation and lung pathology during tuberculosis. *Am. J. Respir. Crit. Care Med.* **188**, 1137–1146 (2013).
175. Nouailles, G. *et al.* CXCL5-secreting pulmonary epithelial cells drive destructive neutrophilic inflammation in tuberculosis. *J. Clin. Invest.* (2014).
176. Blomgran, R. & Ernst, J. D. Lung neutrophils facilitate activation of naive antigen-specific CD4+ T cells during Mycobacterium tuberculosis infection. *J. Immunol.* **186**, 7110–7119 (2011).
177. Lowe, D. M., Redford, P. S., Wilkinson, R. J., O’Garra, A. & Martineau, A. R. Neutrophils in tuberculosis: friend or foe? *Trends Immunol.* **33**, 14–25 (2012).
178. Lovewell, R. R., Baer, C. E., Mishra, B. B., Smith, C. M. & Sasseti, C. M. Granulocytes act as a niche for Mycobacterium tuberculosis growth. *Mucosal Immunol.* **14**, 229–241 (2021).
179. Eruslanov, E. B. *et al.* Neutrophil responses to Mycobacterium tuberculosis infection in genetically susceptible and resistant mice. *Infect. Immun.* **73**, 1744–1753 (2005).
180. Scott, N. R. *et al.* S100A8/A9 regulates CD11b expression and neutrophil recruitment during chronic tuberculosis. *J. Clin. Invest.* **130**, 3098–3112 (2020).
181. Hunter, R. L. Pathology of post primary tuberculosis of the lung: an illustrated critical review. *Tuberculosis (Edinb)* **91**, 497–509 (2011).
182. Nair, S. *et al.* Irg1 expression in myeloid cells prevents immunopathology during M. tuberculosis infection. *J. Exp. Med.* **215**, 1035–1045 (2018).
183. Dorhoi, A. *et al.* The adaptor molecule CARD9 is essential for tuberculosis control. *J. Exp. Med.* **207**, 777–792 (2010).
184. Puttur, F., Gregory, L. G. & Lloyd, C. M. Airway macrophages as the guardians of tissue repair in the lung. *Immunol. Cell Biol.* **97**, 246–257 (2019).
185. Papp, A. C. *et al.* AmpliSeq transcriptome analysis of human alveolar and monocyte-derived macrophages over time in response to Mycobacterium tuberculosis infection. *PLoS One* **13**, e0198221 (2018).

186. Cohen, S. B. *et al.* Alveolar Macrophages Provide an Early Mycobacterium tuberculosis Niche and Initiate Dissemination. *Cell Host Microbe* **24**, 439–446.e4 (2018).
187. Rothchild, A. C. *et al.* Alveolar macrophages generate a noncanonical NRF2-driven transcriptional response to Mycobacterium tuberculosis in vivo. *Sci. Immunol.* **4**, (2019).
188. Leemans, J. C. *et al.* Depletion of alveolar macrophages exerts protective effects in pulmonary tuberculosis in mice. *J. Immunol.* **166**, 4604–4611 (2001).
189. Huang, L., Nazarova, E. V., Tan, S., Liu, Y. & Russell, D. G. Growth of Mycobacterium tuberculosis in vivo segregates with host macrophage metabolism and ontogeny. *J. Exp. Med.* **215**, 1135–1152 (2018).
190. Guirado, E. *et al.* Deletion of PPAR $\gamma$  in lung macrophages provides an immunoprotective response against M. tuberculosis infection in mice. *Tuberculosis (Edinb)* **111**, 170–177 (2018).
191. Wolf, A. J. *et al.* Mycobacterium tuberculosis infects dendritic cells with high frequency and impairs their function in vivo. *J. Immunol.* **179**, 2509–2519 (2007).
192. Repasy, T. *et al.* Intracellular bacillary burden reflects a burst size for Mycobacterium tuberculosis in vivo. *PLoS Pathog.* **9**, e1003190 (2013).
193. Lee, J. *et al.* CD11c<sup>Hi</sup> monocyte-derived macrophages are a major cellular compartment infected by Mycobacterium tuberculosis. *PLoS Pathog.* **16**, e1008621 (2020).
194. Norris, B. A. & Ernst, J. D. Mononuclear cell dynamics in M. tuberculosis infection provide opportunities for therapeutic intervention. *PLoS Pathog.* **14**, e1007154 (2018).
195. Marino, S. *et al.* Dendritic cell trafficking and antigen presentation in the human immune response to Mycobacterium tuberculosis. *J. Immunol.* **173**, 494–506 (2004).
196. Tian, T., Woodworth, J., Sköld, M. & Behar, S. M. In vivo depletion of CD11c+ cells delays the CD4+ T cell response to Mycobacterium tuberculosis and exacerbates the outcome of infection. *J. Immunol.* **175**, 3268–3272 (2005).
197. Peters, W. *et al.* Chemokine receptor 2 serves an early and essential role in resistance to Mycobacterium tuberculosis. *Proc. Natl. Acad. Sci. USA* **98**, 7958–7963 (2001).
198. Peters, W. *et al.* CCR2-dependent trafficking of F4/80<sup>dim</sup> macrophages and CD11c<sup>dim/intermediate</sup> dendritic cells is crucial for T cell recruitment to lungs infected with Mycobacterium tuberculosis. *J. Immunol.* **172**, 7647–7653 (2004).
199. Samstein, M. *et al.* Essential yet limited role for CCR2<sup>+</sup> inflammatory monocytes during Mycobacterium tuberculosis-specific T cell priming. *Elife* **2**, e01086 (2013).
200. Miller, J. D. *et al.* Human effector and memory CD8+ T cell responses to smallpox and yellow fever vaccines. *Immunity* **28**, 710–722 (2008).
201. Poulsen, A. Some clinical features of tuberculosis. 1. Incubation period. *Acta Tuberc Scand* **24**, 311–346 (1950).
202. Wallgren, A. The time-table of tuberculosis. *Tubercle* **29**, 245–251 (1948).
203. Madan-Lala, R. *et al.* Mycobacterium tuberculosis impairs dendritic cell functions through the serine hydrolase Hip1. *J. Immunol.* **192**, 4263–4272 (2014).
204. Garcia-Romo, G. S. *et al.* Mycobacterium tuberculosis manipulates pulmonary APCs subverting early immune responses. *Immunobiology* **218**, 393–401 (2013).
205. Wolf, A. J. *et al.* Initiation of the adaptive immune response to Mycobacterium tuberculosis depends on antigen production in the local lymph node, not the lungs. *J. Exp. Med.* **205**, 105–115 (2008).
206. Griffiths, K. L. *et al.* Targeting dendritic cells to accelerate T-cell activation overcomes a bottleneck in tuberculosis vaccine efficacy. *Nat. Commun.* **7**, 13894 (2016).
207. Khader, S. A. *et al.* IL-23 and IL-17 in the establishment of protective pulmonary CD4+ T cell responses after vaccination and during Mycobacterium tuberculosis challenge. *Nat. Immunol.* **8**, 369–377 (2007).

208. Gallegos, A. M., Pamer, E. G. & Glickman, M. S. Delayed protection by ESAT-6-specific effector CD4+ T cells after airborne M. tuberculosis infection. *J. Exp. Med.* **205**, 2359–2368 (2008).
209. Bozzano, F. *et al.* Functionally relevant decreases in activatory receptor expression on NK cells are associated with pulmonary tuberculosis in vivo and persist after successful treatment. *Int. Immunol.* **21**, 779–791 (2009).
210. Roy Chowdhury, R. *et al.* A multi-cohort study of the immune factors associated with M. tuberculosis infection outcomes. *Nature* **560**, 644–648 (2018).
211. Vankayalapati, R. *et al.* Role of NK cell-activating receptors and their ligands in the lysis of mononuclear phagocytes infected with an intracellular bacterium. *J. Immunol.* **175**, 4611–4617 (2005).
212. Brill, K. J. *et al.* Human natural killer cells mediate killing of intracellular Mycobacterium tuberculosis H37Rv via granule-independent mechanisms. *Infect. Immun.* **69**, 1755–1765 (2001).
213. Lu, C.-C. *et al.* NK cells kill mycobacteria directly by releasing perforin and granulysin. *J. Leukoc. Biol.* **96**, 1119–1129 (2014).
214. Denis, M. Interleukin-12 (IL-12) augments cytolytic activity of natural killer cells toward Mycobacterium tuberculosis-infected human monocytes. *Cell Immunol.* **156**, 529–536 (1994).
215. Junqueira-Kipnis, A. P. *et al.* NK cells respond to pulmonary infection with Mycobacterium tuberculosis, but play a minimal role in protection. *J. Immunol.* **171**, 6039–6045 (2003).
216. Feng, C. G. *et al.* NK cell-derived IFN-gamma differentially regulates innate resistance and neutrophil response in T cell-deficient hosts infected with Mycobacterium tuberculosis. *J. Immunol.* **177**, 7086–7093 (2006).
217. Howson, L. J., Salio, M. & Cerundolo, V. MR1-Restricted Mucosal-Associated Invariant T Cells and Their Activation during Infectious Diseases. *Front. Immunol.* **6**, 303 (2015).
218. Kauffman, K. D. *et al.* Limited Pulmonary Mucosal-Associated Invariant T Cell Accumulation and Activation during Mycobacterium tuberculosis Infection in Rhesus Macaques. *Infect. Immun.* **86**, (2018).
219. Ellis-Connell, A. L. *et al.* MAIT cells are minimally responsive to Mycobacterium tuberculosis within granulomas, but are functionally impaired by SIV in a macaque model of SIV and Mtb co-infection. *BioRxiv* (2020). doi:10.1101/2020.01.07.897447
220. Sakala, I. G. *et al.* Functional Heterogeneity and Antimycobacterial Effects of Mouse Mucosal-Associated Invariant T Cells Specific for Riboflavin Metabolites. *J. Immunol.* **195**, 587–601 (2015).
221. Suliman, S. *et al.* MR1-Independent Activation of Human Mucosal-Associated Invariant T Cells by Mycobacteria. *J. Immunol.* **203**, 2917–2927 (2019).
222. Greene, J. M. *et al.* MR1-restricted mucosal-associated invariant T (MAIT) cells respond to mycobacterial vaccination and infection in nonhuman primates. *Mucosal Immunol.* **10**, 802–813 (2017).
223. Chua, W.-J. *et al.* Polyclonal mucosa-associated invariant T cells have unique innate functions in bacterial infection. *Infect. Immun.* **80**, 3256–3267 (2012).
224. Janis, E. M., Kaufmann, S. H., Schwartz, R. H. & Pardoll, D. M. Activation of gamma delta T cells in the primary immune response to Mycobacterium tuberculosis. *Science* **244**, 713–716 (1989).
225. Vorkas, C. K. *et al.* Mucosal-associated invariant and  $\gamma\delta$  T cell subsets respond to initial Mycobacterium tuberculosis infection. *JCI Insight* **3**, (2018).
226. Peng, M. Y. *et al.* Interleukin 17-producing gamma delta T cells increased in patients with active pulmonary tuberculosis. *Cell Mol Immunol* **5**, 203–208 (2008).
227. Tanaka, Y. *et al.* Nonpeptide ligands for human gamma delta T cells. *Proc. Natl. Acad. Sci. USA* **91**, 8175–8179 (1994).

228. Balaji, K. N., Schwander, S. K., Rich, E. A. & Boom, W. H. Alveolar macrophages as accessory cells for human gamma delta T cells activated by Mycobacterium tuberculosis. *J. Immunol.* **154**, 5959–5968 (1995).
229. Dieli, F. *et al.* Granulysin-dependent killing of intracellular and extracellular Mycobacterium tuberculosis by Vgamma9/Vdelta2 T lymphocytes. *J. Infect. Dis.* **184**, 1082–1085 (2001).
230. Tsukaguchi, K., Balaji, K. N. & Boom, W. H. CD4+ alpha beta T cell and gamma delta T cell responses to Mycobacterium tuberculosis. Similarities and differences in Ag recognition, cytotoxic effector function, and cytokine production. *J. Immunol.* **154**, 1786–1796 (1995).
231. Ladel, C. H., Blum, C., Dreher, A., Reifenberg, K. & Kaufmann, S. H. Protective role of gamma/delta T cells and alpha/beta T cells in tuberculosis. *Eur. J. Immunol.* **25**, 2877–2881 (1995).
232. Chen, Z. W. Multifunctional immune responses of HMBPP-specific Vγ2Vδ2 T cells in M. tuberculosis and other infections. *Cell Mol Immunol* **10**, 58–64 (2013).
233. De Libero, G. *et al.* Selection by two powerful antigens may account for the presence of the major population of human peripheral gamma/delta T cells. *J. Exp. Med.* **173**, 1311–1322 (1991).
234. Panchamoorthy, G. *et al.* A predominance of the T cell receptor V gamma 2/V delta 2 subset in human mycobacteria-responsive T cells suggests germline gene encoded recognition. *J. Immunol.* **147**, 3360–3369 (1991).
235. Shen, Y. *et al.* Adaptive immune response of Vgamma2Vdelta2+ T cells during mycobacterial infections. *Science* **295**, 2255–2258 (2002).
236. Shen, L. *et al.* Immunization of Vγ2Vδ2 T cells programs sustained effector memory responses that control tuberculosis in nonhuman primates. *Proc. Natl. Acad. Sci. USA* **116**, 6371–6378 (2019).
237. Van Der Meeren, O. *et al.* Phase 2b controlled trial of M72/AS01E vaccine to prevent tuberculosis. *N. Engl. J. Med.* **379**, 1621–1634 (2018).
238. Stewart, E., Triccas, J. A. & Petrovsky, N. Adjuvant strategies for more effective tuberculosis vaccine immunity. *Microorganisms* **7**, (2019).
239. Nanishi, E., Dowling, D. J. & Levy, O. Toward precision adjuvants: optimizing science and safety. *Curr. Opin. Pediatr.* **32**, 125–138 (2020).
240. Billeskov, R. *et al.* High Antigen Dose Is Detrimental to Post-Exposure Vaccine Protection against Tuberculosis. *Front. Immunol.* **8**, 1973 (2017).
241. Sallin, M. A. *et al.* Th1 Differentiation Drives the Accumulation of Intravascular, Non-protective CD4 T Cells during Tuberculosis. *Cell Rep.* **18**, 3091–3104 (2017).
242. Van Dis, E. *et al.* STING-Activating Adjuvants Elicit a Th17 Immune Response and Protect against Mycobacterium tuberculosis Infection. *Cell Rep.* **23**, 1435–1447 (2018).
243. Hart, P. *et al.* Nanoparticle-Fusion Protein Complexes Protect against Mycobacterium tuberculosis Infection. *Mol. Ther.* **26**, 822–833 (2018).
244. Shann, F. The non-specific effects of vaccines. *Arch. Dis. Child.* **95**, 662–667 (2010).
245. Spencer, J. C., Ganguly, R. & Waldman, R. H. Nonspecific protection of mice against influenza virus infection by local or systemic immunization with Bacille Calmette-Guérin. *J. Infect. Dis.* **136**, 171–175 (1977).
246. Starr, S. E., Visintine, A. M., Tomeh, M. O. & Nahmias, A. J. Effects of immunostimulants on resistance of newborn mice to herpes simplex type 2 infection. *Proc Soc Exp Biol Med* **152**, 57–60 (1976).
247. O’Neill, L. A. J. & Netea, M. G. BCG-induced trained immunity: can it offer protection against COVID-19? *Nat. Rev. Immunol.* **20**, 335–337 (2020).
248. Kaufmann, E. *et al.* BCG Educates Hematopoietic Stem Cells to Generate Protective Innate Immunity against Tuberculosis. *Cell* **172**, 176–190.e19 (2018).
249. Darrah, P. A. *et al.* Prevention of tuberculosis in macaques after intravenous BCG immunization. *Nature* **577**, 95–102 (2020).

250. Barclay, W. R., Anacker, R. L., Brehmer, W., Leif, W. & Ribí, E. Aerosol-Induced Tuberculosis in Subhuman Primates and the Course of the Disease After Intravenous BCG Vaccination. *Infect. Immun.* **2**, 574–582 (1970).
251. Joosten, S. A. *et al.* Mycobacterial growth inhibition is associated with trained innate immunity. *J. Clin. Invest.* (2018).
252. Schutz, C. *et al.* Corticosteroids as an adjunct to tuberculosis therapy. *Expert Rev Respir Med* **12**, 881–891 (2018).
253. Cadena, A. M., Fortune, S. M. & Flynn, J. L. Heterogeneity in tuberculosis. *Nat. Rev. Immunol.* **17**, 691–702 (2017).
254. Qu, H.-Q., Li, Q., McCormick, J. B. & Fisher-Hoch, S. P. What did we learn from the genome-wide association study for tuberculosis susceptibility? *J. Med. Genet.* **48**, 217–218 (2011).
255. Green, A. M., Difazio, R. & Flynn, J. L. IFN- $\gamma$  from CD4 T cells is essential for host survival and enhances CD8 T cell function during Mycobacterium tuberculosis infection. *J. Immunol.* **190**, 270–277 (2013).
256. Caruso, A. M. *et al.* Mice deficient in CD4 T cells have only transiently diminished levels of IFN- $\gamma$ , yet succumb to tuberculosis. *J. Immunol.* **162**, 5407–5416 (1999).
257. Scanga, C. A. *et al.* Depletion of CD4(+) T cells causes reactivation of murine persistent tuberculosis despite continued expression of interferon gamma and nitric oxide synthase 2. *J. Exp. Med.* **192**, 347–358 (2000).
258. Cooper, A. M. *et al.* Disseminated tuberculosis in interferon gamma gene-disrupted mice. *J. Exp. Med.* **178**, 2243–2247 (1993).
259. Kramnik, I., Demant, P. & Bloom, B. B. Susceptibility to tuberculosis as a complex genetic trait: analysis using recombinant congenic strains of mice. *Novartis Found Symp* **217**, 120–31; discussion 132 (1998).
260. Kramnik, I., Dietrich, W. F., Demant, P. & Bloom, B. R. Genetic control of resistance to experimental infection with virulent Mycobacterium tuberculosis. *Proc. Natl. Acad. Sci. USA* **97**, 8560–8565 (2000).
261. Pan, H. *et al.* Ipr1 gene mediates innate immunity to tuberculosis. *Nature* **434**, 767–772 (2005).
262. Ji, D. X. *et al.* Role of the transcriptional regulator SP140 in resistance to bacterial infections via repression of type I interferons. *Elife* **10**, (2021).
263. Churchill, G. A. *et al.* The Collaborative Cross, a community resource for the genetic analysis of complex traits. *Nat. Genet.* **36**, 1133–1137 (2004).
264. Svenson, K. L. *et al.* High-resolution genetic mapping using the Mouse Diversity Outbred population. *Genetics* **190**, 437–447 (2012).
265. Smith, C. M. *et al.* Tuberculosis susceptibility and vaccine protection are independently controlled by host genotype. *MBio* **7**, (2016).
266. Niazi, M. K. K. *et al.* Lung necrosis and neutrophils reflect common pathways of susceptibility to Mycobacterium tuberculosis in genetically diverse, immune-competent mice. *Dis. Model. Mech.* **8**, 1141–1153 (2015).
267. Koyuncu, D. *et al.* Tuberculosis biomarkers discovered using Diversity Outbred mice. *medRxiv* (2021). doi:10.1101/2021.01.08.20249024
268. Smith, C. M. *et al.* Host-pathogen genetic interactions underlie tuberculosis susceptibility in genetically diverse mice. *Elife* **11**, (2022).
269. Salcedo, T., Geraldès, A. & Nachman, M. W. Nucleotide variation in wild and inbred mice. *Genetics* **177**, 2277–2291 (2007).
270. Yang, H. *et al.* Subspecific origin and haplotype diversity in the laboratory mouse. *Nat. Genet.* **43**, 648–655 (2011).

271. Phifer-Rixey, M. *et al.* The genomic basis of environmental adaptation in house mice. *PLoS Genet.* **14**, e1007672 (2018).
272. Ferris, K. G. *et al.* The genomics of rapid climatic adaptation and parallel evolution in North American house mice. *PLoS Genet.* **17**, e1009495 (2021).
273. Lönnroth, K., Williams, B. G., Cegielski, P. & Dye, C. A consistent log-linear relationship between tuberculosis incidence and body mass index. *Int. J. Epidemiol.* **39**, 149–155 (2010).
274. Bold, T. D. & Ernst, J. D. CD4+ T cell-dependent IFN- $\gamma$  production by CD8+ effector T cells in Mycobacterium tuberculosis infection. *J. Immunol.* **189**, 2530–2536 (2012).
275. Sakai, S. *et al.* CD4 T Cell-Derived IFN- $\gamma$  Plays a Minimal Role in Control of Pulmonary Mycobacterium tuberculosis Infection and Must Be Actively Repressed by PD-1 to Prevent Lethal Disease. *PLoS Pathog.* **12**, e1005667 (2016).
276. Bustamante, J., Boisson-Dupuis, S., Abel, L. & Casanova, J.-L. Mendelian susceptibility to mycobacterial disease: genetic, immunological, and clinical features of inborn errors of IFN- $\gamma$  immunity. *Semin. Immunol.* **26**, 454–470 (2014).
277. Casanova, J.-L. & Abel, L. Genetic dissection of immunity to mycobacteria: the human model. *Annu. Rev. Immunol.* **20**, 581–620 (2002).
278. Rodríguez-Prados, J.-C. *et al.* Substrate fate in activated macrophages: a comparison between innate, classic, and alternative activation. *J. Immunol.* **185**, 605–614 (2010).
279. Viola, A., Munari, F., Sánchez-Rodríguez, R., Scolaro, T. & Castegna, A. The metabolic signature of macrophage responses. *Front. Immunol.* **10**, 1462 (2019).
280. Wellen, K. E. & Thompson, C. B. A two-way street: reciprocal regulation of metabolism and signalling. *Nat. Rev. Mol. Cell Biol.* **13**, 270–276 (2012).
281. Wang, T. *et al.* HIF1 $\alpha$ -Induced Glycolysis Metabolism Is Essential to the Activation of Inflammatory Macrophages. *Mediators Inflamm.* **2017**, 9029327 (2017).
282. Ferreira, J. V. *et al.* STUB1/CHIP is required for HIF1A degradation by chaperone-mediated autophagy. *Autophagy* **9**, 1349–1366 (2013).
283. Lin, L., Yee, S. W., Kim, R. B. & Giacomini, K. M. SLC transporters as therapeutic targets: emerging opportunities. *Nat. Rev. Drug Discov.* **14**, 543–560 (2015).
284. Freerman, A. J. *et al.* Myeloid Slc2a1-Deficient Murine Model Revealed Macrophage Activation and Metabolic Phenotype Are Fueled by GLUT1. *J. Immunol.* **202**, 1265–1286 (2019).
285. Sedlyarov, V. *et al.* The bicarbonate transporter SLC4A7 plays a key role in macrophage phagosome acidification. *Cell Host Microbe* **23**, 766–774.e5 (2018).
286. Bejarano, E. & Cuervo, A. M. Chaperone-mediated autophagy. *Proc Am Thorac Soc* **7**, 29–39 (2010).
287. Komander, D. & Rape, M. The ubiquitin code. *Annu. Rev. Biochem.* **81**, 203–229 (2012).
288. Roberts, A. W. *et al.* Cas9+ conditionally-immortalized macrophages as a tool for bacterial pathogenesis and beyond. *Elife* **8**, (2019).
289. Morgens, D. W. *et al.* Genome-scale measurement of off-target activity using Cas9 toxicity in high-throughput screens. *Nat. Commun.* **8**, 15178 (2017).
290. Cai, W. & Yang, H. The structure and regulation of Cullin 2 based E3 ubiquitin ligases and their biological functions. *Cell Div.* **11**, 7 (2016).
291. Luo, W. *et al.* Hsp70 and CHIP selectively mediate ubiquitination and degradation of hypoxia-inducible factor (HIF)-1 $\alpha$  but Not HIF-2 $\alpha$ . *J. Biol. Chem.* **285**, 3651–3663 (2010).
292. Bento, C. F. *et al.* The chaperone-dependent ubiquitin ligase CHIP targets HIF-1 $\alpha$  for degradation in the presence of methylglyoxal. *PLoS One* **5**, e15062 (2010).
293. Joshi, V. *et al.* A decade of boon or burden: what has the CHIP ever done for cellular protein quality control mechanism implicated in neurodegeneration and aging? *Front. Mol. Neurosci.* **9**, 93 (2016).

294. Hess, D. T., Matsumoto, A., Kim, S.-O., Marshall, H. E. & Stamler, J. S. Protein S-nitrosylation: purview and parameters. *Nat. Rev. Mol. Cell Biol.* **6**, 150–166 (2005).
295. Yasinska, I. M. & Sumbayev, V. V. S-nitrosation of Cys-800 of HIF-1alpha protein activates its interaction with p300 and stimulates its transcriptional activity. *FEBS Lett.* **549**, 105–109 (2003).
296. Sumbayev, V. V., Budde, A., Zhou, J. & Brüne, B. HIF-1 alpha protein as a target for S-nitrosation. *FEBS Lett.* **535**, 106–112 (2003).
297. Metzen, E., Zhou, J., Jelkmann, W., Fandrey, J. & Brüne, B. Nitric oxide impairs normoxic degradation of HIF-1alpha by inhibition of prolyl hydroxylases. *Mol. Biol. Cell* **14**, 3470–3481 (2003).
298. Ben-Lulu, S., Ziv, T., Admon, A., Weisman-Shomer, P. & Benhar, M. A substrate trapping approach identifies proteins regulated by reversible S-nitrosylation. *Mol. Cell Proteomics* **13**, 2573–2583 (2014).
299. Forrester, M. T., Foster, M. W., Benhar, M. & Stamler, J. S. Detection of protein S-nitrosylation with the biotin-switch technique. *Free Radic. Biol. Med.* **46**, 119–126 (2009).
300. Hubbi, M. E. *et al.* Chaperone-mediated autophagy targets hypoxia-inducible factor-1 $\alpha$  (HIF-1 $\alpha$ ) for lysosomal degradation. *J. Biol. Chem.* **288**, 10703–10714 (2013).